



Deliverable 3.2

–

**CORI – SOTA Update on cement-organic-radionuclide interactions
in the context of L/ILW disposal**

Work Package 3, CORI

The project leading to this application has received funding from the European Union's Horizon 2020 research and innovation programme under grant agreement No 847593.



<http://www.ejp-urad.eu/>

Document information

Project Acronym	EURAD
Project Title	European Joint Programme on Radioactive Waste Management
Project Type	European Joint Programme (EJP)
EC grant agreement No.	847593
Project starting / end date	1st June 2019 – 30 May 2024
Work Package No.	3
Work Package Title	Cement Organic Radionuclide Interaction
Work Package Acronym	CORI
Deliverable No.	3.2
Deliverable Title	SOTA update on cement- organic-radionuclide- interactions in the content of L/ILW disposal
Lead Beneficiary	KIT
Contractual Delivery Date	58
Actual Delivery Date	25/05/2024
Type	Report
Dissemination level	PU
Authors	CORI WP Board: Marcus Altmaier [KIT]; Virginie Blin [CEA]; David García [KIT (Amphos21)]; Pierre Henocq [Andra], Nathalie Macé [CEA], Tiziana Missana [CIEMAT]; Denise Ricard [Andra]; Johan Vandendorre [CNRS (SUBATECH)]

To be cited as:

(2024): SOTA update on cement-organic-radionuclide-interactions in the context of L/ILW disposal. Final version as of 25.05.2024 of Deliverable D3.2 of the HORIZON 2020 project EURAD. EC Grant agreement no: 847593.

Disclaimer

All information in this document is provided "as is" and no guarantee or warranty is given that the information is fit for any particular purpose. The user, therefore, uses the information at its sole risk and liability. For the avoidance of all doubts, the European Commission has no liability in respect of this document, which is merely representing the authors' view.

Acknowledgement

This document is a deliverable of the European Joint Programme on Radioactive Waste Management (EURAD). EURAD has received funding from the European Union's Horizon 2020 research and innovation programme under grant agreement No 847593.

Status of deliverable		
	By	Date
Delivered (Lead Beneficiary)	KIT	25/05/2024
Verified (PMO)	B. Grambow	27/05/2024
Reviewed (Bureau)		
Approved (General Assembly)		
Submitted to EC (Coordinator)	Andra (Coordinator)	31/05/2024

Executive Summary

This document presents the state-of-art on key topics addressed in CORI and provides supporting background information relevant to the specific scientific and technical context investigated in this project. New advances made within CORI are highlighted for the three R&D Tasks.

In the SOTA, a short introductory chapter summarizes the main scope and content of CORI, against which the SOTA is developed.

The degradation of selected organic materials by hydrolytic and radiolytic processes is discussed in Chapter 2. The principal organic materials present in LILW-LL waste are introduced and the main characteristics of the organic polymers studied in CORI explained. Under disposal conditions, radiation and the presence of water are the main factors relevant for polymer ageing. The degradation of polymers through radiolysis is discussed and the factors affecting the radiolytic yields for gas production explained. Radiolysis leads also to the production of non-gaseous degradation products. Some of the oxidised species generated can be dissolved in water and released when polymer waste comes into contact with water. The main steps characterizing the degradation of polymers due to the dual effect of radiolysis and hydrolysis are described by the polymer reaching equilibrium, the solubility of water-soluble species, and the hydrolysis of the polymer. The release of water-soluble degradation products depends on several controlling factors, and the organic species released by each polymer are likewise rather specific. The different materials under investigation in CORI are discussed with both mechanistic understanding and quantitative information on degradation processes being provided. Chapter 2 has been updated to include new results derived in CORI.

The current understanding on the behaviour of organic molecules in cement-based material is summarized in Chapter 3 focusing on the binary systems featuring organics and cement materials. The provided overview on organic molecules addresses their properties in solutions related to cementitious environments, their sorption behaviour and their diffusion behaviour. An overview of the different organic molecules potentially relevant in this context is given according to present ThermoChimie database selections. Interaction processes of organic molecules with cement materials are explained, with examples from literature mainly taken from the ISA system. Information on organics diffusion in cement materials is provided. The need of providing new data and understanding on organics retention in cement systems is emphasized, in view of the scarcity of present data, the large range of systems in terms of cement degradation states and cement formulations, as well as the complexity of organics speciation in high pH environments. Recent advances by CORI are indicated.

Adding further complexity and focusing on ternary systems containing radionuclides, organics and cement materials, the SOTA Chapter 4 provides an overview on the current knowledge regarding radionuclide and organic ligands interactions in cementitious environments. The main processes controlling RN migration are solubility, retention processes and physical transport. Radionuclide chemistry in cementitious environments needs to take into account the specific characteristics of speciation and solubility under alkaline conditions. This is especially relevant when considering the presence of organics materials. The radionuclide uptake in cementitious materials is summarized and references made to main publications in this field. By introducing organic ligands, the radionuclide retention on cement materials can be significantly influenced, as is explained by several examples from recent literature. A mechanistic approach to the understanding and description of retention processes in complex materials like cement needs the application of a bottom-up approach, focusing on the behaviour of the main sorbing minerals (e.g. C-S-H phases). This approach requires focused experiments to understand the extent of the effects of organics on RN retention, but also a thermodynamic description of the aqueous and solid species formed. After introducing main theoretical concepts and equations, the radionuclide diffusion in cementitious materials under the presence of organics is discussed. Main results from CORI are described and an overview of systems studied provided.

To provide fundamental information on the topic which may not be available with the average reader, the final Chapter 5 of the SOTA provides an introduction to fundamental cement chemistry. Different types of cement are available, and the chemical properties of the cement-based materials and their mineralogy depend on the chemical composition of the cement. The compositions of the main types of cement are introduced and shown in a ternary diagram for $\text{CaO-SiO}_2\text{-Al}_2\text{O}_3$. Once cement is hydrated with water, solid phases including water molecules are formed, called cement hydrates. The Calcium Silicate Hydrate (C-S-H) system is discussed in more detail, based on examples from literature. Separate sub-chapters address topics related to the composition of pore solutions and the specific case of superplasticisers. The degradation of cement-based materials is explained, considering the corresponding pH decrease as a function of time and the definition of the degradation stages. The cement-based materials form a complex chemical system, which is not in equilibrium in most of the cases, especially in the context of a deep geological radioactive waste repository. The cementitious matrix is composed of several minerals, which play a role for the chemical evolution and the related radionuclide sorption processes. A new sub-chapter has been included to highlight the studies in CORI related to the surface charge of solid phases in relation to the chemical environment including selected organics. There is generally a good knowledge regarding the cement chemistry and a wide literature dedicated to the various cement types, which allows to characterize their chemical evolution with time and their contribution in terms of sorption.

Each sub-chapter is supported by the list of relevant key literature cited. The SOTA includes more than 150 references in total, thus providing direct references to more detailed information on the cement-organic-radionuclide interactions studied in CORI.

CORI had prepared an initial State-of-Art report within EURAD on cement-organic-radionuclide interactions as Deliverable D3.1. The present document is the update of the initial SOTA in view of the results generated in CORI and prepared as Deliverable D3.2. Feeding into D3.2 are Technical Reports developed on CORI at Task level (especially D.3,6,7,8), integrating the new findings generated in CORI and focussing on specific topics. All Task leaders in CORI contributed to the writing of the SOTA documents. The leading authors of the individual technical chapters are indicated.

The Deliverable is written as a consistent document covering the main aspects addressed in CORI. However, the sub-chapters were also prepared in a way so that they can be read as stand-alone documents on the respective sub-topics. Each section features an extended list of further literature.

Table of content

Executive Summary.....	4
Table of content.....	6
List of Figures.....	8
List of Tables.....	10
Glossary.....	11
1. Definition of scope and content of EURAD-CORI.....	13
2. Organic degradation by hydrolytic and radiolytic processes.....	15
2.1 Organic waste.....	15
2.2 Organic materials selected in EURAD-CORI.....	17
2.2.1 Cellulose.....	18
2.2.2 Polyvinyl chloride (PVC).....	18
2.2.3 Ion Exchange Resins (IER).....	19
2.2.4 Superplasticizers.....	20
2.3 Ageing of polymers.....	21
2.3.1 Degradation of polymers through radiolysis.....	21
2.3.2 Production of gas through radiolysis.....	21
2.3.3 Variability of radiolytic yields for gas production.....	22
2.3.4 Summary of radiolytic yield values.....	25
2.3.5 Gas production calculation method.....	27
2.4 Degradation of polymers - dual effect of radiolysis + hydrolysis.....	28
2.4.1 The polymer reaching equilibrium.....	28
2.4.2 Solubility of water-soluble species.....	29
2.4.3 Hydrolysis of the polymer.....	29
2.5 Identification and release of water-soluble molecules.....	30
2.5.1 Variability of the release of water-soluble degradation products.....	30
2.5.2 Organic species released by each polymer.....	34
2.6 Degradation of ion-exchange resins (IER).....	37
2.6.1 Radiolytic degradation of “dry” polystyrene backbone IERs.....	37
2.6.2 Radiolytic degradation of polystyrene backbone IERs in the presence of water.....	38
2.6.3 Leaching of ion-exchange resins.....	40
2.6.4 Degradation of polystyrene backbone IERs under the effect of temperature.....	41
2.7 References for Chapter 2.....	42
3. Organic-cement interactions.....	45
3.1 Properties in solution.....	45
3.2 Sorption on cement-based materials.....	48
3.3 Diffusion in cement-based materials.....	51

3.4 CORI Results: Update on organic sorption and adsorption	52
3.4.1 Sorption results from CORI	52
3.4.1 Diffusion results	53
3.5 Conclusion	53
3.6 References for Chapter 3	54
4. Radionuclide-organic-cement interactions	57
4.1 Introduction to WP CORI Task 4 objectives	57
4.2 Radionuclide chemistry in cementitious environments	59
4.2.1 Speciation/solubility under alkaline conditions	59
4.2.2 Speciation/solubility in the presence of organic ligands	59
4.2.3 Speciation/solubility calculations	63
4.3 Radionuclide uptake in cementitious materials	64
4.3.1 Uptake of RN onto cementitious materials	64
4.3.2 Uptake of RN in the presence of organic ligands	65
4.4 Radionuclide diffusion in cementitious materials	67
4.5 CORI results: RN migration in cement-organic systems	69
4.5.1 Results obtained in CORI for U(VI)	70
4.5.2 Results obtained in CORI for Th(IV)/Pu(IV)	72
4.5.3 Results obtained in CORI for Eu(III)/ Cm(III)/ Pu(III)	73
4.5.4 Results obtained in CORI for Pb(II)/Ni(II)	74
4.6 References Chapter 4	76
5. Fundamental cement chemistry	83
5.1 Anhydrous cement	83
5.2 Cement hydrates	84
5.3 Pore solution	87
5.4 Superplasticizers	88
5.5 Chemical evolution	88
5.6 Effect of the sorption on chemical properties	90
5.7 CORI Results: effects of organics sorption on chemical properties	90
5.7.1 Organic molecules	91
5.7.2 Superplasticizers	92
5.8 Conclusion	94
5.9 References Chapter 5	95

List of Figures

The list of Figures is organised according to the different chapters of this SOTA. (For instance, abbreviation 2-1 indicates that it is the first Figure in the second Chapter of this document).

FIGURE 2-1: *Distribution of organic materials present in the French ILW waste in percentage by mass (information provided by Andra).*

FIGURE 2-2: *ONDRAF/NIRAS organic inventory (information provided by ONDRAF/NIRAS).*

FIGURE 2-3: *Mass distribution of L/ILW organics based on the waste package inventory from Nagra (Nagra 2023).*

FIGURE 2-4: *Formation of a polystyrene skeleton (De Dardel, 1998).*

FIGURE 2-5: *Formation of a polyacrylic skeleton (De Dardel, 1998).*

FIGURE 2-6: *Chemical structure of SPs (a) sulphonated naphthalene formaldehyde, (b) sulphonated melamine formaldehyde (c) ligninsulphonates and (d) polycarboxylate ether.*

FIGURE 2-7: *Variation of H₂ production yields as function of LET for polyethylene (PE), polypropylene (PP), poly(methyl methacrylate) (PMMA) and polystyrene (PS).*

FIGURE 2-8: *A: Sampled solutions from suspensions of (non-)irradiated tissues in ACW, with an absorbed dose during pre-irradiation increasing from left to right. B,C: Evolution of DOC (B) and ISA (C) concentrations as a function of time, in suspensions of (non-) irradiated cellulose in ACW. Pre-irradiation was performed under anoxic conditions at different absorbed doses (10 kGy to ~1.4 MGy) and at a dose rate of ~0.6 kGy/h. The error bars represent the measurement uncertainty for a 95% confidence interval [SCK CEN].*

FIGURE 2-9: *Leached organic-content in solution quantified by NPOC measurements after filtration through 0.1 µm syringe PTFE disk filters as a function of allowed contact time for UP2W degradation samples equilibrated in 0.1 M NaOH, pH = 12.5 NaOH solutions (up) and Ca(OH)₂-saturated solutions with or without Fe(0) [KIT].*

FIGURE 2-10: *Leached organic-content in solution quantified by NPOC measurements as a function of allowed contact time for UP2W degradation samples equilibrated in Ca(OH)₂-saturated solutions with or without Fe(0) at T = 22 ± 3 °C and 80°C [KIT].*

FIGURE 3-1: *Sorption isotherm of on Portland cement at pH=13.3. Empty circles stand for experimental data, the solid line represents the modelling considering a two-site Langmuir model and the dashed line a one-site Langmuir model. (Van Loon & Glaus, 1998).*

FIGURE 3-2: *Sorption isotherm of β-ISA on Portland cement at pH=13.3. Solid line indicates the modelling of the data obtained for α-ISA using a two-site Langmuir model (Van Loon & Glaus, 1998).*

FIGURE 3-3: *Sorption isotherm of α-ISA on C-S-H and C-A-S-H phases at pH=13.3 (Van Loon & Glaus, 1998).*

FIGURE 3-4: Evolution of (a) gluconate (GLU) and (b) ISA contents (mol/g) sorbed on fresh (stage I) and degraded (stage III) cement pastes (Pointeau et al., 2006).

FIGURE 3-5: Comparison of adsorption distribution coefficients (K_d) against pH in fresh and degraded cement pastes. Non-filled symbols are results from Garcia et al. (2020) ('this work' in the legend); black filled symbols by Pointeau et al. (2008); grey filled symbols by Bruno et al. (2018).

FIGURE 3-6: Uptake of low molecular weight organic compounds by HCP as a function of reaction time.

FIGURE 4-1: Experimentally measured $m(\text{Pu})_{\text{tot}}$ in equilibrium with $\text{PuO}_2(\text{ncr,hyd})$ at $I = 0.10 \text{ m NaCl}$ in Sn(II)-buffered systems with $\text{pH}_m = 8.0\text{--}12.9$ in the presence of $m(\text{ISA})_{\text{tot}} = 10^{-3} \text{ m}$ and in hydroquinone-buffered systems, at $\text{pH}_m > 11$ with $m(\text{ISA})_{\text{tot}} = 10^{-3} \text{ m}$.

FIGURE 4-2: Predominance diagrams of Eu(III) $10^{-6} \text{ mol}\cdot\text{kg}_w^{-1}$ vs. pH with increasing total adipic acid concentration, $I = 0.1 \text{ mol}\cdot\text{kg}_w^{-1}$ (NaClO_4) at $P(\text{CO}_2) = 10^{-12} \text{ atm}$. Diagram obtained using Phreeplot software (Kinniburgh and Cooper, 2011) (Fig. 10a taken from Fromentin and Reiller, 2018).

FIGURE 5-1: Ternary diagram $\text{CaO-SiO}_2\text{-Al}_2\text{O}_3$ showing the compositions of the main types of cement (from Damtoft et al., 1999).

FIGURE 5-2: Solubility of C-S-H: C/S as a function of calcium concentration in a solution in equilibrium with the C-S-H from Berner (1992) and Henocq (2005).

FIGURE 5-3: Solubility of C-S-H: calcium concentration as a function of C/S for different NaOH concentrations (from Henocq, 2005).

FIGURE 5-4: ^{29}Si NMR spectra of C-S-H samples with various C/S ratios (from Roosz, 2016).

FIGURE 5-5: Effect of the pozzolanic reaction: A) hydration of Ordinary Portland cement, and B) hydration of a cement/slag mix (from Surech & Nagaraju (2015)).

FIGURE 5-6: Schematic diagram illustrating the evolution of pH associated to the gradual degradation of cement-based materials defining four degradation stages (I to IV) (Ochs et al., 2016).

FIGURE 5-7: Effect of the Na^+ sorption on the chemistry of C-S-H: evolution of the calcium concentration of C-S-H (C/S=0.8) at equilibrium as a function of NaCl concentration with different liquid-to-solid ratios (L/S). Experiments and modelling (Henocq, 2017).

List of Tables

The list of Tables is organised according to the different chapters of this SOTA. (For instance, abbreviation 2-1 indicates that it is the first Table in the second Chapter of this document).

TABLE 2-1: *Principal organic materials present in LILW-LL waste.*

TABLE 2-2: *Bulk amount of organic materials in SKB inventory (information provided by SKB).*

TABLE 2-3: *Radiolytic gas yield values (including 95% confidence intervals) for gamma irradiation of cellulosic tissues determined by [SCK CEN]. The indicated uncertainties on the G values represent the 95% confidence interval and take into account the uncertainties on the pressure, gas concentration, weight of tissues and volumetric measurements.*

TABLE 2-4: *Maximum gas radiolytic yields for several polymers present in ILW waste packages (values were obtained by the CEA/Orano, unless otherwise specified).*

TABLE 2-5: *Formation yields of carbonate, formate and acetate ions after alpha (α) and gamma (γ) radiolysis of PCE superplasticizer in various solutions.*

TABLE 3-1: *List of the main organic ligands and their sources considered in ThermoChimie database (www.thermochimie-tdb.com).*

TABLE 3-2: *Structure of organic ligands currently considered in the ThermoChimie database.*

TABLE 3-3: *Availability of key thermodynamic data for various organic/species complexes; the considered species are radionuclides and/or major ions such as Ca and Mg. (ThermoChimie, version 10a, 2016).*

TABLE 3-4: *Calculated maximum concentrations of α -ISA and gluconate in the cement pore water for different stages of cement degradation (Van Loon et al., 1999).*

TABLE 5-1: *Pore solution composition from CEM-V/A HCP samples at 102 days of curing (Olmeda et al., 2017).*

Glossary

An	Actinide(s)
ACW	Artificial young cement water
C-A-S-H	Calcium aluminium silicate hydrate
C-S-H	Calcium silicate hydrate
CAST	Carbon-14 Source Term, EC project
CEM 1-5	Cement degradation stages
CORI	Cement Organic Radionuclide Interactions
DINP	Di-isononylphthalate
DVB	Divinylbenzene
EPDM	Ethylene propylene diene monomer terpolymer
EPR	Ethylene propylene rubber copolymer
EDTA	Ethylenediaminetetraacetic acid
PHREEQC	Geochemical modelling code (pH redox equilibria in C)
GLU	Gluconate
GTA	Glutaric acid
Gy	Gray
HPC	Hardened cement paste
HRWR	High range water reducers
HBA	3-Hydroxybutyric acid
HIBA	α -Hydroxyisobutyric acid
ILW	Intermediate level waste
S.I.	International system of units
IER	Ion exchange resins
ISA	Isosaccharinic acid
Ln	Lanthanide(s)
LET	Linear energy transfer, "stopping power"
LFER	Linear free-energy relationships
LS	Ligninsulphonates
LLW/VLLW	Low-level waste / Very low-level waste
LILW-LL	Long lived low and intermediate level waste
NPOC	Non-purgable organic carbon-content
OPC	Ordinary Portland cement
PAN	Polyacrylonitrile
PC	Polycarbonate
PCE	Polycarboxylate ether
PE	Polyethylene
PI	Polyimide
PMMA	Polymethyl methacrylate
PP	Polypropylene
PTFE	Polytetrafluoroethylene
PUR	Polyurethane
PVC	Polyvinyl chloride
PVDF	Polyvinylidene fluoride
RCM	Reference cement material, HCP based on CEM II
RDP	Real degradation products

RWMD	Radioactive waste management and disposal
G	Radiolytic yield
RN	Radionuclide(s)
Eh	Redox potential
RD&D	Research development and demonstration
SCM	Supplementary cement materials
SOTA	State of art report
SP	Superplasticiser(s)
SMF	Sulphonated melamine formaldehyde
SNF	Sulphonated naphthalene formaldehyde
NEA-TDB	Thermochemical database project of the OECD-NEA
TDB	Thermodynamic database
TOC	Total organic carbon
TBP	Tributyl phosphate
WMO	Waste management organisation

1. Definition of scope and content of EURAD-CORI

The Workpackage CORI in EURAD has improved the knowledge on the organic release issues which can accelerate the radionuclide migration in the context of the post closure phase of geological repositories for ILW and LLW/VLLW, including surface/shallow disposal. CORI has addressed topics in the context of cement-organic-radionuclide interactions. Organic materials are present in some nuclear waste and as admixtures in cement-based materials and can potentially influence the performance of a geological disposal system, especially in the context of low and intermediate level waste disposal. This potential effect of organic molecules is caused by the formation of complexes in solution with radionuclides of interest (actinides and lanthanides, but also other metal cations like Ni) which can (i) increase the radionuclide solubility and (ii) decrease the radionuclide sorption. Organic substances require increased attention since a significant quantity exists in the waste and in the cementitious materials, with a large degree of chemical diversity. Cement-based materials will be degraded with time in the context of waste disposal inducing a large range of alkaline pH conditions according to their degradation stage. Alkaline pH provides specific conditions under which the organics can degrade, which contributes to increasing their impact on repository performance. The most critical open topics and data needs required to better assess and quantify cement-organics-radionuclides interactions were reflected in the three RD&D oriented CORI Tasks.

CORI Task 2 - Organics Degradation. Focus was put on the characterization of soluble organic species generated by radiolytic and hydrolytic degradation of selected organics (PVC, cellulose, resins, superplasticizers). Studies also included the analysis of degradation/stability of small organic molecules such as carboxylic acids. Determination of degradation rates of polymeric materials and small molecular weights molecules were also performed.

CORI Task 3 - Organic-Cement Interactions. Studies focused on investigating the mobility of selected organic molecules in cement-based materials. Understanding the mobility of organic molecules requires knowledge on retention and transport properties. Organics also include small ^{14}C bearing molecules as identified in the previous EC funded project CAST. Both retention on individual cement minerals and actual cementitious systems were investigated. Analysing the fate of the organics in cementitious environments is a key requirement to understand and model the radionuclide behaviour in single and complex systems.

CORI Task 4 - Radionuclide-Organic-Cement Interactions. Processes of radionuclide migration were studied in the ternary system. The role of organic molecules on the transfer properties of radionuclides were investigated through retention and transport experiments, covering a range of experimental conditions (relative amounts of radionuclide–cement–organics solutions). Selected radionuclides cover a range of chemical characteristics and redox states relevant for the expected conditions in L/ILW disposal.

Predicting and assessing radionuclide transport is a key topic in nuclear waste disposal. For radionuclide behaviour in cementitious environments where large inventories of organic materials may be present, CORI has significantly improved the previous knowledge. The improved quantification of radionuclide solubility and retention phenomena in cementitious environments provides important input into predicting radionuclide transport. In view of this general motivation in CORI, specific benefits in terms of impacting implementation or safety are described below.

Regarding RWMD implementation needs:

Issues of interest at the repository scale are:

- Improved scientific basis for the Safety Case for L/ILW waste repositories featuring relevant organics content.
- Co-storage of waste: support decisions regarding the question whether a mix of various wastes (organics, soluble salts, exothermic waste) can be foreseen.
- Optimization of vault design: limitations of interactions between the vaults regarding their content. CORI will provide information on the organic plume by characterizing the transfer behavior in cement-based materials.
- Optimization of concrete formulations as regards the potential effect of superplasticizers on radionuclide transfer properties.

Regarding safety:

- Characterizing the effect of the organic plume on the behavior of radionuclides in terms of:
 - solubility (limitation of solubility increase),
 - sorption (limitation of retention decrease) in terms of K_d values.
 - retention of potentially ^{14}C -bearing organic molecules (determined in CAST project) in cementitious environments in the case of specific waste.
- This project has:
 - reduced the uncertainties on the current knowledge (mainly K_d values),
 - improved the knowledge on the known organic molecules present in degradation solutions (not considered so far) with their complexing properties: better definition of the organic inventory regarding the waste and the concrete vault (geological and surface repositories).

CORI had established a focused Workplan based on the three identified RD&D Tasks given above. To perform cutting-edge research and make best use of available resources, it was essential to focus and not to investigate a too broad set of topics. It was therefore decided from the start that CORI will NOT study several other related topics like microbial degradation of organics, bitumised waste, iron corrosion in cementitious environments, work related to the conditioning of waste in cement materials or studies on natural organics present in certain host-rocks. Studies primarily targeting to derive new thermodynamic data for databases were not included, although it is acknowledged that complete and reliable thermodynamic data and databases are essential. The limited modelling performed within CORI is necessary to analyse and systematize the new experimental data and findings from CORI in the RD&D Tasks. CORI does not perform any PA related modelling studies. These limitations regarding the scope of CORI is also reflected in the initial and updated SOTA document prepared, which focus on the main topics addressed in CORI and thus cannot at all be considered a comprehensive exhaustive survey of all relevant topics.

This Deliverable report D3.2 updates the initial D3.1 SOTA report prepared by CORI within EURAD on cement-organic-radionuclide interactions. As the main text body of the initial SOTA D3.1 remains identical, new sections were added in order to highlight the improvements in data, process understanding and knowledge derived in CORI. Further information on the technical results in the three R&D Tasks in CORI is available from the combined Deliverable D3.6,7,8, in which detailed information is given on research at Task level. An integrated view on CORI including the potential application to the Safety Case is likewise available as public Deliverable D3.5.

2. Organic degradation by hydrolytic and radiolytic processes

Authors: Denise Ricard [Andra]

2.1 Organic waste

Organic materials are present in various forms in low or intermediate level wastes: as paper, gloves, over-clothing, flasks, filters, seals, cables, ion exchange resins, etc.. Organic materials can also be part of the cement matrix, like in the form of superplasticizers. The radioactivity of organic waste is due mostly to the presence of contamination on the surface of the waste by fission products, activation products and/or actinides. Principal polymers present in long-lived low and intermediate level waste (LILW-LL) are summarized in TABLE 2-1.

TABLE 2-1: Principal organic materials present in LILW-LL waste.

<p>Chloropolymers</p> <p>Polyvinyl chloride (PVC)</p> <p>Polychloroprene (Neoprene®)</p> <p>Chlorosulfonated polyethylene (Hypalon®)</p> <p>Fluoropolymers</p> <p>Polytetrafluoroethylene (PTFE, Teflon®)</p> <p>Polyvinylidene fluoride (PVDF)</p> <p>Vinylidene fluoride-hexafluoropropylene copolymer (Viton®)</p> <p>Polyacrylate</p> <p>Polymethyl methacrylate (PMMA)</p> <p>Polyacrylonitrile (PAN)</p> <p>Ion exchange resins (IER)</p> <p>Styrene-divinylbenzene copolymer</p> <p>Polyacrylonitrile based resins</p>	<p>Polyolefins and associated copolymers</p> <p>Polyethylene (PE)</p> <p>Polypropylene (PP)</p> <p>Ethylene propylene rubber (EPR) copolymer</p> <p>Ethylene propylene diene monomer (EPDM) terpolymer</p> <p>Miscellaneous</p> <p>Polycarbonate (PC)</p> <p>Polyurethane (PUR)</p> <p>Polyamides (Nylon®)</p> <p>Polyimide (PI)</p> <p>Cellulose</p> <p>Epoxy resin</p> <p>Silicone</p> <p>Polybutadiene</p> <p>Superplasticizers</p>
-----------------------------------------------------------------------------------------------------------------------------------------------------------------------------------------------------------------------------------------------------------------------------------------------------------------------------------------------------------------------------------------------------------------------------------------------------------------------------------------------------------------------------------------------------------	------------------------------------------------------------------------------------------------------------------------------------------------------------------------------------------------------------------------------------------------------------------------------------------------------------------------------------------------------------------------------------------------------------------------------------------------------

The percentages by mass of the various organic materials present in the French ILW waste are presented in FIGURE 2-1. The total mass of polymer ILW waste is listed as 1.600 tonnes (PIGD, 2014). FIGURE 2-2, FIGURE 2-3 and TABLE 2-2 show the organic waste inventories for ONDRAF/NIRAS, NAGRA and SKB, respectively.

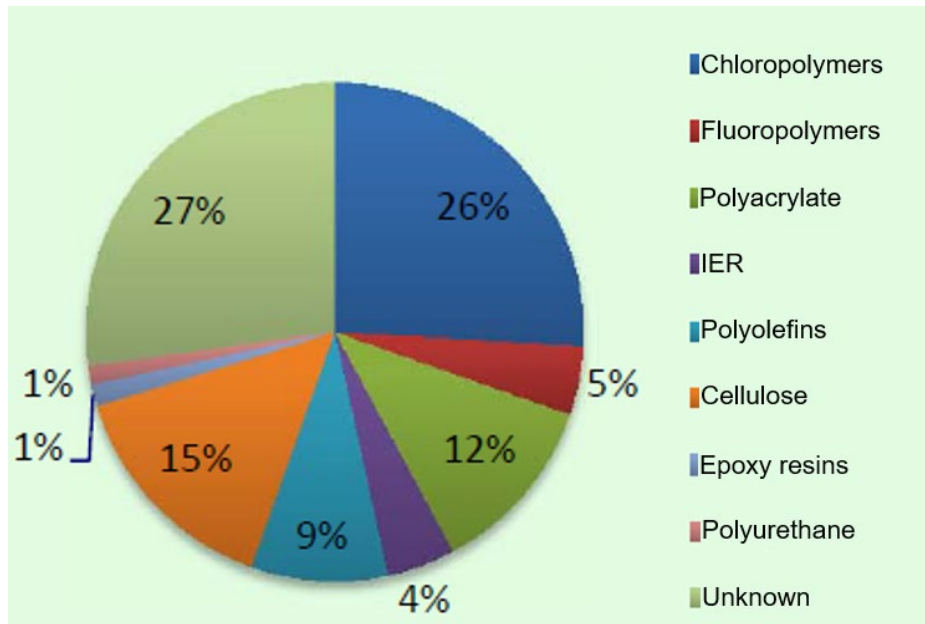


FIGURE 2-1: Distribution of organic materials present in the French ILW waste in percentage by mass (information provided by Andra).

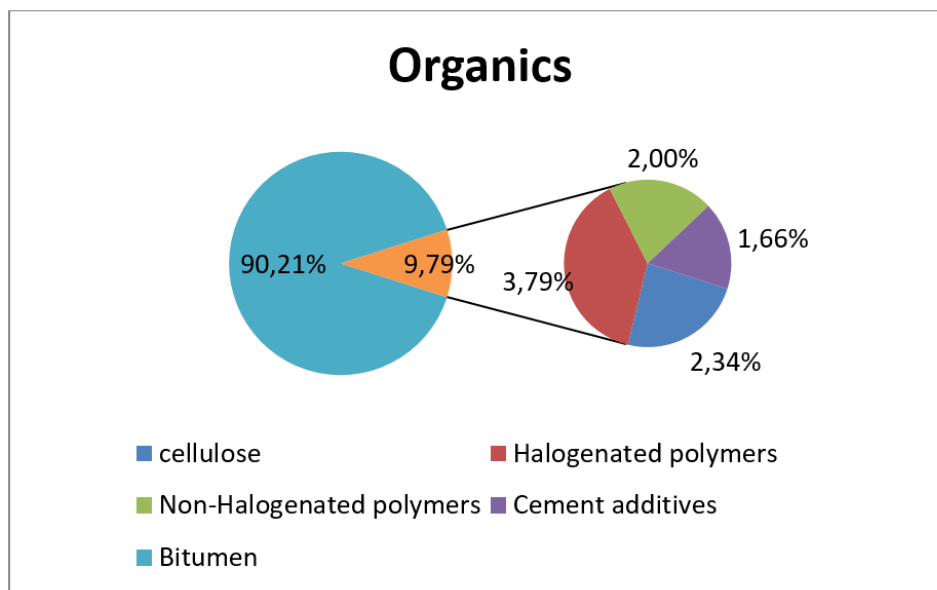


FIGURE 2-2: ONDRAF/NIRAS organic inventory (information provided by ONDRAF/NIRAS).

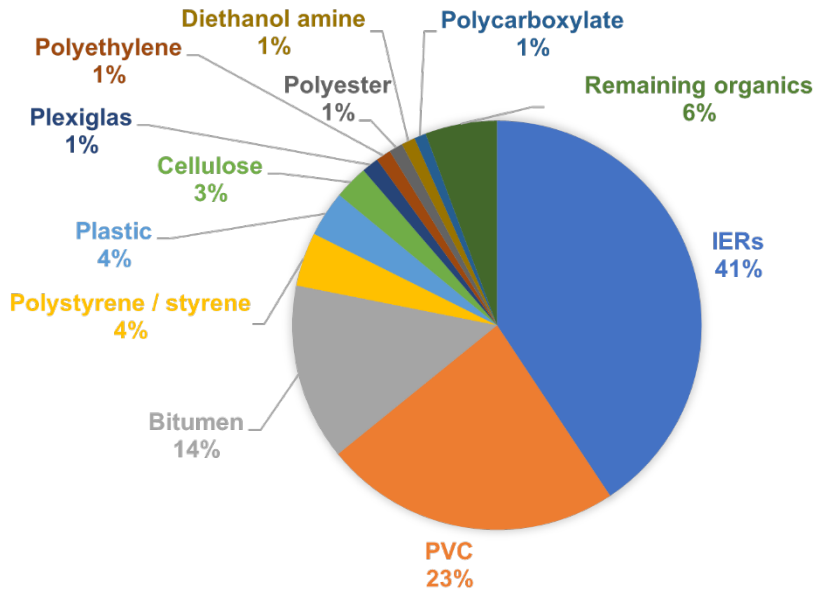


FIGURE 2-3: Mass distribution of L/ILW organics based on the waste package inventory from Nagra (Nagra 2023).

TABLE 2-2: Bulk amount of organic materials in SKB inventory (information provided by SKB).

Bulk material	In SFR [t]	Source	Interest
Ash	700	Pyrolysed legacy waste	
Cellulose	700	Various, e.g. concrete	Microbes, gas production. ISA
Ion-exchange resin	11 700	Treatment of active water	
Filter aids	1 300	With ion-exchanger	Degrades to complexing agents
Evaporator concentrate	400	Wash water	
Rubber and plastics	1 400	Various, e.g. packaging	
Sludge	300	Decont., filter aids, etc.	
Sand and soil	6 200	Mostly inorganic	
"Other organic"	1 200	Catch-all. Previously included some above materials	Microbes, gas production
Bitumen	2 900	Solidification of fluid waste	Assumed low porosity & diffusivity. Inert (?)

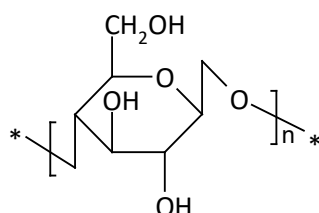
2.2 Organic materials selected in EURAD-CORI

The following organic materials were selected to be studied in Task 2 of EURAD-CORI: polyvinyl chloride (PVC), cellulose, ion exchange resins (IER) and superplasticizers. These organics represent the most abundant/important materials in the WMO's inventories.

Polymers used in the nuclear sector are industrial materials used in equipment such as electric cable sheathing, seals, and the gloves, sleeves or panes of glove boxes. The characteristics of commercial materials based on cellulose, PVC, IER and superplasticizers frequently used in the nuclear sector are discussed in the following.

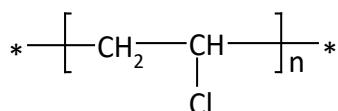
2.2.1 Cellulose

Cellulose is a polymer made up of D-glucose groups with the chemical formula presented below. This material is historically used in the nuclear industry as tissue for smear-testing potentially radioactive particles. However, in some countries, like Belgium and Sweden, other materials have replaced the cellulose in order to decrease their amounts in disposal. Cellulose can also be found in paper textile, filters, wood and cardboard materials.



2.2.2 Polyvinyl chloride (PVC)

Polyvinyl chloride (PVC) is a chloropolymer with the chemical formula presented below.



This material is primarily present in the waste as bags or glove box sleeves, but also as thicker material such as used in filter casings. For ventilation filter seals, an example of the composition is:

- 27 % of pure PVC (50/50 mixture by mass of Solvin® 266 SF and Solvin® 372 LD);
- 14 % CaCO₃;
- 2 to 3 % Ca(OH)₂;
- 30 % plasticisers (di-n-butyl phthalate, diisononyl phthalate, 2-ethylhexyl diphenyl phosphate);
- 24 % inorganic fire retardants (Al(OH)₃ and Sb₂O₃).

For bags or glove box sleeves, an example of the composition is:

- 63 % resin (PVC K70 and PVC K75);
- 31 % plasticisers (di-isononyl phthalate (DINP));
- 1.4% heat stabilisers (organic derivatives of Ca/Zn metals);
- 2.25% of additives (stearic acid, calcium stearate, talc powder).

2.2.3 Ion Exchange Resins (IER)

Ion exchange resins (IER) are solids that have the capacity to exchange the ions they contain with other ions from a solution, often with specific selectivity. IERs are primarily used by the nuclear industry for treating and decontaminating the water used in spent fuel unloading and storage pools. IERs are made up of:

- an organic polymer skeleton (with a three-dimensional network);
- functional groups fixed to the polymer skeleton that provide the ion exchange function within the material (cationic or anionic).

There are several types of polymer skeletons, including for example:

- polystyrene skeleton: this is obtained by polymerisation of styrene followed by cross-linking using divinylbenzene (DVB), see *FIGURE 2-4*.

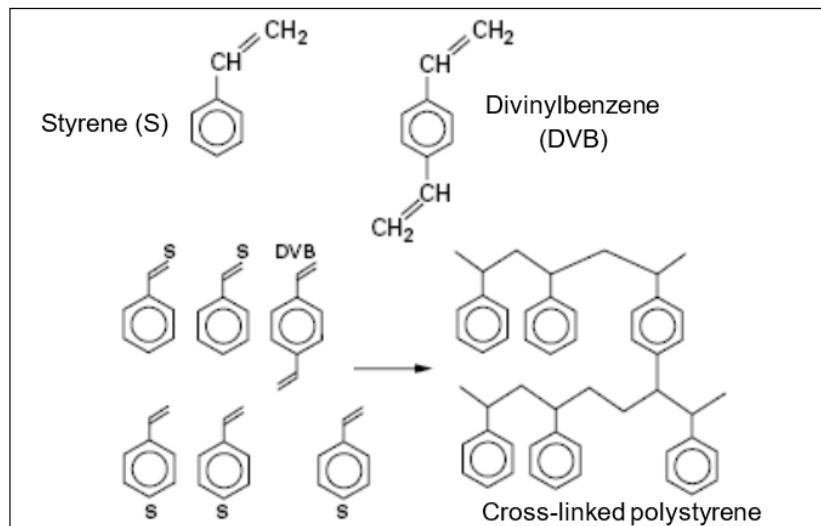


FIGURE 2-4: Formation of a polystyrene skeleton (De Dardel, 1998).

- polyacrylic skeleton: obtained by polymerisation of a methacrylate and cross-linking with divinylbenzene (see *FIGURE 2-5*).

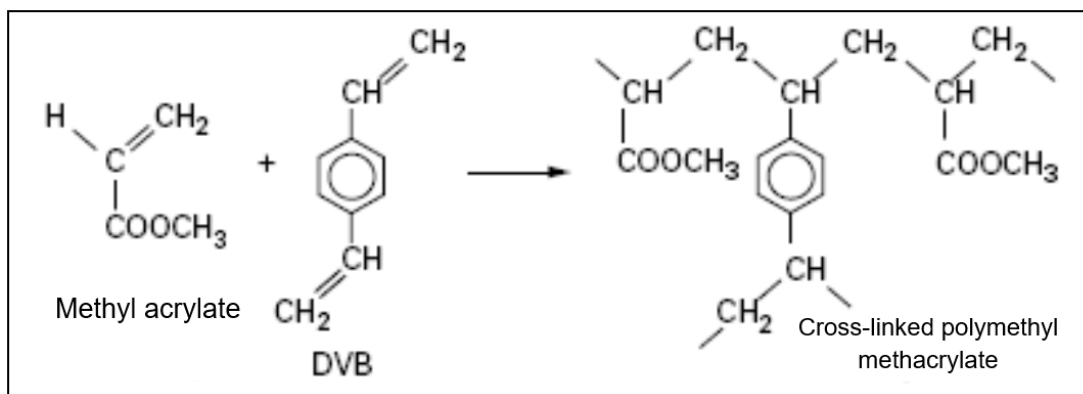


FIGURE 2-5: Formation of a polyacrylic skeleton (De Dardel, 1998).

2.2.4 Superplasticizers

Superplasticisers (SPs) belong to a group of cement additives known as High Range Water Reducers (HRWR). These water-miscible organic polymers have properties to prevent premature particle aggregation in cement mixtures. The addition of SP to these mixtures allows for a reduction of the water to cement ratio, increasing the early strength of the concrete whilst improving the flow characteristics (rheology) of the mixture (Nagra, 2023; NDA, 2019).

Several types of SPs are used in conditioning cement. The first generation of SP was made from polymerised sulphonated naphthalene formaldehyde (SNF), sulphonated melamine formaldehyde (SMF) and modified ligninsulphonates (LS). The modern generation SPs are represented by polycarboxylate ether (PCE). The general chemical structures of SP are shown in the FIGURE 2-6.

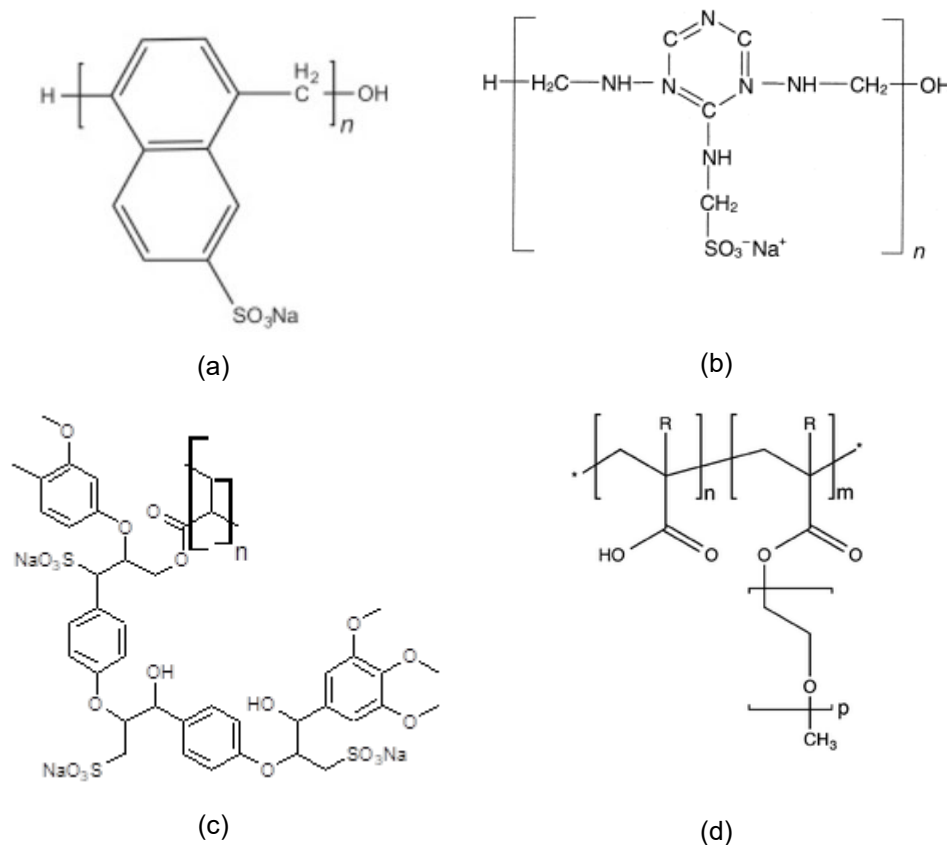


FIGURE 2-6: Chemical structure of SPs (a) sulphonated naphthalene formaldehyde, (b) sulphonated melamine formaldehyde (c) ligninsulphonates and (d) polycarboxylate ether.

2.3 Ageing of polymers

Under disposal conditions, radiation and the presence of water are the main factors of polymer ageing. These two processes of ageing or degradation are described below.

2.3.1 Degradation of polymers through radiolysis

In polymers, molecular changes induced by irradiation can be of various kinds (O'Donnell, 1989), including:

- chain cross-links and splits;
- release of volatile compounds (hydrogen H₂, carbon oxides CO and CO₂, molecules with low molecular mass (e.g. methane CH₄, etc.);
- formation of unsaturated species (“double bonds”);
- formation of non-gaseous degradation products (*i.e.* molecules with a low molecular mass (alcohols, carboxylic acids, etc.).

2.3.2 Production of gas through radiolysis

Production of gas through the radiolysis of organic material is a process that occurs already from the manufacturing of the packages. It diminishes over time due to the decreasing radioactive decay and hence activity of the waste, and the changes in the materials under radiation.

The main gases produced by radiolysis are hydrogen (H₂), carbon dioxide (CO₂), carbon monoxide (CO), and methane (CH₄). If the polymer is chlorinated or fluorinated, hydrogen chloride (HCl) or hydrogen fluoride (HF) can also form.

Hydrogen is produced by most of the polymers to be considered in disposal, while CO and CO₂ are mainly formed under oxidising conditions. If C-O or O-O-O bonds are present within the structure of polymers, production of CO and CO₂ may also occur under anaerobic conditions (for example cellulose or polyurethane). As specified above, hydrogen chloride is produced from chlorinated organic materials. These are the most abundant polymers in the waste considered for deep geological disposal. In some packages, the presence of fluorinated polymers can lead to the formation of hydrogen fluoride. It is essential to quantify gaseous hydrogen production because it is a flammable gas that may even cause explosions in the presence of air (O₂). Hydrogen chloride and hydrogen fluoride need to be specifically quantified due to their corrosive action on steels. These corrosive gases can thus have consequences on the stability of primary packages, especially during storage and disposal phases.

The production of gases from a waste package containing organic polymers is calculated by considering:

- the nature and activity of the radionuclides associated with the organic waste, and
- the gas production radiolytic yield values for each organic material present in the package.

Radiolytic yield is defined as the concentration of the radiolytic species formed in relation to the quantity of energy deposited by ionising radiation. The radiolytic yield is denoted G and expressed, in S.I. units, in mol·J⁻¹. For polymer irradiation, G can represent the yield for the creation of a new group in the

polymer chain, the yield for the release generation of a gas or small molecule, or the yield for destruction of a group initially present in the irradiated compound.

In the following paragraphs, the discussion will focus mainly on the radiolytic gas generation.

2.3.3 Variability of radiolytic yields for gas production

Various parameters can affect the radiolytic yield values for gas production, such as:

- the effect of additives / the formula;
- the effect of LET¹ (Linear Energy Transfer);
- the effect of the dose²;
- the effect of the relative humidity;
- the effect of the temperature.

Detailed results on the effect of these parameters are given in document (EURAD-CORI, MS17).

Influence of the formulation

In industrial polymers, the presence of fillers and additives can influence gas production. Since there is generally a low quantity of stabilisers, their effect can only be seen at low radiation doses.

Industrial halogenated polymers contain additives like calcium fillers $\text{Ca}(\text{OH})_2$ or CaCO_3 which offer the advantage of capturing corrosive gases like HCl. For some industrial PVC, the HCl can be completely captured by additives while for others the HCl capture will only be partial.

Influence of LET

LET (linear energy transfer) represents the deposit of energy transferred by the particle encountering the environment per unit of length in the material considered. This parameter is characteristic of ionising radiation. The β particles and γ radiation on the one hand, and the α particles and the neutrons on the other differ by their energy deposit induced in the irradiated materials. The former induce low LET, while the latter lead to higher LETs (difference of a factor ~ 1000).

FIGURE 2-7 shows the variation in the H_2 formation yield with LET for several polymers: polyethylene, polypropylene, poly(methyl methacrylate) and polystyrene (Chang & Laverne, 2000). Increasing the LET from 0.2 eV/nm (associated to γ radiation) to 800 eV/nm leads to an increase of G_{H_2} . However, this increase also depends on the chemical composition of the polymers: a factor of about 2 is observed between lowest and higher G_{H_2} values for saturated polyolefins, (polyethylene or polypropylene type), about 10 for poly(methyl methacrylate) and around 30 for polystyrene.

¹ LET refers to the quantity of energy transferred by the particle to the material per unit of distance covered in the material.

² Dose refers to the energy deposited per target unit of mass. This is normally expressed in Gray (Gy), where $1 \text{ Gy} = 1 \text{ J}\cdot\text{kg}^{-1}$.

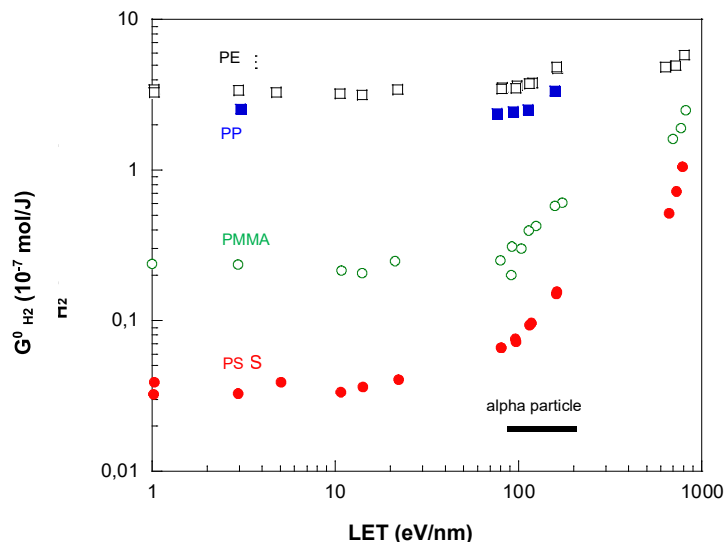


FIGURE 2-7: Variation of H₂ production yields as function of LET for polyethylene (PE), polypropylene (PP), poly(methyl methacrylate) (PMMA) and polystyrene (PS) (Chang & Laverne, 2000).

The observed different behaviour verified according to the polymer composition can be interpreted as follows:

- For saturated polyolefins, the yield is virtually independent of LET. H₂ is formed very quickly and is insensitive to the density of ionisation and excitation in the lobes. This is attributed to the reactivity of H^o radicals.
- For polymers containing unsaturated groups, G_{H₂} is practically constant for low LET values and then increases from a threshold LET value. However, these materials benefit from a protective effect associated with the presence of unsaturated groups. Increased LET leads to densification of energy deposition which seems to have the effect of reducing this protection.

In summary, the effects of LET are more important for unsaturated polymers and, in some conditions, for halogenated polymers. Oxidation also seems to depend significantly on the type of ionising particles.

Influence of the dose and dose rate

The main effect of the dose is to modify the chemical composition of the polymer. The structure of the material changes during irradiation, leading to variations in the way in which energy is deposited in the medium.

The instantaneous radiolytic yield for H₂ formation for polyethylene (PE) has been described by (Venture *et al.*, 2016) for doses up to 12 MGy. For these studies, PE was subjected to irradiation under inert conditions with 1 MeV electrons and ²⁰Ne high-energy ions. The results show that G_{H₂} drops with the dose, for both types of irradiation, and that these values tend to stabilise at high doses. High-dose G_{H₂} values are around 2 × 10⁻⁷ mol·J⁻¹ and 3 × 10⁻⁷ mol·J⁻¹ for electron and ²⁰Ne ion irradiations, respectively. These values correspond, respectively, to ≈ 50 % and ≈ 65 % of the G_{H₂} values of PE at the initial dose (G_{0,H₂}).

For pure PVC and industrial PVC, a decrease in the yield of H₂ and HCl with the dose was recorded (Colombani; 2007).

The instantaneous radiolytic yields of gas production for cellulose tissues were determined in Task 2 of WP CORI by [SCK CEN] under different absorbed dose (Bleyen et al., 2023). The results of G_{H₂}, G_{CO} and G_{CO₂} are shown in TABLE 2-3. The applied twofold difference in the dose rate during gamma irradiation did not result in a significant difference in the G values for gas production. Either there is no dose rate effect, or it would only be detectable at greater dose rate differences. Furthermore, the G_{CO} (though not statistically significant) and the G_{CO₂} values increase with absorbed dose during oxic irradiation. In anoxic conditions, the G_{H₂} and G_{CO} values decrease with absorbed dose, while the CO₂ production increases proportionally with the dose up to ~1.4 MGy.

TABLE 2-3: Radiolytic gas yield values (including 95% confidence intervals) for gamma irradiation of cellulosic tissues determined by [SCK CEN]. The indicated uncertainties on the G values represent the 95% confidence interval and take into account the uncertainties on the pressure, gas concentration, weight of tissues and volumetric measurements.

Absorbed dose (kGy)	Dose rate (kGy/h)	Irradiation atmosphere	G values (x 10 ⁻⁷ moles/J)		
			H ₂	CO ₂	CO
10 ± 2	0.63 ± 0.14	Ar	2.8 ± 0.7	1.3 ± 0.3	0.3 ± 0.1
47 ± 11	0.63 ± 0.14	Ar	2.5 ± 0.6	1.1 ± 0.3	0.3 ± 0.1
47 ± 11	0.63 ± 0.14	Air	2.3 ± 0.6	6.0 ± 1.4	1.4 ± 0.3
48 ± 7	0.34 ± 0.05	Ar	2.3 ± 0.4	1.1 ± 0.2	0.22 ± 0.04
48 ± 7	0.34 ± 0.05	Air	2.3 ± 0.4	6.4 ± 1.0	1.5 ± 0.2
180 ± 40	0.69 ± 0.16	Ar	2.0 ± 0.5	1.1 ± 0.2	0.23 ± 0.05
352 ± 56	0.67 ± 0.11	Ar	1.8 ± 0.3	1.0 ± 0.2	0.21 ± 0.03
760 ± 92	0.62 ± 0.08	Ar	1.6 ± 0.4	1.1 ± 0.4	0.24 ± 0.09
760 ± 92	0.62 ± 0.08	Air	1.4 ± 0.2	11.1 ± 3.2	1.9 ± 0.6
764 ± 91	0.31 ± 0.04	Ar	1.4 ± 0.2	0.7 ± 0.2	0.15 ± 0.05
764 ± 91	0.31 ± 0.04	Air	1.2 ± 0.2	10.6 ± 3.2	1.7 ± 0.5
1368 ± 160	0.55 ± 0.06	Ar	1.1 ± 0.2	1.1 ± 0.3	0.10 ± 0.03

In conclusion, it is evident that the dose influences the yields of gas formation. The instantaneous yields G_{H₂} and G_{HCl} decrease with the dose. For H₂, this decrease is mainly due to the formation of unsaturated defects, whereas for HCl the mechanism is via dehydrochlorination of the material. For the other gases and particularly for gases produced by the oxidation of materials (CO, CO₂), the yields can increase with the dose, being related to the accumulation of oxidation products.

The dose rate does not seem to have an effect on the gas production, or it would only be detectable at larger dose rate differences.

Influence of relative humidity

Few studies have been conducted regarding the effect of humidity on the degradation of polymers used in the nuclear industry under irradiation.

A recent study was carried out by CEA/ORANO on a formulated PVC at a high dose rate (3-4 kGy·h⁻¹), under aerobic conditions and integrated doses from 0.1 to 4 MGy. The difference of radiolytic yields of HCl_{trapped} for PVC irradiated under low relative humidity conditions (of around 10%) and high relative humidity (74%), is less than 10%. For H₂ production, G_{H₂}^{βγ} is equal to 0.95 molecules/100 eV for 10% of relative humidity and equal to 1.07 molecules/100 eV for 74% of relative humidity conditions (Andra).

In summary, the yields of HCl and H₂ formation from industrial PVC are influenced little by relative humidity.

For cellulose, A.R. Kazanjian (Kazanjian, 1976) compared the gas emission of a dry cellulose and a mixture containing 40% cellulose and 60% water by weight. The apparent yields measured are higher for dry cellulose. This result is expected since the yield of H₂ formation by the radiolysis of water is lower than the yield of cellulose. It seems that the effect of the presence of water is therefore limited.

Although the effect of relative humidity has not been studied extensively, the available data suggests that this factor does not play a significant role in the radiolysis of organic polymers.

Influence of temperature

The effect of temperature on the production of gas was studied on polyethylene by CEA/ORANO. Series of irradiations were carried out on a polyethylene under helium and under air at ambient temperature and at 120°C. An increase in H₂ production was observed at 120°C. This increase is much more marked in the presence of oxygen (radiolytic yield of H₂ is $17.1 \times 10^{-7} \text{ mol} \cdot \text{J}^{-1}$ under air, and $5.5 \times 10^{-7} \text{ mol} \cdot \text{J}^{-1}$ under helium) (Andra).

The effect of temperature on the production of gas from PVC under radiolytic conditions was studied for pure and industrial polymers. Boughattas (Boughattas, 2014) studied, for example, the effect of temperature on the radiolytic yields of HCl, H₂ and benzene formation, measured during irradiation campaigns on pure PVC and industrial PVC under helium and under air at different temperatures (80°C, 100°C, 120°C and 150°C). Results indicate that the temperature has a relatively small effect on the production of H₂ for pure or commercial PVC. On the other hand, the radiolytic yield G_{HCl} for pure PVC increases with temperature. The generation of HCl under air is systematically higher than that recorded under inert conditions.

2.3.4 Summary of radiolytic yield values

TABLE 2-4 summarises the values of maximum radiolytic yields obtained for the polymers considered in Task 2 of EURAD-CORI. The values available for the other organic materials present in ILW waste packages are available in the document (Eurad-CORI Milestone 17). Most of these values were obtained by the CEA/ORANO from γ irradiation and heavy ion irradiation at ambient temperature and under homogeneous oxidation conditions (Andra). Some of the values given apply to industrial polymers present in packages of waste (gloves, cables, filters, etc.). The rest apply to pure polymers with no fillers or additives. TABLE 2-4 specifies whether the values of radiolytic yields reported are taken from the literature rather than the work of the CEA.

For some polymers, the only available values of radiolytic yields refer to γ radiation. Estimates are therefore used to establish values of α radiolytic yields. Therefore, two approximations concerning the radiolytic yields of H₂ formation under α radiolysis can be made if data is unavailable. Either the radiolytic yield of formation of this gas is taken as equal to that from polyethylene, or it is taken as equal to 4.5 times that of the material in question under γ radiolysis. The first approximation is used when the material is aliphatic. The second approximation is used when the material contains unsaturated groups. Furthermore, for the other gases (CO, CO₂, CH₄, HCl, HF), it is always considered that G^α is equivalent to $G^\beta \gamma$.

The values of radiolytic yields of CO₂ and CO production are particularly high. The production of these gases depends on the oxidation rate of the polymer and is therefore highly dependent on the conditions

under which the material is exposed to oxidation and radiation. In the case of irradiation carried out at the CEA, sufficiently thin polymers were generally used so that oxidation occurred evenly across the entire thickness under irradiation. However, in ILW packages containing polymer organic materials, organic materials are thicker as the waste is compacted or packaged in bulk in the packages. Oxidation of the various organic materials will therefore not necessarily occur evenly within the materials. The maximum values of radiolytic yields of CO₂ and CO are thus very conservative. For some of the polymers, greater quantities of these two gases will be produced during the repository operating phase under oxidic conditions.

TABLE 2-4: Maximum gas radiolytic yields for several polymers present in ILW waste packages (values were obtained by the CEA/Orano, unless otherwise specified) (Andra).

Polymer	Radiolytic yield ($\times 10^{-7}$ mol·J ⁻¹)	Material/ Dose
Polyethylene (PE)	$G_{0, H_2}^{\beta\gamma} = 3.4$ $G_{CO_2}^{\beta\gamma} = 1.8$ $G_{0, CO}^{\beta\gamma} = 0.41$ $G_{0, CH_4}^{\beta\gamma} = 0.026$	Pure PE under air, G at zero dose
	$G_{0, H_2}^{\alpha} = 3.9$ $G_{0, CO_2}^{\alpha} = 3.6$ $G_{0, CO}^{\alpha} = 1.2$ $G_{0, CH_4}^{\alpha} = 0.162$	Pure EPDM under air, G at zero dose Pure EPDM under air, G at 8 MGy Pure PP under air, G at zero dose Pure PP under air, G at zero dose
Cellulose	$G_{0, H_2}^{\beta\gamma} = 2.8$ $G_{CO_2}^{\beta\gamma} = 6.0$ $G_{CO}^{\beta\gamma} = 1.9$ $G_{CH_4}^{\beta\gamma} = 0.02$	Cellulose tissues under air, G at 0,01 MGy [SCK CEN] Cellulose tissues under air, G at 0,047 MGy [SCK CEN] Cellulose tissues under air, G at 0,76 MGy [SCK CEN] Cellulose tissues under air, G at 0,76 MGy [SCK CEN]
	$G_{0, H_2}^{\alpha} = 2.5$ $G_{CO_2}^{\alpha} = 1.7$ $G_{CO}^{\alpha} = 0.84$ $G_{CH_4}^{\alpha} = 0.005$	$G_{0, H_2}^{\alpha} = G_{0, H_2}^{\beta\gamma}$ industrial cotton under air, G at zero dose Industrial Cotton under air, G at 3.9 MGy Industrial Cotton under air, G at 3.9 MGy Industrial Cotton under air, G at 7.1 MGy
Polyacrylonitrile	$G_{0, H_2}^{\beta\gamma} = 0.25$ $G_{0, HCN}^{\beta\gamma} = 0.04$	G at zero dose (Burlant & Taylor, 1955)
	$G_{0, H_2}^{\alpha} = 1.1$	$G_{0, H_2}^{\alpha} = 4.5 \times G_{0, H_2}^{\beta\gamma}$ (ratio observed for pure polystyrene at zero dose (Chang & Laverne, 2000))
IER	$G_{H_2}^{\beta\gamma} = 1.2$	IER anionic Amberlite® IRA 400 OH under air, G at 0,5 MGy

Polymer	Radiolytic yield ($\times 10^{-7} \text{ mol} \cdot \text{J}^{-1}$)	Material/ Dose
	$G_{\text{CO}_2}^{\beta\gamma} = 8.1$	IER (75% cationic, 25% anionic) Microionex® MB400 HOH under air, G at 0.5 MGy
	$G_{\text{H}_2}^{\alpha} = 3.9$	Polyethylene value (EPDM under air, G at zero dose)
Polyvinyl chloride (PVC)	$G_{0, \text{H}_2}^{\beta\gamma} = 0.31$ $G_{\text{CO}_2}^{\beta\gamma} = 4.2$ $G_{\text{CO}}^{\beta\gamma} = 1.0$ $G_{\text{CH}_4}^{\beta\gamma} = 0.071$ $G_{\text{HCl}}^{\beta\gamma} = 6.4$	Industrial PVC (Plastunion) under air, G at zero dose Industrial PVC (Plastunion) under air, G at 6 MGy Industrial PVC (Plastunion) under air, G at 10 MGy Industrial PVC (Plastunion) under air, G at 2 MGy Industrial PVC (Plastunion) under air, G at 10 MGy
	$G_{0, \text{H}_2}^{\alpha} = 0.62$ $G_{\text{CO}_2}^{\alpha} = 2.1$ $G_{\text{CO}}^{\alpha} = 1.2$ $G_{\text{CH}_4}^{\alpha} = 0.081$ $G_{\text{HCl}}^{\alpha} = 3.2$	Industrial PVC (Plastunion) under air, G at zero dose Industrial PVC (Plastunion) under air, G at 7.4 MGy Industrial PVC (Plastunion) under air, G at 7.4 MGy Industrial PVC (Plastunion) under air, G at 3.8 MGy
Superplasticizer (SP) - PCE	$G_{0, \text{H}_2}^{\beta\gamma} = 1.12$ $G_{0, \text{CO}_2}^{\beta\gamma} = 0.44$	“Homemade” PCE in pure water under air, G at zero dose [CNRS(Subatech)] “Homemade” PCE in pure water under air, G at zero dose [CNRS(Subatech)]
	$G_{0, \text{H}_2}^{\alpha} = 1.34$	“Homemade” PCE in pure water under air, G at zero dose [CNRS(Subatech)]

2.3.5 Gas production calculation method

The gas production rate at each instant “t” can be calculated using the following formula:

$$d_x = A_x \sum_i F^i \frac{1}{100} (e_{x,\alpha} \times G_i^{\alpha} + e_{x,\beta\gamma} \times G_i^{\beta,\gamma}) \quad (\text{eq. 2-1})$$

where:

- A_x : activity of a radionuclide X at the time t considered;
- d_x : gas production rate, in molecules per second, associated with radionuclide X;
- F^i : mass fraction of the “radiolysable” material i in the package. This mass fraction is given considering the mass of packaged waste and that of the packaging matrix (therefore excluding the container);
- $e_{x,\alpha}, e_{x,\beta\gamma}$: energy deposited by α or β/γ radiation in the package per 1 Bq by radionuclide X in eV/disintegration. The values of energy deposited for each radionuclide are taken from the literature;

- $G_i^\alpha, G_i^{\beta,\gamma}$: radiolytic yield of radiolysable material i under α or β/γ irradiation in molecules/100 eV. These values of yields are considered to be constant over time.

Following this method, all energy from disintegration is assumed to dissipate evenly in the waste and matrix mass. This assumption is conservative for γ rays, which have a longer path than the average dimensions of the waste. This means that the γ irradiation from adjacent packages in the waste cell is effectively taken into account. This assumption is also conservative with respect to the estimate of gas production associated with α radiation. It does not take into account self-absorption phenomena for α particle radiation or the fact that the energy deposited by α particles varies across the thickness of the material.

2.4 Degradation of polymers - dual effect of radiolysis + hydrolysis

When ionising radiation interacts with polymers, non-gaseous radiolytic degradation products are produced. Some of the products generated by the radio-oxidation of the material are low molar mass oxidised species, such as alcohols, ketones or esters. These oxidised species can be dissolved in water and released when polymer waste comes into contact with water. These organic compounds can alter the mobility of radionuclides and potentially increase their migration away from the disposal site, either because of an increase in their solubility or because of a change in their retention by the different engineered barriers.

The pH values and the chemical composition of water in contact with ILW packages containing organic materials are directly connected to the physical and chemical changes to the cement-based materials that make up the disposal packages and structures of ILW disposal cells. In most of the currently designed disposal facilities, the leaching solution is expected to be cementitious water with a pH between 10.5 and 13.5. The phenomena that occur when the radiation-degraded polymer and cementitious leaching solution come into contact are summarized as follows, and described in more detail in the subsequent sections:

- the polymer in solution reaches equilibrium with the aqueous phase (water diffusion inside the polymer and solubilisation of soluble species), mainly influenced by the pH of the solution;
- diffusion of the water-soluble species which formed during the polymer irradiation, the process depending on the contacting solution and nature of the compounds formed under radiation;
- hydrolysis of the oxidised polymer.

These phenomena can occur at different time scales depending on the diffusion phenomena, the nature of the irradiated polymer (little oxidised, cross-linked, etc.), and the reactivity of the species in water.

2.4.1 The polymer reaching equilibrium

Thermodynamic equilibrium of the polymer with the aqueous solution requires permeation of water into the polymer. This depends on the composition of the polymer. The more the polymer contains polar groups, the more quickly water will permeate. A polymer that is hydrophobic when non-irradiated can become highly hydrophilic after oxidation under irradiation, as the formation of oxidised groups such as ketones, alcohols, carboxylic acids will facilitate the permeation of water. In contrast, polymer cross-linking will make it more impermeable to water.

2.4.2 Solubility of water-soluble species

After the water/polymer system has reached equilibrium, the water-soluble degradation products dissolve. Solubility depends on the following factors:

- the aliphatic chain length;
- polarity;
- the geometry of molecules;
- pH;
- the presence of metal ions or salts.

As a general chemical rule, the longer the carbonated aliphatic chain length, the lower the solubility of the compound in water. Solubility also depends on the dipole moment of the molecule that arises from bond polarity and geometry of the molecule. A dipole exists when a molecule has areas of asymmetrical positive and negative charge. The polarity of a bond is associated to the electronegativity difference between two atoms of a bond. The atom with larger electronegativity will have more pull for the bonded electrons than the atom with smaller electronegativity; the greater the difference in electronegativity, the larger the dipole. In a diatomic molecule (X_2 or XY), there is only one bond, and the polarity of that bond determines the polarity of the molecule. When a molecule contains more than one bond, the geometry must be taken into account. If the bonds in a molecule are arranged so that their bond moments cancel (vector sum equals zero), the molecule is nonpolar.

The main chemical functions of organic compounds can therefore be classified according to their polarity. The following order is obtained, from the most polar function to the least polar function:

amide > carboxylic acid > alcohol > ketone ~ aldehyde > amine > ester > ether > alkane.

Since water is a polar solvent, amides, carboxylic acids and alcohols are the compounds that will be mostly solubilised in the aqueous phase. Furthermore, the more polar chemical functions there are, the more solubility is favoured. In addition, the geometry of the compound influences the solubility of the compound. A non-linear geometry favours the solubility of the compound because branching lowers intermolecular forces and decreases intermolecular attraction. Finally, the solubility of the compound depends on the ionic strength and pH of the aqueous solution. Carboxylic acids and alcohols can be in protonated or non-protonated form. Their concentration in a solution depends on its pH and their acidity constant.

The pH of the solution can also alter the solubility of compounds. The ionised (*i.e.* deprotonated) compound is easier to solubilise in water. The solubility of acids therefore increases with the pH. In the ILW repository, the water in contact with the packages will generally be cementitious water with a pH between 10.5 and 13.5. The solubilisation of acids under these conditions will be greater than in pure water. Finally, the presence of metal ions or alkalis generally increases the solubility of species by forming soluble complexes.

The diffusion of water-soluble compounds depends on temperature, as well as the steric bulk of the compound and of the solute concentration to solubilise. Therefore, the higher the temperature, the greater the diffusion coefficient. Similarly, the more the solute concentration decreases, the greater the diffusion coefficient.

2.4.3 Hydrolysis of the polymer

Independent of the previous steps, the polymer hydrolyses in contact with water. As it diffuses in the material, water reacts with the chemical functions of the polymer and can cause additional degradation. This hydrolysis mainly depends on the functional groups carried by the polymer and the pH of the aqueous solution. Furthermore, the more water-permeable the material, the greater the hydrolysis of the polymer.

The hydrolysis of degraded polymers is therefore far from negligible in cementitious water. For some materials such as polyester-based polymers, the contribution of basic hydrolysis to the degradation of the material is more significant than radiolysis.

2.5 Identification and release of water-soluble molecules

The chemical characteristics and quantities of water-soluble molecules released by organic materials in the repository depend on the nature of polymers present within the waste packages, as well as the conditions under which materials were exposed to ionising radiation and their accessibility to water from the geological medium.

2.5.1 Variability of the release of water-soluble degradation products

Several factors can influence the release of water-soluble degradation products such as:

- the irradiation conditions: dose and LET that can influence the oxidation rate of the material;
- the leaching solution: pH, presence of counter-ions, *etc.*;
- the formulation of the material: nature of the polymer, composition of the material (pure or industrial), presence of additives, presence of mineral fillers which can trap HCl, *etc.*

Detailed results on the effect of these parameters are given in document (EURAD-CORI Milestone 17).

Influence of irradiation conditions

The effect of the type of irradiation on the release of soluble species was evaluated by CEA/ORANO for various polyurethanes (PUR Estane, PUR Mapa, PUR Piercan, PUR Manche), for the PVC representative of glove box bags or sleeves (Plastunion PVC), Hypalon®, Neoprene® and PC (Lexan). These polymers were irradiated at 4 MGy and then leached for one month in pure water. The following carboxylic acids were investigated in the leaching solution: formic, glutaric, acetic, phthalic acids.

The highest concentrations of organic acids are obtained for polymers irradiated under γ rays, as the oxidation rate is greater under this type of radiation. Only polycarbonate produces more acids when it is irradiated with heavy ions than under γ radiation. This behaviour can be associated with the presence of aromatic groups that are sensitive to a stopping power effect (Andra).

Influence of LET (stopping power)

The effect of LET or stopping power on the nature and quantity of water-soluble degradation products released in a solution was evaluated by CEA/ORANO for the following polymers: EPDM, PP, PVC and PUR. Irradiation was carried out using ^{36}S and ^{22}Ne light ions of energy equal to approximately $11.5 \text{ MeV}\cdot\text{A}^{-1}$. The concentrations of carboxylic acids measured are of the same order of magnitude regardless of the LET studied, ranging between 15 and $4 \text{ MeV}\cdot\text{mg}^{-1}\cdot\text{cm}^{-2}$ (Andra).

Influence of dose

The effect of the dose was studied by CEA/ORANO for certain polymers (PUR, EPR, PVC) irradiated under γ rays at dose rate of $0.7 \text{ kGy}\cdot\text{h}^{-1}$ and at doses of 6 and 10 MGy. Irradiation was followed by

leaching in cementitious water (pH 13.2). The following carboxylic acids were investigated in the leaching solution: formic, oxalic, glutaric, acetic, adipic acids and phthalic acid for industrial PVC. The release of phthalic acid observed in the case of industrial PVC is associated with leaching of phthalate, present in this medium as a plasticiser.

The total quantity of organic carbon TOC, and thus the water-soluble degradation product concentration is similar for the two doses of radiation. From 6 MGy, the release of certain water-soluble degradation products tends to reach saturation (Andra).

It is currently impossible to establish an exhaustive list of all the compounds formed under irradiation of carbon chains and heterochains polymers containing oxygen. The majority of compounds identified are alcohols and carboxylic acids. The carboxylic acids are of various types and can be grouped into families:

- monoacids, which come from a single chain break: acetic acid and formic acid;
- diacids, which come from two chain breaks: glutaric acid and adipic acid;
- triacids, which can come from bridging between a diacid and monoacid: carballylic acid;
- α -hydroxy acids: lactic acid;
- keto acids: acetoacetic acid;
- hydroxy diacids: malic acid;
- monounsaturated acids: fumaric acid;
- aromatic acids: phthalic acid and benzoic acid.

The identification of soluble species in artificial young cement water (ACW) of pre-irradiated cellulose tissues was studied by [SCK CEN] in Task 2 of CORI. The TOC of solution and the carboxylic acid concentration were measured up to 2 years of alkaline degradation. As shown in the FIGURE 2-8, the DOC and isosaccharinic acid (ISA) concentrations increased with increasing absorbed dose.

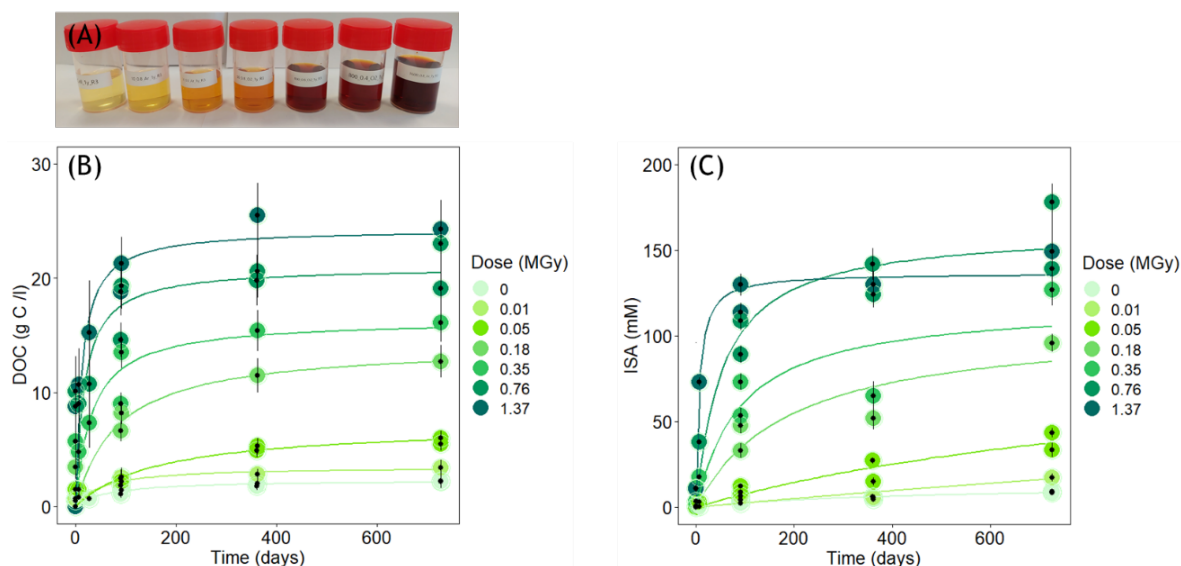


FIGURE 2-8: A: Sampled solutions from suspensions of (non-)irradiated tissues in ACW, with an absorbed dose during pre-irradiation increasing from left to right. B,C: Evolution of DOC (B) and ISA (C) concentrations as a function of time, in suspensions of (non-) irradiated cellulose in ACW. Pre-irradiation was performed under anoxic conditions at different absorbed doses (10 kGy to ~1.4 MGy) and at a dose rate of ~0.6 kGy/h. The error bars represent the measurement uncertainty for a 95% confidence interval [SCK CEN].

In conclusion: the water-soluble degradation products generated by the degradation of organic polymers under radiation are mainly carboxylic acids and alcohols. Among the carboxylic acids, several families of compounds have been identified (monoacids, diacids, keto acids, aromatic acids, *etc.*). At a high dose, the release of certain water-soluble degradation products tends to reach a saturation peak.

Influence of the leaching solution

The chemistry of the contacting leaching solution is an important factor influencing the release of water-soluble degradation products. In cementitious water, the main release phenomenon for water-soluble degradation products is basic hydrolysis. The release therefore depends on the phenomenon of basic hydrolysis, whose speed depends on the composition of the degraded polymer.

The polymer leaching protocol can also play a role in the release of water-soluble products. Two types of basic water leaching protocols have been studied by Fromentin (Fromentin, 2017) during polyurethane leaching: (i) leaching with pH adjustment and (i) leaching with solution renewal. The results obtained in the work indicated that losses of mass and TOC values are higher for leaching with solution renewal as the reaction is forced towards degradation.

The leaching of a filter aid based on polyacrylonitrile (PAN) in different alkaline solution was studied by [KIT] in the framework of CORI. The evolution of NPOC (non-purgable organic carbon content) values show that degradation kinetics at $T = 25^{\circ}\text{C}$ in $\text{Ca}(\text{OH})_2$ -buffered media are substantially slower compared to the Ca-free systems (NaOH) at $\text{pH} = 12.5$ (FIGURE 2-9). This highlights the key role of Ca in the degradation experiments. The degradation were also performed in presence or absence of Fe(0). The studies show no effect of the iron on the PAN degradation.

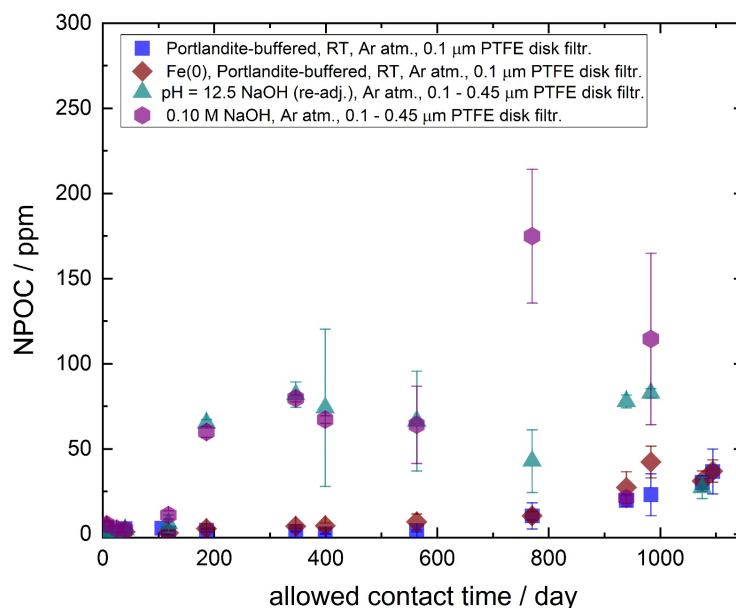


FIGURE 2-9: Leached organic-content in solution quantified by NPOC measurements after filtration through $0.1\ \mu\text{m}$ syringe PTFE disk filters as a function of allowed contact time for UP2W degradation samples equilibrated in $0.1\ \text{M NaOH}$, $\text{pH} = 12.5\ \text{NaOH}$ solutions (up) and $\text{Ca}(\text{OH})_2$ -saturated solutions with or without Fe(0) [KIT].

Degradation experiments with Aldrich cellulose under alkaline conditions in ACW at 90°C was carried out by [PSI] in Task 2 of WP CORI, in the absence and in the presence of portlandite and Fe(0) powder. The results showed that the presence of Fe(0) have no significant influence neither on the degradation rate nor on the type of degradation products formed.

In conclusion, the main leaching solution parameters affecting the release of water-soluble degradation products and the associated effects are as follows:

- basic pH influences the solubilisation of ionic carboxylate species and generates basic hydrolysis of the material, which produces additional degradation of the material by splitting the chains;
- presence of counter-ions that stabilises the ionic species;
- presence of cations like K^+ , Ca^{2+} , etc. that can form complexes with the water-soluble degradation products and whose stability will depend on the presence and concentration of metal ions (competition reactions). The results obtained in the framework of CORI have shown that Fe(0) has no influence on the degradation of PAN and cellulose materials;
- solution renewal that leads to greater material degradation.

Influence of the leaching temperature

The effect of the leaching solution temperature on the release of water-soluble products was studied by Fromentin (Fromentin, 2017) for the industrial polyurethane MAPA used in glove box gloves. During these studies, non-irradiated and irradiated polymers were subjected to basic leaching in an inert atmosphere at three temperatures (ambient temperature, 40°C and 60°C). The author observed that the higher the temperature, the greater the TOC and the faster the loss of mass, for both irradiated polymers and non-irradiated polymers. Differences in the leaching kinetics are also observed at ambient temperature compared to the leaching carried out at 40°C and 60°C. This difference appears less significant for irradiated polymers.

[KIT] carried out hydrolytic degradation experiments of PAN based filter aid (UP2W) in $Ca(OH)_2$ -buffered media at 25°C and 80°C. The content of NPOC values (FIGURE 2-10) after ~700 days of contact time showed an increase at room temperature. As for the system at $T = 80^\circ C$, detected NPOC values were in the range of the background level even after 1000 days of contact time, indicating that chain scission did not take place to a relevant extent at this temperature.

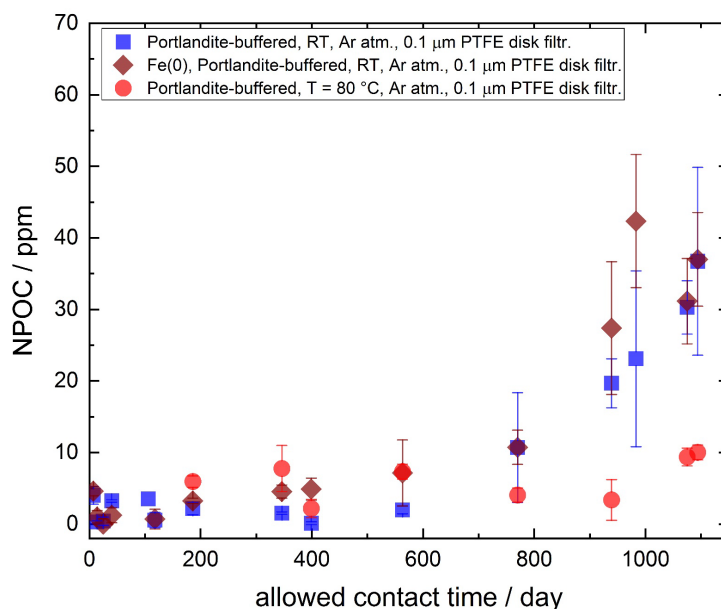


FIGURE 2-10: Leached organic-content in solution quantified by NPOC measurements as a function of allowed contact time for UP2W degradation samples equilibrated in $Ca(OH)_2$ -saturated solutions with or without Fe(0) at $T = 22 \pm 3^\circ C$ and $80^\circ C$. (data at $80^\circ C$ in red, all other data at $T = 22^\circ C$) [KIT].

Influence of the formulation

The type of polymer determines the oxidation rate of the material under irradiation and also its hydrolysis when it is degraded. The higher the polymer's oxidation rate, the higher the release of water-soluble degradation products. This can be explained by a high concentration of oxidised chemical functions such as ketones, esters, carboxylic acids, *etc.*. The more oxidised functions are present in the material, the more they make the material polar and thus allow for the solubilisation of increasingly long carbon chains.

In general, the behaviour of industrial polymers is similar to that of pure polymers, except for their degradation level, which is generally lower than for the pure polymers. The soluble fraction of industrial polymers depends on the polymer's oxidation rate, as for pure polymers. However, the soluble fractions are generally lower, because (i) they contain a percentage by mass of pure polymer ranging from 25% to 95% depending on the material, and (ii) due to the presence of additives, which delays oxidation of the material.

As example, we can cite the radiolytic experiments on industrial and pure PVC performed by [CNRS(ISTO)] in the framework of CORI. Industrial PVC and pure PVC were irradiated in NaOH pH 13 solutions. For industrial PVC, TOC release is lower than the TOC of pure plastics after 2.5 MGy of irradiation. This can be explained by the presence of additives that protect the polymer chain and slow down its degradation.

2.5.2 Organic species released by each polymer

Cellulose

Radiolytic and subsequent hydrolytic degradation (at pH ~13) of cellulosic tissues was investigated by [SCK CEN] under various conditions. After 2 years of alkaline degradation of irradiated cellulosic tissues, ISA, the main degradation product, made up to ~30 to 60% of the dissolved organic carbon. Comparisons can be made with the results of studies performed with cellulose materials only considering hydrolysis degradation process. For pure cellulose, according to (Glaus et Van Loon, 2008), the content of ISA was 80 to 90% of total TOC in alkaline degradation after 12 years. [PSI] determined the concentration of ISA after 21 and 28 years of alkaline degradation. For cellulose tissues, the amount of ISA was about 75% after 21 years and 64% after 28 years.

Other soluble species were also identified par [SCK CEN] as degradation products after alkaline degradation of pre-irradiated cellulose tissues:

- Lactic and formic acid, mostly making up 1 to 3% of the TOC concentration.
- Glycolic acid and acetic acid at lower concentrations and not in the suspensions with non-irradiated samples.
- The concentrations of valeric, butyric and malonic acid were below the detection limit, while the concentrations of oxalic and propionic acid were always low ($\leq 0.1\%$ of the TOC), suggesting that these organics were not major degradation products of (irradiated) cellulosic tissues.
- The following molecules were identified but could not be dosed: xylo-isosaccharinic acid (alkaline degradation of hemicellulose), sugars and oligosaccharides such as glucose, cellobiose, cellotriose, cellotetraose, and cellopentaose.

Some of these species were also identified and quantified by (Glaus et Van Loon, 2008) after hydrolytic degradation of non-irradiated cellulose. Besides ISA, the other acids identified in low quantities, include formic, lactic, glycolic, pyruvic, glyceric, threonic and 2-hydroxybutanoic acids (Glaus *et al.*, 1999; Van

Loon *et al.*, 1999). The works performed by [PSI] after 21 and 28 years of alkaline cellulose degradation, identified the following degradation species in addition to ISA:

- Formic acid, acetic, glycolic, lactic acid (3-10 %);
- Succinic, oxalic acid and fumaric acid only detected in negligible amounts.

The kinetics for cellulose degradation by hydrolysis in a cementitious medium and the release of ISA was studied in the past by two groups: Van Loon and colleagues (Glaus & Van Loon, 1998; Glaus & Van Loon, 2008); Pavasars and colleagues (Pavasars *et al.*, 2003). In the framework of Task 2 of CORI, [PSI] performed sampling campaigns carried out after 19.2, 21 and 28 years of degradation. The long-term experiments of anaerobic alkaline hydrolysis of cellulose at ambient temperature confirm the earlier observation, of Glaus & Van Loon, that cellulose degradation slowly progressed after a rather short (~3 years) first phase of fast removal ("peeling-off") of glucose units from the reducing end of the cellulose chain. The secondary slow phase of peeling-off is assumed to proceed via the same reaction paths as the fast process. However, it is slowed down by the strongly reduced availability of reducing end groups in the cellulose chain compared to the initial phase of reaction.

The results obtained by [SCK CEN] also showed that pre-irradiation of cellulosic tissues does not seem to alter the alkaline degradation pathways, but rather accelerates the overall degradation.

The model previously proposed by [PSI] to predict cellulose degradation and ISA production is still applicable.

Polyvinyl chloride (PVC)

The water-soluble degradation products under radiolysis combined with hydrolysis of a soft industrial PVC used as glove-box sleeves have been characterised by the CEA/ORANO. For these studies, the industrial PVC was irradiated under gamma radiation up to 10 MGy and then leached in cementitious water (pH 13.2) at 60°C. The species identified/quantified are the following: acetic, formic, glutaric, succinic, adipic, oxalic, malonic, phthalic and benzoic acid (CEA, 2014). The release of phthalic acid observed in the case of industrial PVC is associated with leaching of phthalate, present in this substance as a plasticiser (≈ 30% mass). The release of benzoic acid is associated with the degradation of phthalate. The fraction of TOC identified in the leachate is around 49%.

Studies to identify the water-soluble molecules from PVC degradation have also been carried out by RWN (Baston *et al.*, 2017). In these studies, the material used was a flexible PVC representative of glove-box gloves, like in the CEA study. In this instance, the polymer contains three different types of phthalates (plasticisers): di-2-ethylhexyl phthalate (DEHP), diisononyl phthalate (DINP) and diisodecyl phthalate (DIDP). The PVC and plasticisers were irradiated at various dose rates (0.25; 0.5; 0.75 and 1 MGy) in the presence of a saturated Ca(OH)₂ solution and ambient temperature. Irradiation was also performed at high temperature (80°C) on PVC samples at a dose of 0.75 MGy. The species identified in the RWN studies are: phthalic acid, 2-ethylhexanoic acid, 2-ethyl-1-hexanol and several phenolic compounds (phenol, 2-Isopropylphenol, 3-Isopropylphenol, 4-Isopropylphenol and 4,4-(1-Methyl-ethylidene)-bisphenol).

The degradation of soft commercial PVC by radiolysis and alkaline degradation was studied by (Chantreux, 2021; Chantreux *et al.*, 2021). The degradation products were extensively characterised and quantified. The main degradation product from alkaline degradation of pre-irradiated industrial PVC is phthalic acid. This degradation product originates from the radiolytic degradation of the diisononylphthalate (DINP), present as additive in soft commercial PVC. In addition, it was proved that DINP is a major source of byproducts such as phthalic derivatives, alcohols and mono carboxylic acids from C4 to C9 and dicarboxylic acids from C2 to C8. Other additives are also suspected to contribute. In the present case, dicarboxylic acids from C6 to C9 were also generated from the radiooxidation of stearic acid used as lubricant in the commercial PVC. The species release by the degradation of PVC chain are formic, acetic, oxalic, propanedioic, pentanoic, glycolic, chloroacetic and butanedioic acids.

In the framework of WP CORI, [CNRS[ISTO]] studied the degradation of hard commercial PVC polymers by radiolysis followed by hydrolysis. Similar results were obtained like described in the literature for soft PVC. The main difference is that phthalate is one the most important degradation product of soft PVC and not found as degradation product of hard PVC. This can be explained by the fact that phthalate is added in high concentrations to the commercial soft PVC as plasticizer additive and is found only in very low concentration in formulation of the hard PVC.

Ethylene propylene rubber (EPR) copolymer

Two types of EPR copolymer have been studied by the CEA/ORANO, a pure EPR and an industrial EPR in the form of an O-ring. The EPR was chosen as a PE simulant.

The characterisation of water-soluble products from the degradation of these polymers by radiolysis/hydrolysis in cementitious water at 60°C identified and quantified the following species: oxalic, acetic, formic, glutaric, succinic, adipic, malonic and pimelic acid. The contribution of unidentified organic compounds to the TOC increases with the dose; the identified TOC is approximately 4% at 10 MGy (Andra).

Superplasticizers

NDA studies were carried out to measure the degradation of SP in alkaline solution and the effects of temperature and gamma radiation on the degradation process (NDA, 2019). The SP studied was a PCE for which the full chemical structure was unknown. SP in alkaline solution were relatively unchanged over nine months, both at ambient temperature and at 80°C. However, gamma irradiation to 200 kGy produced a drop in TOC by ~80% and a detectable decrease in the average molecular weight. There is significant uncertainty in the identification of the SP degradation products. Analysis of SP solutions after irradiation tentatively identified some radiolysis products (hexagol, 3,6,9,12-tetraoxatetradecan-1-ol), additionally some products could not be identified.

The radiolytic and hydrolytic degradation of two types of SP, a PCE and a PNS, was studied by (Legand, 2023). The results highlighted the degradation of the two superplasticizers under irradiation, leading to chain scission and crosslinking. For the PCE superplasticizer, two degradation products were identified and dosed: acetate and sulphite that comes from degradation of sulphonate lateral groups. For the PNS superplasticizer, sulphate was identified as degradation product, associated to the degradation of sulphonate groups of the SP.

In the framework of CORI, radiolytic degradation of “homemade PCE” was studied by [CNRS(Subatech)]. Carbonate, formate and acetate were identified as degradation products. The radiolytic yield of formation for these soluble species are shown in TABLE 2-5 for gamma and alpha irradiation of PCE in three media or solution, ultrapure water, K⁺ medium or ACW medium. This table also shows the radiolytic yield of the respective medium without PCE. If there is no yield given, either the species is not concentrated enough (very low concentration measured), or its formation does not follow any tendency with the dose.

The formation of carbonate ions is negative, indicating that carbonate ions accumulated in the solution are degraded with the dose. The carbonate ion formation for K⁺ and ACW media show very important yields both with and without PCE. The difference of CO₃²⁻ that might come from CO₂ from the PCE radiolytic degradation is too small compared to the dissolution of atmospheric CO₂ and even in favour of the solution without PCE.

The influence of the medium and pH on the formation of formate ions shows a higher production of HCOO⁻ in the presence of PCE in ultrapure water. This can be explained by the fact that radicals formed during water radiolysis, like H[•] and HO[•], can react with PCE carboxylate moieties to form formate. At pH

13.7 these species are mainly in their basic form, which might be less reactive towards the PCE molecule and explain this weaker formation of formate at pH 13.7.

Regarding acetate formation, the radiolytic yields are quite low and no significant difference was observed in solutions of PCE in ultrapure water and K⁺ or ACW media.

TABLE 2-5: Formation yields of carbonate, formate and acetate ions after alpha (α) and gamma (γ) radiolysis of PCE superplasticizer in various solutions and media without PCE.

Systems	pH	$G_0(\text{CO}_3^{2-})$ ($\times 10^{-7} \text{ mol.J}^{-1}$)	$G_0(\text{HCOO}^-)$ ($\times 10^{-7} \text{ mol.J}^{-1}$)	$G_0(\text{CH}_3\text{COO}^-)$ ($\times 10^{-7} \text{ mol.J}^{-1}$)
PCE 1 g.L⁻¹ H₂O	8.2	α: -0.24 ± 0.001 γ: -0.42 ± 0.01	α: 0.71 ± 0.04 γ: 1.32 ± 0.05	α: 0.023 ± 0.001 γ: -
H₂O	6.9	α: - γ: -	α: - γ: -	α: - γ: -
PCE 1 g.L⁻¹ K⁺	13.7	α: 8.85 ± 0.24 γ: 6.50 ± 0.33	α: 0.10 ± 0.01 γ: 1.13 ± 0.07	α: 0.07 ± 0.03 γ: 0.42 ± 0.03
K⁺	13.7	α: 9.70 ± 0.34 γ: 8.01 ± 0.40	α: 0.039 ± 0.001 γ: -	α: - γ: -
PCE 1 g.L⁻¹ ACW	13.7	α: 7.50 ± 0.24 γ: -	α: 0.35 ± 0.01 γ: 1.19 ± 0.08	α: 0.08 ± 0.01 γ: 0.47 ± 0.03
ACW	13.7	α: 7.57 ± 0.24 γ: 8.13 ± 0.40	α: 0.017 ± 0.001 γ: -	α: 0.026 ± 0.001 γ: -

2.6 Degradation of ion-exchange resins (IER)

The effects of ionising radiation on ion-exchange resins are similar to those observed for the other organic polymers. The main difference resides in the presence of functional groups grafted onto the polymer skeleton of IERs, which may be subject to cleavage phenomena under radiolysis.

Two cases can be considered for the radiolysis of IERs, differentiating whether radiolysis occurs in the presence of water or under dry conditions. It is also worth mentioning that so-called “dry” resins still contain interstitial water in their structure.

2.6.1 Radiolytic degradation of “dry” polystyrene backbone IERs

Degradation of the polystyrene skeleton

The presence of benzene rings in the resin skeleton provides good stability to ionising radiation. Under radiolysis, cross-linkage phenomena are dominant, associated with the production of H₂. Skeleton degradations remain minor up to doses exceeding 10 MGy.

Radiolytic degradation of cationic IERs

For cationic resins, radiolytic cleavage phenomena between functional groups and the organic skeleton are observed for doses exceeding 1 MGy.

Many authors propose mechanisms to explain the radiolytic degradation of cationic resins (Karpukhina *et al.*, 1976 ; Ichikawa & Hagiwara, 1973). For dry resins, the functional groups will be degraded according to a redox mechanism leading to the formation of sulfones by a reaction between two functional groups (note that Ar represents the aryl group in eq. 2-2):



Radiolytic yields

The gas production radiolytic yields γ (G_{H_2} , G_{SO_2} and G_{CO_2}) have been determined by Gangwer *et al.* for two types of cationic resins, Dowex 50W and KU-2 (Gangwer *et al.*, 1977). Gas production radiolytic yield measurements were also carried out by (Traboulsi, 2012) for a cationic resin (Amberlite IR 120) by considering various γ radiation doses under aerobic and anaerobic conditions. The results of (Traboulsi, 2012) indicate that the radiolytic H_2 production is independent of the irradiation atmosphere and the radiolytic yield remains low (lower than $0.10 \times 10^{-7} \text{ mol}\cdot\text{J}^{-1}$), similar to that determined by (Gangwer *et al.*, 1977) for a Dowex 50W cationic resin.

Radiolytic degradation of anionic IERs

Anionic resins are degraded under irradiation at lower integrated doses than for cationic resins with an identical skeleton. At 0.1 MGy, degradation can already be significant for anionic resins with primary, secondary or tertiary amine functional groups (Pillay, 1986). Many authors also mention a cleavage of functional groups, leading to the formation of nitrogenous compounds, primarily trimethylamine (TMA) (Swyler *et al.*, 1983; Rébufa, 2015).

Mechanisms for anionic resin radiolysis and more particularly the degradation of functional groups have been proposed by Ahmed *et al.* (Ahmed *et al.*, 1996) and Hall (Hall, 1963). Trimethylamine is formed from a dried resin, by anionic group cleavage following a Hofmann reaction induced under radiolysis (note that Ar represents the aryl group in eq. 2-3):



Radiolytic yields

The gas production γ radiolytic yields of two types of anionic resins in the form containing NO_3^- (Dowex 1 and 11) have been determined by Gangwer *et al.* (Gangwer *et al.*, 1977). G_{H_2} , for the two resins is about $0.10 \times 10^{-7} \text{ mol}\cdot\text{J}^{-1}$. The gas production radiolytic yields of an Amberlite IRA 400 anionic resin were measured by (Traboulsi, 2012) at various doses, under aerobic and anaerobic conditions. The hydrogen gas production radiolytic yield values (from $0.24 \times 10^{-7} \text{ mol}\cdot\text{J}^{-1}$ to $1.15 \times 10^{-7} \text{ mol}\cdot\text{J}^{-1}$) are higher than for cationic IERs. The values of G_{H_2} vary with dose in a complex manner. The verified behaviour is not similar to that observed for a large number of polymers, i.e. G_{H_2} declines with the dose. According to (Traboulsi, 2013), this complex behaviour may be associated with the degradation of the function groups of the IERs generating amines; these amines may then decompose and also produce H_2 . These two degradation stages may occur at different doses and lead to a complex evolution of G_{H_2} with the dose.

2.6.2 Radiolytic degradation of polystyrene backbone IERs in the presence of water

Under the action of ionising radiation, the ion-exchange resins can incur additional degradation caused by the reactive species generated by water radiolysis.

Radiolytic degradation of cationic IERs

The following degradation processes are typically observed for cationic resins irradiated under water:

- cleavage of functional groups at doses exceeding 1 MGy;
- formation of sulfate ions;
- release of volatile products such as H₂, CO₂, CO and methane.

In the presence of oxygen and water, some authors (Kiseleva *et al.*, 1961) note the formation of hydroxylic and carboxyphenolic functions. The form of the resin (H⁺ acid or saline form) also influences its stability under radiation. Many authors report that a saturated IER is more radiation resistant (Gangwer *et al.*, 1977).

Formation of sulfate ions

In the presence of water, the cleavage of sulfonic groups results in the formation of sulfate ions, in the form of sulfuric acid for resins in H⁺ acid form, and a H₂SO₄/counter-ion salt mixture for resins in the saline form. When the resin is initially charged with Fe²⁺ or Fe³⁺ ions, fewer sulfate ions are released (Swyler *et al.*, 1983). Swyler *et al.* (Swyler *et al.*, 1983) showed that the increase in the production of sulfate ions is linear with the dose up to 5 MGy, before levelling out at higher doses.

Radiolytic yields

The radiolytic yield values for gas production were determined by Gangwer *et al.* (Gangwer *et al.*, 1977) for a Dowex 50W resin and were also measured recently by the CEA for an Amberlite IR 120 resin. No effect of the irradiation dose (from 0.5 to 4 MGy) on the radiolytic yield values was found for the doses studied (Traboulsi, 2012).

Radiolytic degradation of anionic IERs

The following degradation processes are typically observed for anionic resins irradiated under water:

- loss of the resin's water of hydration and a reduction in grain diameter (Swyler *et al.*, 1983; Vannoorenberghe, 1991);
- increase in the pH of the solution in contact with the resin, especially if the resin is charged with OH⁻ species;
- cleavage of functional groups at doses exceeding 0.1 MGy;
- production of nitrogenous compounds (primarily TMA);
- release of H₂ gas and traces of methane and CO₂.

As for cationic resins, radiolysis leads to the loss of the quaternary ammonium functional group, and in some cases, the formation of hydroxylic and carboxyphenolic groups, which are slightly acidic cationic exchange sites in the anionic resin network.

Radiolytic yields

Baidak and Laverne (Baidak & Laverne, 2010) have studied the influence of the water content of an Amberlite 400 anionic resin with quaternary ammonium in three different forms (Cl⁻, NO₃⁻, OH⁻) on the radiolytic yield for H₂ production. The results show that for resins in Cl⁻ or OH⁻ form, H₂ production increases with higher water content, whereas the resin in NO₃⁻ form has lower H₂ production for equivalent water contents.

The CEA performed γ irradiation to determine the radiolytic yields of H₂ production for the same type of anionic IER in the OH⁻ form (Amberlite 400). Irradiation was performed under water in anaerobic conditions at doses between 0.5 and 4 MGy. The radiolytic yield seems to increase slightly up to a dose of 3 MGy (from 0.68×10^{-7} mol·J⁻¹ to 0.99×10^{-7} mol·J⁻¹) (Traboulsi, 2012).

Radiolytic degradation of mixed-bed resins

The radiolytic yields of H₂ production under γ radiation have been measured by the CEA. The resins studied consisted of a mixture of 25% mass of anionic resin (in OH⁻ form) and 75% mass of cationic resin (in H⁺ form). The radiolytic yield values are relatively low and appear to increase for doses exceeding 3 MGy (from $0.04 \times 10^{-7} \text{ mol}\cdot\text{J}^{-1}$ to $0.46 \times 10^{-7} \text{ mol}\cdot\text{J}^{-1}$).

2.6.3 Leaching of ion-exchange resins

Polystyrene backbone IER

Post-irradiation leaching of ion-exchange resins is studied in order to assess the behaviour of these materials with regard to the coupled phenomena of radiolysis and hydrolysis. The information provided in this section was acquired through studies carried out by the CEA for cationic, anionic and mixed-bed resins (Traboulsi, 2012).

Leaching of post-irradiation anionic resin at 4 MGy

The quantity of Total Organic Carbon (TOC) in a leaching solution for an anionic resin that has previously been irradiated under “dry” and anaerobic conditions at 4 MGy was followed during 140 days. The release of water-soluble compounds occurs very quickly after the irradiated resin is placed into contact with pure water. The cumulative quantity of TOC released by the resins changes little as a function of leaching time, from $8 \text{ mg}\cdot\text{g}^{-1}$ to $18 \text{ mg}\cdot\text{g}^{-1}$ of dry resins.

The following main species were identified during the leaching of pre-irradiated resins: acetic acid, formic acid, TriMethylAmine (TMA), DiMethylAmine (DMA), MonoMethylAmine (MMA) and the NH₄⁺ ion.

Leaching of post-irradiation cationic resin at 4 MGy

The quantities of TOC released from non-irradiated resins are higher for the cationic resin than for the anionic resin studied. According to (Traboulsi, 2012), the release of TOC from the cationic resin is most probably due to the presence of admixtures used in the industrial resin manufacturing process. As for the anionic resin, cationic resins irradiated in the presence of water release little TOC. However, the presence of air during irradiation increases the quantity of TOC released by the leaching of this material. This release of water-soluble species increases above a dose of 4 MGy (to around $25 \text{ mg}\cdot\text{g}^{-1}$ of dry resins).

Post-irradiation leaching of a mixed-bed resin MB 400

For a pre-irradiated mixed-bed resin, the quantities of TOC released after 1 day of leaching are low for most irradiation conditions. Under oxidising conditions, the release of TOC only becomes significant for radiation doses exceeding 4 MGy (around $25 \text{ mg}\cdot\text{g}^{-1}$ of dry resins).

Comparison of the TOC quantities released by the mixed-bed resin compared to those released by the fully cationic or anionic resins shows that:

- for doses up to 1 MGy, the quantities of TOC released by the mixed-bed resin remain below those released by its cationic and anionic components considered separately, regardless of the irradiation conditions (anaerobic or aerobic medium, presence of water, *etc.*);
- for irradiation in an anaerobic or aerobic medium with a dose of approximately 4 MGy, the quantities of TOC released by the mixed-bed resin are close to those of its cationic component.

The following main water-soluble species are released during post-irradiation leaching of mixed-bed resins: acetic acid, formic acid, oxalic acid, TMA, DMA, MMA, ammonium ion and SO_4^{2-} .

PAN based IER

The leaching of a filter aid based on polyacrylonitrile (PAN) in different basic solutions was studied by [KIT] in the framework of Task 2 of CORI. NPOC values determined in $\text{Ca}(\text{OH})_2$ -buffered systems show a significant increase after a contact time of ca. 800 days. Based on the analysis of solid phases and degraded leachates three proxy ligands were proposed to simulate the chemical characteristics of the UP2W degradation products: glutaric acid (GTA) representing the bulk chain of the generated polymer fragments, whilst α -hydroxyisobutyric acid (HIBA) and 3-hydroxybutyric acid (HBA) simulate the effect of the end groups.

2.6.4 Degradation of polystyrene backbone IERs under the effect of temperature

IERs are especially sensitive to the influence of temperature. Under the action of temperature, three consecutive degradation reactions occur:

- loss of absorbed humidity and the water of hydration contained in the resin (80 - 120°C);
- cleavage of functional groups grafted onto the resin's polystyrene skeleton (50-150°C);
- decomposition of the resin's polystyrene skeleton (> 150°C).

For cationic resins, the sulfonic functional group is stable. The bond cleavage reaction between the sulfonic functional group and polymer skeleton occurs at between 120-150°C (Li & Sengupta, 2000). For anionic resins, the Hofmann degradation can transform quaternary ammonium functional groups (strong bases) into tertiary amines (weak bases), or even fully degrade the functional group. This reaction occurs in an alkaline media. The Hofmann degradation only significantly occurs above 50°C. Degradation of the polystyrene skeleton occurs at a high temperature and its carbonisation only observed at around 300°C.

2.7 References for Chapter 2

- Andra. Le socle de connaissances scientifiques et techniques de Cigéo - Les référentiels de connaissances, Le comportement des déchets MA-VL, under progress.
- Ahmed M.T., Clay P.G. & Hall G.R. (1966) Radiation induced decomposition of ion-exchange resins, Part II. The mechanism of the deamination of anion-exchange resins. *J. Chem. Soc.*, 12, 1155-1157.
- Baidak A. & LaVerne J.A. (2010) Radiation-induced decomposition of anion exchange resins. *J. Nucl. Mater.*, 407, 211-219.
- Baston G., Cowper M., Davies P., Dawson J., Farahani B., Heath T., Schofield J., Smith V., Watson S. & Wilson J. (2017) The impacts of PVC additives and their degradation products on radionuclide behavior. Rapport RWM, RWM005769.
- Bleyen D., Van Gompel V., Smeta S., Eyley S., Verwimp W., Thielemans W., Valcke E. (2023) Radiolytic degradation of cellulosic materials in nuclear waste: Effect of oxygen and absorbed dose. *Radiation Physics and Chemistry* 212, 111177.
- Boughattas I. (2014) Etude de la dégradation thermique du polychlorure de vinyle: Effet couplé de l'irradiation et de la température. Thèse de doctorat, Université de Caen Basse-Normandie.
- Burlant W.J. & Taylor C.R. (1955) Effect of radiation on polyacrylonitrile and poly- α -methacrylonitrile. *J. Phys. Chem.*, 62, 247- 247.
- CEA (2014) Inventaires de matières organiques et complexants dans les colis MA-VL. Rapport PNGMDR 2013-2015.
- Chang Z. & LaVerne J.A. (2000) Hydrogen Production in the Heavy Ion Radiolysis of Polymers. 1. Polyethylene, Polypropylene, Poly(methyl methacrylate), and Polystyrene. *J. Phys. Chem. B.* 104, 10557-10562.
- Chantreux M. (2021) Étude de la dégradation par radiolyse et/ou hydrolyse basique de PVC présents dans les stockages de déchets radioactifs, PhD manuscript.
- Chantreux M., Ricard D., Asia L., Rossignol S., Wong-Wah-Chung P. (2021) Additives as a major source of radiolytic organic byproducts of polyvinyl chloride (PVC). *Radiation Physics and Chemistry* 188, 109671.
- Colombani J. (2007) Étude de la radiolyse gamma du poly(chlorure de vinyle) : application à l'étude de la dégradation par irradiation et par lixiviation du PVC industriel. Thèse de doctorat, Faculté des Sciences et Techniques de Marseille Saint Jérôme.
- De Dardel F. (1998) Echange d'ions – Principes de base. *Techniques de l'Ingénieur* J2783.
- EURAD-CORI Milestone 17 - CORI Technical Report - Task 2 State-of-art report on organic degradation by radiolytic and hydrolytic processes.
- Fromentin (2017) Lixiviation des polymères irradiés: caractérisation de la solution et complexation des actinides. PhD manuscript, Ecole doctorale Chimie Physique et Chimie Analytique de Paris Centre.
- Gangwer T.E., Golstein M. & Pillay K.K.S. (1977) Radiation effects on ion exchange materials. DOE BNL 50781.
- Glaus M. A. & Van Loon L.R. (1998) Experimental and Theoretical studies on alkaline degradation of cellulose and its impact on the sorption of radionuclides. Rapport PSI 98-07.
- Glaus M. A., Van Loon L. R., Achatz S., Chodura A. & Fischer K (1999) Degradation of cellulosic materials under the alkaline conditions of a cementitious repository for low and intermediate level radioactive waste. Part I: Identification of degradation products. *Analytica Chimica Acta*, 398, 111 – 122.

- Glaus M. A. & Van Loon L.R. (2008) Degradation of cellulose under alkaline conditions: news insights from a 12 years degradation study. *Environ. Sci. Technol.*, 42, 2906- 2911.
- Hall G.R. (1963) Radiation induced decomposition of ion-exchange resins. Part 1. Anion exchange resins. *J. Chem. Soc.*, 5, 5205- 5211.
- Ichikawa T. & Hagiwara Z. (1973) Effect of Gamma Irradiation on Cation Exchange Resin. *J. Nucl. Sci. Technol.*, 10, 746-752.
- Karpukhina T.E., Kiselava T.E. & Chutov K.V. (1976) Electron Spin Resonance Study of the low temperature Radiolysis of Ion-Exchange Resins: II, The KU-2 Cation Exchange Resin. *Russ. J. Phys. Chem.*, 50, 712- 714.
- Kazanjian A.R. (1976) Radiolytic Gas Generation in Plutonium Contaminated Waste Materials. Rockwell International RFP-2469.
- Kiselava E.D. Chmutov K.V. & Kruptova V.N. (1961) Effect of Accelerated Electrons on KU-2 Cation-Exchange Resin. *Russ. J. Phys.Chem.* 35, 892-895.
- Legand S. (2023) Effets de la radiolyse sur le transfert et la spéciation de radionucléides en milieu cimentaire adjuvanté, PhD manuscript.
- Li P. & Sengupta A.K. (2000) Intraparticle Diffusion during Selective Sorption of Trace Contaminants: The Effects of Gel versus Macroporous Morphology. *Environ. Sci. Technol.*, 34, 5193-5200.
- Nagra (2023), Degradation of organic materials in an L/ILW Repository. Technical Report 23-11.
- NDA, 2019, Further Studies to Underpin the Use of PCE Superplasticisers in the Packaging of Low-heat-generating Wastes. Updates on the effects of radiolysis products on sorption and solubility. DA Report no. RWM/Contr/19/035.
- O'Donnell J.H. (1989) The effects of radiation on high-technology polymers. American Chemical Society, Washington DC.
- Pavasars I., Hagberg J., Borén H. & Allard B. (2003) Alkaline Degradation of Cellulose: Mechanisms and Kinetics. *Journal of Polymers and the Environment*, 11, 39-47.
- PIDG (2014) Programme Industriel De Gestion des déchets - Projet Cigéo, version D. Document technique Andra CGPEADPC110074.
- Pillay K.K.S. (1986) The effects of ionizing-radiations on synthetic organic ion-exchangers. *J. Radioanal. Nucl. Chem.*, 97, 135- 210.
- Rébufa C., Traboulsi A., Labeled V., Dupuy N. & Sergent M. (2015) Experimental design approach for identification of the factors influencing the γ -radiolysis of ion exchange resins. *Radiation Physics and Chemistry*, 106, 223- 234.
- Swyler K.J., Dodge C.J. & Dayal R. (1983) Irradiation effects on the storage and disposal of radwaste containing organic ion-exchange media. Rapport NUREG/CR-3383.
- Traboulsi A. (2012) Radiolyse gamma et lixiviation post-irradiation de résines échangeuses d'ions. Thèse de doctorat, Université Paul Cézanne.
- Traboulsi A., Labeled V., Dauvois V., Dupuy N. & Rébufa C. (2013) Gamma radiation effect on gas production in anion exchange resins. *Nuclear Instruments and Methods in Physics Research B*, 312, 7- 14.
- Van Loon L. R., Glaus M. A., Laube A. & Stallone S. (1999) Degradation of cellulosic materials under the alkaline conditions of a cementitious repository for low and intermediate-level radioactive waste II. Degradation kinetics, *Journal of environmental polymer degradation*, 7, 41 – 51.
- Vannoorenberghe H. (1991) Étude du comportement à long terme des déchets conditionnés dans les résines époxydes et/ou polyesters polymérisés. Thèse de doctorat, Faculté des Sciences et Techniques de Marseille Saint Jérôme.

Ventura A., Ngono-Ravache Y., Marie H., Levavasseur-Marie D., Legay R., Dauvois V., Chenal T., Visseaux M., Balanzat E. (2016) Hydrogen Emission and Macromolecular Radiation-Induced Defects in Polyethylene Irradiated under an Inert Atmosphere: The Role of Energy Transfers toward trans-Vinylene Unsaturations. *The Journal of Physical Chemistry B*, 120, 10367–10380.

3. Organic-cement interactions

Authors: David García [KIT (Amphos21)] and Pierre Henocq [Andra]

This chapter summarizes the current understanding of the behaviour of organic molecules in cement-based materials.

Organic materials can be present in ILW and LLW radioactive waste. As seen in the framework of the CORI Task 2 and the previous SOTA chapter, the origin of these organic compounds is varied and includes (i) radiolysis and/or hydrolytic degradation of cellulosic materials, polymers, ionic-exchange resins (IERS) or other organic materials, (ii) wastes from effluent extraction processes such as EDTA, NTA, TBP, and (iii) cementitious admixtures such as superplasticisers. These compounds are subject to degradation processes that can release organic molecules to solution. The products that are formed are, to some extent, controlled by the specific chemical conditions imposed by the cement-based materials in the repository. Some of these degradation products are ligands which can react with radionuclides to form complexes in solution (Allard, 2005; Allard and Ekberg, 2006; Androniuk, 2017; Androniuk *et al.*, 2017; Boggs *et al.*, 2010; Colàs, 2014; Colàs *et al.*, 2013; Dario *et al.*, 2004; Evans, 2003; Felipe-Sotelo *et al.*, 2012; Gaona *et al.*, 2008; Garcia *et al.*, 2020; González-Siso *et al.*, 2018; Holgersson *et al.*, 1998; Holgersson *et al.*, 2011; Keith-Roach, 2008; Pointeau *et al.*, 2006; Tasi *et al.*, 2018a, 2018b; Thakur *et al.*, 2006; Tits *et al.*, 2002; Vercammen, 2000; Vercammen *et al.*, 2001). The complexation of the radionuclides by organic ligands can cause an increase in their mobility by (i) increasing their solubility and (ii) decreasing their sorption to cement-based materials (Ochs *et al.*, 2014).

In order to understand the mechanisms enhancing the mobility of radionuclides as organic complexes, this chapter describes the fundamental properties driving the behaviour of organic molecules in the presence of cement-based materials. This overview of organic molecules includes (i) their properties in solutions related to cementitious environments, (ii) their sorption behaviour, and (iii) their diffusion behaviour.

3.1 Properties in solution

The properties of organic molecules in solution are characterized by their speciation and their solubility (Hummel *et al.*, 2005). According to IUPAC conventions, the analytical composition of a saturated solution, expressed in terms of the proportion of a designated solute (*e.g.* M^i or Org^j) in a designated solvent, is the solubility of that solute. The solubility may be expressed in a number of ways, including as a concentration, molality, mole fraction, or mole ratio. Solubility considers not just the amount of free ion, M_i , in solution but the sum of all aqueous species of the M^i as shown in eq.3-1, where L^k stands for the different ligands (hydroxyl ion, organics, *etc.*) present in solution.

$$Solubility = [M]_{TOTAL} = [M^i] + [ML^{i+k}] + [ML_2^{i+2k}] + \dots \quad (\text{eq. 3-1})$$

The distribution of all aqueous chemical species of M^i or Org^j in a system is defined as the element chemical speciation by IUPAC and is therefore dependent on the nature of the solution. For example, the speciation of calcium in basic solution is predominantly Ca^{2+} and $CaOH^+$. However, in the presence of organic molecules such as GLU, the complex species $Ca(OH)(HGLU)(aq)$ and $Ca(HGLU)^+$ can appear (Gaona *et al.*, 2008), and can be the predominant forms at high GLU concentrations.

The speciation of an element or an organic compound under a given set of conditions can be estimated through thermodynamic calculations based on data integrated into a thermodynamic database. This database includes the necessary parameters for each species related to their properties in solution. As an example of this, *TABLE 3-1* and *TABLE 3-2* detail the source and chemical structure, respectively, of the organic molecules deemed important from a radioactive waste disposal perspective that are considered in ThermoChimie (Giffaut *et al.*, 2014), a thermodynamic database managed by the French (Andra), British (RWM) and Belgian (Ondraf-Niras) waste management agencies. Organic ligands are commonly considered as its negatively charged form as indicated in *TABLE 3-1*; note that *TABLE 3-2* includes the general structure of the main organic ligands but does not reflect their most common protonation state. *TABLE 3-3* provides a matrix of the element complexation data available for these organic molecules in ThermoChimie.

TABLE 3-1: List of the main organic ligands and their sources considered in ThermoChimie database (www.thermochimie-tdb.com).

Organics in wastes	Organic ligands in ThermoChimie
Cement additives*	Gluconate
Plastics, Filters, Resins**	Adipate
	Phthalate
Bitumen degradation products	Oxalate
	Acetate
Cleaning/extraction agents	EDTA
	NTA
	Citrate
Cellulose degradation products	Isosaccharinate
Organic species in clay***	Malonate
	Succinate
	Suberate

TABLE 3-2: Structure of organic ligands currently considered in the ThermoChimie database.

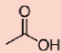
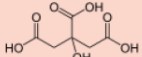
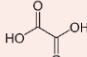
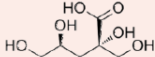
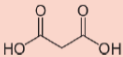
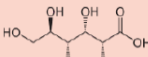
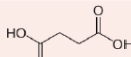
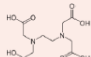

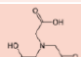

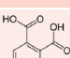
Monocarboxylic	Acetic		Hydroxycarboxylic	Citric		
	Dicarboxylic	Oxalic			ISA	
Malonic				Gluconic		
Succinic				Aminocarboxylic	EDTA	
Adipic					NTA	
Suberic				Aromatic Carboxylic	Phthalic	

TABLE 3-3: Availability of key thermodynamic data for various organic/species complexes; the considered species are radionuclides and/or major ions such as Ca and Mg. (ThermoChimie, version 10a, 2016).

acid/base	Monocarboxylic	Dicarboxylic					Hydroxycarboxylic			Aminocarboxylic		Aromatic carboxylic
	Acetic	Oxalic	Malonic	Succinic	Adipic	Suberic	Citric	Gluconate	ISA	EDTA	Nta	Phthalic
Ca	✓	✓	✓	✓	✓	✓	✓	✓	✓	✓	✓	✓
Mg	✓	✓	✓	✓			✓			✓	✓	
Ni	✓	✓	✓				✓			✓	✓	✓
Eu	✓	✓	✓	✓					✓			✓
Am	✓	✓					✓	✓	✓	✓	✓	✓
Cm		✓										✓
Tc	✓	✓								✓	✓	
Th	✓	✓	✓	✓			✓	✓	✓	✓	✓	
U	✓	✓		✓			✓	✓	✓	✓	✓	✓
Np	✓	✓					✓	✓	✓	✓	✓	
Pu	✓	✓						✓	✓	✓	✓	✓

✓ Data available in ThermoChimie vs. 10a

The work on the solubility of $\text{Ca}(\alpha\text{-ISA})_2(\text{s})$ and $(\text{CaGLU})_2(\text{s})$ by Van Loon *et al.* (1999) is a good illustration of how thermodynamic data can be used to predict the concentrations of organic species in solution. From the reported thermodynamic constants, Van Loon *et al.* were able to estimate the maximum concentration of $\alpha\text{-ISA}$ and gluconate that might be expected in a cement pore water (Van Loon *et al.*, 1999). Importantly, this estimation took into account stage I and II degradation of the cement-based materials (see Chapter 5 of this SOTA), and thus provided realistic concentrations to be expected under repository conditions, as illustrated in TABLE 3-4.

TABLE 3-4: Calculated maximum concentrations of $\alpha\text{-ISA}$ and gluconate in the cement pore water for different stages of cement degradation (Van Loon *et al.*, 1999).

Stage	pH	[Ca]/mM	I^a /M	$[\alpha\text{-ISA}]_{\text{max}}^b$ /mM	$[\text{GLUC}]_{\text{max}}^b$ /mM
I	13.3	2	0.3	44	930
II	12.5	20	0.05	10	220

^a I , ionic strength. ^bCalculated by eqn. (12).

3.2 Sorption on cement-based materials

In the context of underground waste repositories, cement-based materials will contribute not only as structural materials but will also influence the behaviour of species (radionuclides, organics, *etc.*) in solution in terms of retention and stabilization (Berckmans *et al.*, 2013). The retention properties of the cementitious materials can be very strong for some radionuclides such as actinides or lanthanides (Albrecht *et al.*, 2005; Ochs *et al.*, 2010, Wang *et al.*, 2008; Wieland 2014), as further discussed in Chapter 4 of this SOTA.

Relatively little information is available on the sorption of organic molecules to cement-based materials, although this is a relevant effect to consider within an integrated description of sorption phenomena. The existing information suggests that low-weight organic molecules (propionic acid, formic acid for instance) are weakly sorbed in cement-based materials (Wieland *et al.*, 2016, see FIGURE 3.6). On the other hand, some organic ligands (*i.e.* ISA, GLU, EDTA, NTA, ...) can be strongly sorbed, and in the specific case of citric and oxalic acids, even precipitation can occur (Dario *et al.*, 2004) under the presence of Ca cations. The high amount and volume of cement-based materials in a repository, even if sorption of a certain organic molecule may be rather low per unit mass, suggests that they may significantly impact the behaviour of organic molecules.

The interactions of isosaccharinic acid (ISA) with cement-based materials have been investigated by several authors and are now described as a good example in more detail. As the main degradation product of cellulose, ISA has been particularly studied because of (i) the high quantity of cellulose in the waste streams and (ii) its complexing properties for radionuclides (see references). The sorption of ISA on cement pastes and on C-S-H/C-A-S-H phases, the main hydration products of cement pastes (see SOTA Chapter 5 on fundamental cement chemistry), has been studied by Van Loon & Glaus (1998). FIGURE 3-1 and FIGURE 3-2 present the amounts of sorbed ISA for two ISA diastereomers, α -ISA and β -ISA. Note that α -ISA has been extensively studied because of (i) the very well know synthesis process, and (ii) higher expected sorption and complexation capacities than β -ISA (Brinkmann *et al.*, 2019).

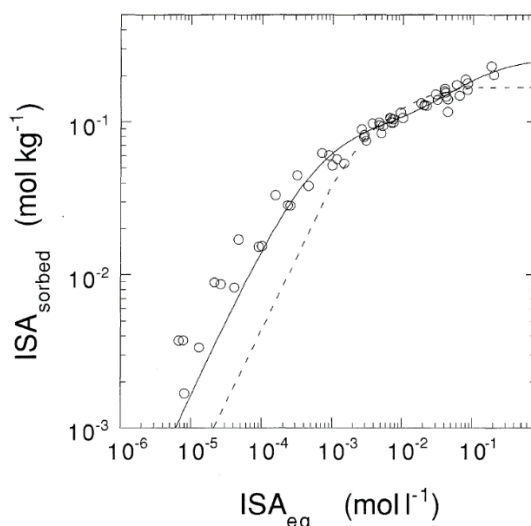


FIGURE 3-1: Sorption isotherm of on Portland cement at pH=13.3. Empty circles stand for experimental data, the solid line represents the modelling considering a two-sites-Langmuir model and the dashed line a one-site Langmuir model. (Van Loon & Glaus, 1998).

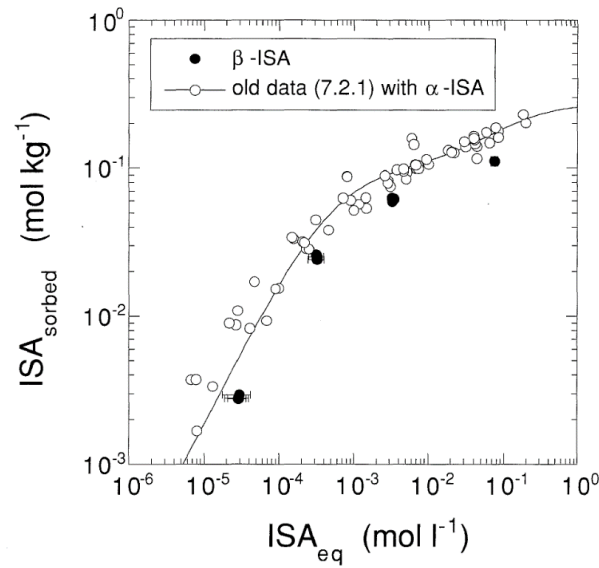


FIGURE 3-2: Sorption isotherm of β -ISA on Portland cement at $\text{pH}=13.3$. Solid line indicates the modelling of the data obtained for α -ISA using a two-sites-Langmuir model (Van Loon & Glaus, 1998).

FIGURE 3-3 shows the sorption isotherms for α -ISA on C-S-H and C-A-S-H phases. These results confirm that C-S-H/C-A-S-H phases can make a significant contribution to the sorption of ISA on cement-based materials.

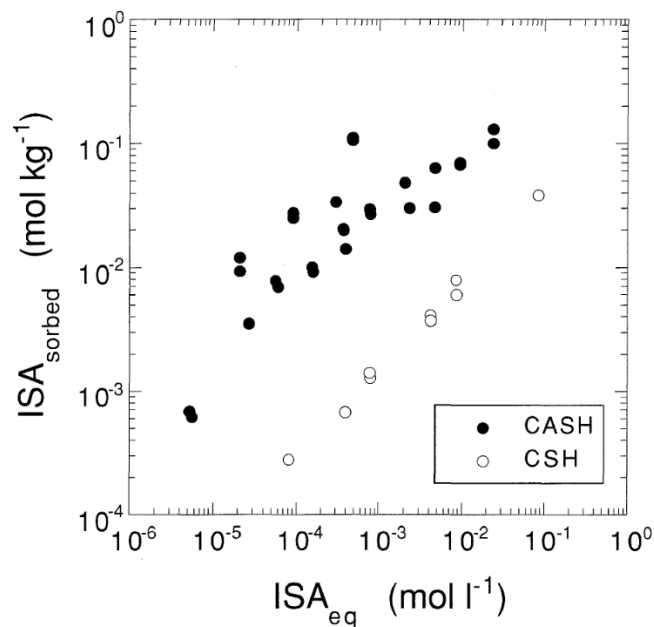


FIGURE 3-3: Sorption isotherm of α -ISA on C-S-H and C-A-S-H phases at $\text{pH}=13.3$ (Van Loon & Glaus, 1998).

FIGURE 3-4 displays sorption data for ISA and GLU on hardened cement pastes for degradation stages I (pH=13.2) and III (pH=11.9) as function of time (Pointeau *et al.*, 2006). These results show a kinetic evolution of the sorption for both ISA and GLU: as expected, the sorbed content increased during the first days (3 days for stage I and 10 days for stage III) but a decrease was then observed until a near-complete desorption was observed. As proposed by the authors, this desorption process could be explained by a carbonation of the HCP grains as (i) cement-based materials are very sensitive to carbonation and (ii) sorption tests of ISA and GLU on calcite (CaCO₃) under pH 13.3 conditions showed no sorption. Calcite could be formed at the surface of the HCP grains and, consequently, that would prevent the sorption of ISA and GLU. This assumption is important because host-rock waters contain carbonate ions which could promote the degradation of cement pastes to stage IV also called carbonated state (see SOTA Chapter 5).

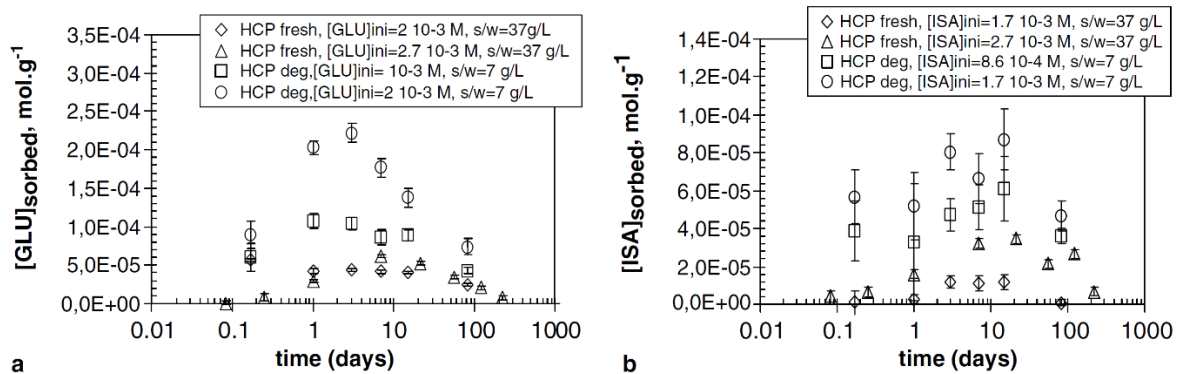


FIGURE 3-4: Evolution of (a) gluconate (GLU) and (b) ISA contents (mol·g⁻¹) sorbed on fresh (stage I) and degraded (stage III) cement pastes (Pointeau *et al.*, 2006).

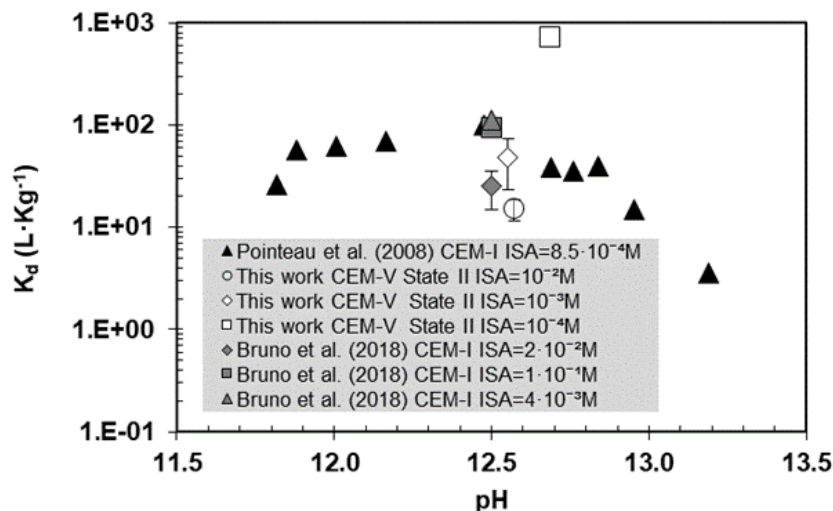


FIGURE 3-5: Comparison of adsorption distribution coefficients (K_d) for ISA against pH in fresh and degraded cement pastes. Non-filled symbols are results from Garcia *et al.* (2020) ('this work' in the legend); black filled symbols by Pointeau *et al.* (2008); grey filled symbols by Bruno *et al.* (2018).

More recently, Bruno *et al.* (2018), Garcia *et al.* (2020) and Pointeau *et al.* (2008) studied the sorption of ISA on cement pastes at degradation stage II. Pointeau *et al.* (2008) and Bruno *et al.* (2018) studied CEM I cement pastes whereas Garcia *et al.* (2020) studied CEM-V (see SOTA Chapter 5 for a description of the different cement degradation stages). A comparison of the results from these studies is provided above in FIGURE 3-5. The results show that the sorption affinity of ISA for the two cement types is similar, except for the lowest ISA concentration studied.

Despite being less studied in the literature, the adsorption of small organic molecules on cement pastes is known to be very low. Wieland *et al.* (2016) obtained distribution coefficients for several low molecular weight organic compounds such as acetic and formic acid, formaldehyde, acetaldehyde, methanol, and ethanol. FIGURE 3-6 shows the evolution of the uptake of these organic molecules as a function of reaction time; the distribution coefficients obtained ($\leq 1 \text{ L}\cdot\text{kg}^{-1}$) are much lower than those obtained for ISA ($K_d \approx 100 \text{ L}\cdot\text{kg}^{-1}$).

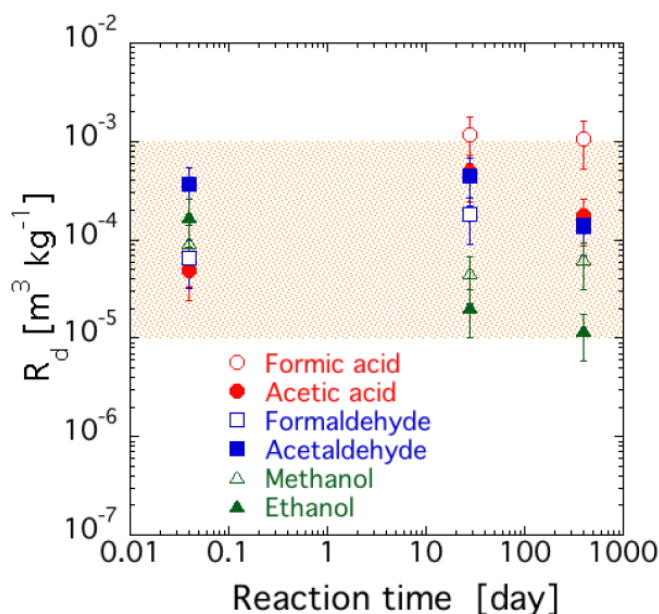


FIGURE 3-6: Uptake of low molecular weight organic compounds by HCP as a function of reaction time.

3.3 Diffusion in cement-based materials

The relevant theoretical concepts and the main equations are given in more detail in sub-chapter 4.4 of the present SOTA.

Very few studies (Chida and Sugiyama, 2008; Kaneko *et al.*, 2003; Matsumoto *et al.*, 1995; Sasoh, 2008; Wieland *et al.*, 2016) are available on the diffusion of organic compounds through cement pastes, mainly because of the poor mobility of organic compounds in compacted materials such as cement pastes. Overall, the available studies focused on small organic compounds (acetic acid, acetaldehyde, ethanol, formaldehyde, formic acid and methanol) providing only rather limited information on the diffusion and sorption properties of the cement pastes. Wieland and co-workers concluded in their work that acetate (CH_3COO^-) diffusion could be fairly well explained with one-site model, while formate (CHOO^-) diffusion required an additional parameter indicative of a second sorption site (Wieland *et al.*,

2016). This means that even a relatively small difference in the organic carbon chain, from 1 carbon to 2 carbons, may have a significant impact on the organic sorption behaviour due to the limited available pore space in the diffusion experiments.

3.4 CORI Results: Update on organic sorption and adsorption

In WP CORI the sorption and diffusion properties of several organic compounds on cement-based materials have been investigated as follows:

- Isosaccherinic acid (ISA), sorption tests.
- EDTA, sorption and diffusion tests.
- NTA, sorption tests.
- Phthalate, sorption and diffusion tests.
- Adipate, sorption tests.
- Gluconate, sorption tests.
- Citrate, sorption tests.
- Formate, sorption tests.
- Glutarate (GTA), sorption tests.
- HIBA and HBA, sorption tests.
- Superplasticizers, sorption tests.
- Real degradation products obtained in the WP CORI, sorption tests.

Cementitious materials studied in WP CORI range from hardened cement paste at different degradation stages (I, II and III) to pure solid phases (i.e. CSH, CASH, Ettringite, etc.). In the following sub-sections a brief description of the results is provided. The most relevant organic sorption results gathered within WP CORI are compiled in the public project Deliverable D3.6,7,8 (Altmaier et al., 2024). The reader is referred to this document for further results and interpretation.

3.4.1 Sorption results from CORI

Overall, a significant amount of new data has been generated in CORI, increasing the knowledge of the different systems as defined in the initial WP CORI State of the Art published in 2020 (D.3.2).

One of the main outcome is the discrepancies between the different types of organics in terms of K_d values. ISA and GLU are significantly sorbed while glutaric acid (GTA), citrate and formate exhibit only very weak sorption on the investigated materials. This confirms previous works on binary systems ORG/cement and support K_d values derived for organic retention on the cement-based materials for use in the context of safety assessments.

Sorption results of ISA, EDTA and phthalate for HCP at degradation stage III compared to the materials at stage I and/or stage II, shown that the sorption is lower at the degradation state III. Also, the trend as a function of the equilibrium concentration (C_{eq}) remains the same whatever the degradation stage. Indeed, for ISA, the K_d value decreases as C_{eq} increases from $C_{eq} = 10^{-5}$ M at stage I and stage III while for EDTA, K_d slightly evolves for stage II, and stage III/IV. Apparently, the chemical degradation of the cement-based materials does not modify the threshold concentrations related to the decrease of the sorption due to the possible saturation of the adsorption sites.

ISA has been one of the most studied molecules due to the high amount of cellulose in the chemical inventory of radioactive waste (from low level to intermediate level waste). All K_d values obtained for ISA in the different cement-based materials investigated in WP CORI can be associated with a general trend

regarding the evolution of K_d values as a function of the ISA concentration, i.e. K_d decrease as ISA concentration increase in the system. In particular, it should be emphasized that there is a remarkable agreement between the existing data.

The measurements of GLU sorption on C-S-H phases provided by Guidone (2023) agree very well with the results given in Androniuk (2017). This observation validates the acquired data on C-S-H but also for the other cement hydrates.

One of the most relevant new outcomes is the determination of sorption properties for cement hydrates other than C-S-H phases. Indeed, WP CORI results have clearly shown that AFm/AFT phases and portlandite can sorb with high affinities organic molecules in the case of citrate and ISA, respectively. The sorption properties of some of individual phases (e.g. AFm, HC) can have similar K_d values like C-S-H. Consequently, this outcome can confirm and explain the higher K_d values observed in HCP relative to C-S-H, and provides consistent information in terms of mechanistic knowledge and understanding of the processes involved in the sorption of organic molecules on cement-based-materials.

3.4.1 Diffusion results

Organic diffusion tests have been conducted by several partners within CORI at different cement degradation stages. Classical through-diffusion cells, in-diffusion tests and novel electro-migration tests were used by the different organizations involved in WP CORI.

The obtained results confirmed the previous observed trends, indicating that organic diffusion is an extremely slow process. Even after four years of experimental tests, organic compounds have not been detected in the downstream cells of the diffusion experiment setups.

3.5 Conclusion

For cementitious materials, little information is available on the behaviour of organic compounds, especially so in comparison with clay-rock materials. That can be explained by challenges arising from the large range of systems (in terms of degradation states and cement formulations), and by the properties of organic species in solution at high pH (in terms of speciation). Even if a general behaviour of the organic molecules in cementitious systems cannot be foreseen at this time, some works on argillaceous materials proposed correlations between the molecular properties (molecular mass, dipolar moment, partition factor) and the transfer properties of organic molecules (solid/liquid distribution coefficient, K_d and effective diffusion coefficient, D_e) which could be extended to cement-based materials (Dagnelie *et al.* 2014, 2018); Rasamimanana *et al.* 2017).

WP CORI has provided a significant amount of new organic sorption data for a wide range of cementitious systems at different geochemical conditions. Several data gaps have been filled by the results obtained in WP CORI. However, other uncertainties have arisen due to the complexity of the cement-based materials investigated and the needs of a better system characterization. Please see CORI Deliverable D.3.6,7,8, for further information on research performed in CORI Task 2 on organics retention.

3.6 References for Chapter 3

- Allard, S., 2005. Investigations of α -D-isosaccharinate: Fundamental Properties and Complexation (PhD Thesis). Chalmers University of Technology.
- Allard, S., Ekberg, Ch., 2006. Complexing properties of alpha-isosaccharinate: Thorium. *Radiochimica Acta* 94, 537–540.
- Albrecht, A., Altmann, S., Buschaert, S., Coelho, D., Gallerand, M.O., Giffaut, E. & Leclerc-Cessac, E. (2005). Dossier 2005 Argile. Référentiel du comportement des radionucléides et des toxiques chimiques d'un stockage dans le Callovo-Oxfordien jusqu'à l'homme. ANDRA.
- Androniuk, I., 2017. Effects of cement organic additives on the adsorption of uranyl ions on calcium silicate hydrate phases : experimental determination and computational molecular modelling (PhD Thesis). Ecole nationale supérieure Mines-Télécom Atlantique Bretagne Pays de la Loire.
- Androniuk, I., Landesman, C., Henocq, P., Kalinichev, A.G., 2017. Adsorption of gluconate and uranyl on C-S-H phases: Combination of wet chemistry experiments and molecular dynamics simulations for the binary systems. *Physics and Chemistry of the Earth, Parts A/B/C, Mechanisms and Modelling of Waste-Cement and Cement-Host Rock Interactions* 99, 194–203.
- Altmaier, M., Ricard D., Vandenborre J., Garcia D., Henocq P., Macé N., Missana T. (2024): Final report of results generated in CORI. Final Deliverables D3.6, D3.7 and D.8 of the HORIZON 2020 project EURAD. EC Grant agreement no: 847593.
- Berckmans, A., Boulanger, D., Brassinnes, S., Capouet, M., Depaus, C., Dorado Lopez, E., Gambi, A., Gens, R., Sillen, X., Van Baelen, H., Van Geet, M., Van Marcke, P., W, W., Wouters, L., Harvey, L., Wickham, S., Pirot, V., 2013. ONDRAF/NIRAS Research, Development and Demonstration (RD&D) plan for the geological disposal of high-level and/or long-lived radioactive waste including irradiated fuel if considered as waste. State-of-the-art report as of December 2012 (No. NIRONDR-TR 2013-12 E). ONDRAF/NIRAS.
- Brinkmann, H., Patzschke, M., Kaden, P., Raiwa, M., Rossberg, A., Kloditz, R., Heim, K., Moll, H. and Stumpf, T. (2019). Complex formation between UO_2^{2+} and α -isosaccharinic acid: insights on a molecular level. *Dalton Transactions*, 48(35), 13440-13457.
- Boggs, M.A., Dong, W., Gu, B., Wall, N.A., 2010. Complexation of Tc(IV) with acetate at varying ionic strengths. *Radiochimica Acta* 98, 583–587.
- Chida, T., Sugiyama, D., 2008. Diffusion behavior of organic carbon and iodine in low-heat Portland cement containing fly ash. *Mater. Res. Soc. Symp. Proc.* 1124, 379-384.
- Colàs, E., 2014. Complexation of Th (IV) and U (VI) by polyhydroxy and polyamino carboxylic acids (PhD Thesis). Universitat Politècnica de Catalunya.
- Colàs, E., Grivé, M., Rojo, I., 2013. Complexation of Uranium(VI) by Gluconate in Alkaline Solutions. *J Solution Chem* 42, 1545–1557. <https://doi.org/10.1007/s10953-013-0048-0>
- Dagnelie, R., Descostes, M., Pointeau, I., Klein, J., Grenut, B., Radwan, J., Lebeau, D., Georgin, D., Giffaut, E. Sorption and diffusion of organic acids through clayrock; comparison with inorganic anions. *Journal of hydrology* (2014). Vol 511, pp.619–27.
- Dagnelie, R. V. H., Rasamimanana, S., Blin, V., Radwan, J., Thory, E., Robinet, J. C., & Lefèvre, G. (2018). Diffusion of organic anions in clay-rich media: Retardation and effect of anion exclusion. *Chemosphere*, 213, 472-480.
- Dario, M., Molera, M., Allard, B., 2004. Effect of organic ligands on the sorption of europium on TiO_2 and cement at high pH (No. SKB-TR--04-04). Swedish Nuclear Fuel and Waste Management Co.

- Evans, N.D.M., 2003. Studies on metal α -isosaccharinic acid complexes (PhD Thesis). Loughborough University.
- Felipe-Sotelo, M., Hinchliff, J., Evans, N., Warwick, P., Read, D., 2012. Sorption of radionuclides to a cementitious backfill material under near-field conditions. *Mineral. mag.* 76, 3401–3410.
- Gaona, X., Montoya, V., Colàs, E., Grivé, M., Duro, L., 2008. Review of the complexation of tetravalent actinides by ISA and gluconate under alkaline to hyperalkaline conditions. *Journal of Contaminant Hydrology* 102, 217–227.
- García, D., Henocq, P., Riba, O., López-García, M., Madé, B., & Robinet, J. C. (2020). Adsorption behaviour of isosaccharinic acid onto cementitious materials. *Applied Geochemistry*, 104625.
- González-Siso, M.R., Gaona, X., Duro, L., Altmaier, M., Bruno, J., 2018. Thermodynamic model of Ni(II) solubility, hydrolysis and complex formation with ISA. *Radiochimica Acta* 106, 31–45.
- Guidone (2023) Impact of formate, citrate and gluconate on the retention of Pu(III/IV), Eu(III) and Cm(III) by cement phases. PhD thesis, KIT, Germany.
- Guidone, R.E., Gaona, X., Winnefeld, F., Altmaier, M., Geckeis, H., Lothenbach, B., 2024. Citrate sorption on cement hydrates. *Cement and Concrete Research* 178, 107404. <https://doi.org/10.1016/j.cemconres.2023.107404>.
- Holgersson, S., Albinsson, Y., Allard, B., Boren, H., Pavasars, I., Engkvist, I., 1998. Effects of glucoisosaccharinate on Cs, Ni, Pm and Th sorption onto, and diffusion into cement. *Radiochimica Acta* 82, 393–398.
- Holgersson, S., Dubois, I., Boerstel, L., 2011. Batch experiments of Cs, Co and Eu sorption onto cement with dissolved fibre mass UP2 in the liquid phase (No. SKB-P--11-24). Swedish Nuclear Fuel and Waste Management Co.
- Kaneko, S., Tanabe, H., Sasoh, M., Takahashi, R., Shibano, T., Tateyama, S., 2003. A study on the chemical forms and migration behavior of carbon-14 leached from the simulated hull waste in the underground condition. *Mater. Res. Soc. Symp. Proc.* 757, 621-626.
- Keith-Roach, M.J., 2008. The speciation, stability, solubility and biodegradation of organic co-contaminant radionuclide complexes: A review. *Science of The Total Environment* 396, 1–11.
- Matsumoto, J., Banba, T., Muraoka, S., 1995. Adsorption of carbon-14 on mortar. *Mater. Res. Soc. Symp. Proc.* 353, 1029-1035.
- Poiteau, I., Coreau, N., Reiller, P.E., 2008. Uptake of anionic radionuclides onto degraded cement pastes and competing effect of organic ligands. *Radiochimica Acta* 96, 367–374.
- Poiteau, I., Hainos, D., Coreau, N., Reiller, P., 2006. Effect of organics on selenite uptake by cementitious materials. *Waste Management, Mechanisms and Modeling of Waste/Cement Interactions* 26, 733–740.
- Ochs, M., Colàs, E., Grivé, M., Olmeda, J., Campos, I., Bruno, J., 2014. Reduction of radionuclide uptake in hydrated cement systems by organic complexing agents: Selection of reduction factors and speciation calculations (No. SKB R-14-22). Swedish Nuclear Fuel and Waste Management Co.
- Ochs, M., Vielle-Petit, L., Wang, L., Mallants, D., & Leterme, B. (2010). Additional sorption parameters for the cementitious barriers of a near-surface repository. ONDRAF/NIRAS, Brussels, Belgium., ONDRAF/NIRAS report NIROND-TR 2010-06 E, 147p., 2010.
- Rasamimanana, S., Lefèvre, G., & Dagnelie, R. V. H. (2017). Adsorption of polar organic molecules on sediments: Case-study on Callovian-Oxfordian claystone. *Chemosphere*, 181, 296-303.
- Sasoh, M., 2008. Investigations of distribution coefficients for C-14 from activated metal. In: Johnson, L., Schwyn, B. (Eds.), *Proceedings of a Nagra/RWMC Workshop on the Release and Transport of*

- C-14 in Repository Environments, pp. 83-86. Nagra Working Report NAB 08-22, Nagra, Wettingen, Switzerland.
- Tasi, A., Gaona, X., Fellhauer, D., Böttle, M., Rothe, J., Dardenne, K., Polly, R., Grivé, M., Colàs, E., Bruno, J., Källström, K., Altmaier, M., Geckeis, H., 2018a. Thermodynamic description of the plutonium – α -D-isosaccharinic acid system II: Formation of quaternary Ca(II)–Pu(IV)–OH–ISA complexes. *Applied Geochemistry* 98, 351–366.
- Tasi, A., Gaona, X., Fellhauer, D., Böttle, M., Rothe, J., Dardenne, K., Polly, R., Grivé, M., Colàs, E., Bruno, J., Källström, K., Altmaier, M., Geckeis, H., 2018b. Thermodynamic description of the plutonium – α -D-isosaccharinic acid system I: Solubility, complexation and redox behavior. *Applied Geochemistry* 98, 247–264.
- Thakur, P., Mathur, J.N., Dodge, C.J., Francis, A.J., Choppin, G.R., 2006. Thermodynamics and the structural aspects of the ternary complexes of Am(III), Cm(III) and Eu(III) with Ox and EDTA + Ox. *Dalton transactions* 4829–4837.
- Tits, J., Bradbury, M., Eckert, P., Schaible, A., Wieland, E., 2002. The Uptake of Eu(III) and Th(IV) by Calcite under Hyperalkaline Conditions: The Influence of Gluconic and Isosaccharinic Acid (No. PSI Nr. 02-03). Paul Scherrer Institut.
- Vercammen, K., 2000. Complexation of Calcium, Thorium and Europium by α -Isosaccharinic Acid under Alkaline Conditions (PhD Thesis). Swiss Federal Institute of Technology Zurich.
- Vercammen, K., Glaus, M.A., Van Loon, L.R., 2001. Complexation of Th(IV) and Eu(III) by α -Isosaccharinic acid under alkaline conditions. *Radiochimica Acta* 89, 393–401.
- Wang, L., Martens, E., Jacques, D., De Cannière, P., Berry, J., & Mallants, D. (2008). Review of sorption values for the cementitious near field of a near surface radioactive waste disposal facility. Project near surface disposal of category A waste at Dessel, NIROND-TR, 23.
- Wieland, E. (2014). Sorption data base for the cementitious near field of L/ILW and ILW repositories for provisional safety analyses for SGT-E2. Nagra, TR 14-08, Nagra, Wettingen, Switzerland.
- Wieland, E., Jakob, A., Tits, J., Lothenbach, B., and Kunz, D. (2016). Sorption and diffusion studies with low molecular weight organic compounds in cementitious systems. *Applied geochemistry*, 67, 101-117.

4. Radionuclide-organic-cement interactions

Authors: Nathalie Macé, Virginie Blin [CEA] and Tiziana Missana [CIEMAT]

This chapter provides an overview of the current knowledge on radionuclide and organic ligands interactions under cementitious environments, focusing on the specific species selected in WP3 CORI.

4.1 Introduction to WP CORI Task 4 objectives

In any international radioactive waste disposal concept, including surface disposal, near surface or deep geological disposal (Andra, 2005; Ochs *et al.*, 2016), the main objective of a multi-barrier system is to prevent radionuclides (RN) from spreading into the environment. After the breach of the primary waste containers, the aim is to slow down as much as possible the dispersion of the radionuclides progressively released from these containers. To guarantee the long-term safety of radioactive waste disposals, one of the main research challenges is to provide a robust understanding of all the processes controlling RN interactions within the materials composing the system. The multi-barrier system is made up of the waste packages, the man-made engineered barriers and, for deep geological disposal, the host rock (geological barrier).

Cementitious materials are amongst the main constituents of waste packages and the engineered barriers for low and intermediate level radioactive waste (L/ILW) disposal. They are typically used as encapsulation matrix, package material, backfill and structural material because their mechanical resistance. These materials, mainly grouts, mortar or concrete, are porous; meaning that they are composed of a solid matrix with reactive surfaces and a porewater with a chemical composition specific for cementitious materials (see SOTA Chapter 5), characterised by highly alkaline pH conditions.

The main processes controlling RN migration are: solubility, retention processes and physical transport.

- The chemical speciation of RN and eventually precipitated solubility limiting solid phases in cementitious pore water govern their solubility. Depending on the chemical composition of the pore water (pH, redox potential E_h , major matrix ions, ligands ...), RN can form different chemical species with potentially distinct chemical behaviour.
- The retention or uptake of RN in cementitious environments is the result of interactions between the dissolved radionuclide species in solution and the surface of the cementitious solid matrix material. This important parameter can be quantified by determining (*e.g.* in batch experiments) the solid/liquid distribution coefficient, K_d , [$L \cdot kg^{-1}$] which represents the ratio between the RN concentration adsorbed onto the solid and the RN concentration remaining in the porewater at equilibrium. Adsorption is one of the most important retention processes, but other processes as (co)precipitation, formation of new minerals or solid solutions may trap RN in the solid matrix irreversibly.
- Radionuclide transport processes in porous materials are induced by several possible gradients (chemical, electric, hydraulic...). That leads to different physical phenomena encountered in the disposal concepts, such as advection and / or diffusion. A key process being studied in cementitious materials is the diffusive transport induced by chemical gradients, like the concentration gradient. Diffusion is quantified by diffusion coefficients which are both species- and material-specific.

Knowing the source term of radionuclides in the waste packages, the combination of the three above-mentioned processes allows explaining the reactive transport (migration) of the RN through the cementitious barrier. All factors affecting RN chemical speciation / solubility and their interactions with mineral surfaces are relevant for contaminant migration. Thus, a thorough analysis of all the factors and mechanisms that can contribute to contaminant mobility is required. This fundamental knowledge is necessary to predict RN behaviour and assess the long-term safety of a repository, minimise the associated risks and support management decisions.

When some additional chemical species are released in a disposal system in significant amounts, *i.e.* organic molecules in the present case, they can affect RN behaviour. The presence of organics is a main cause of contaminant mobility enhancement (Means and Crear, 1978; Santschi *et al.*, 2017). The impact of organic molecules on RN migration is related to RN-organic complexes formation, that increase RN solubility and/or inhibit RN retention on solids (Hummel *et al.*, 2005a and reference therein). Even if these particular effects have been known since a long time, they are far from being elucidated and described in a scientifically advanced mechanistic way (Keith-Roach, 2008). Therefore, it is still very difficult to predict them adequately. EURAD-CORI aims to improve this situation.

The presence of anthropogenic organics is a particular case in L/ILW disposal, mainly because their amount is higher than the organics naturally present in a geological formation and additionally feature a high degree of chemical diversity. As reported in previous in Chapter 2 and 3 of this SOTA, many different types of plastic wastes (halogenated polymers as polyvinyl chloride PVC, non-halogenated polymers as polythene PE), papers, woods, rubber or ion exchange resins (IER) are co-stored with the contaminants. Over time, they can lead to a large variety of degradation products in addition to the organic complexants (EDTA, NTA, ...) disposed of as part of certain waste products.

The impact of organic molecules on RN migration depends on many factors: (i) the type and concentration of organics, (ii) the surrounding solid and aqueous phases which will provide the physicochemical scenario (pH, E_h , ionic strength, type of ion in solution), and (iii) on the characteristics of the contaminant itself (sorption capability, speciation, hydrolysis...). The organic degradation products present in radioactive disposal and the inventories change from one country to another (Abrahamsen *et al.*, 2015). This means that the overall performance can be considered as *site-specific*. To make reliable predictions of RN migration under a wide range of conditions, detailed understanding at the fundamental level is required. CORI Task 4 works to improve the knowledge on organic-radionuclide complexes mobility in cement-based systems by providing mechanistic understanding of interaction processes and provide detailed and new quantitative experimental data.

The cementitious materials and organics studied in CORI Task 4 are prioritised in view of their applied and scientific relevance and are consistent with CORI Tasks 2 and 3:

- CEM I and CEM V cements are used as raw materials for cementitious samples preparation, considering different degradation stages. Amongst the main mineral phases considered, C-S-H (calcium silicate hydrates, $(CaO)_x(SiO)_y(H_2O)_n$) and C-A-S-H (calcium alumina silicate hydrates, $(CaO)_x(SiO)_y(Al_2O_3)_z(H_2O)_n$) will be studied considering different CaO/SiO₂ molar (C/S) ratios;
- organic ligands include, ISA (isosaccharinic acid, C₆H₁₂O₆), EDTA (ethylenediaminetetraacetic acid, C₁₀H₁₆N₂O₈), adipic acid (C₆H₁₀O₄), phthalic acid (C₈H₆O₄) or short-chained carboxylic acids, as well as the degradation products that are identified in CORI Task 2. Finally, organic cement additives as superplasticizers are also considered.

The main radionuclides studied in CORI Task 4 are: nickel isotopes; uranium isotopes; actinides (III/IV) mainly Am, Cm, Pu and Th and/ or chemical homologues as, for example, Eu.

4.2 Radionuclide chemistry in cementitious environments

4.2.1 Speciation/solubility under alkaline conditions

The first information needed to assess the behaviour of radionuclides in cementitious materials, regards their chemical speciation under alkaline conditions. In a cementitious pore water, the speciation is specifically controlled by the interactions with the ubiquitous hydroxyl “OH⁻” ions that create hydrolytic species but also other major/minor dissolved ions or neutral species (see Guillaumont *et al.*, 2003 and especially the recent update from Grenthe *et al.*, 2020 for the main actinides U, Np, Pu, Am and Tc).

The properties of both radionuclides and organic molecules in solution are characterised by their speciation and their solubility (Hummel *et al.*, 2005a). According to IUPAC conventions, the analytical composition of a saturated solution, expressed in terms of the proportion of a designated solute (e.g. Mⁱ or Orgⁱ) in a designated solvent, is the solubility of that solute. The solubility may be expressed in several ways, e.g. concentration, molality, mole fraction, or mole ratio. Solubility does not consider just the amount of the free ion, (Mⁱ) in solution but the sum of all aqueous species of Mⁱ as shown in eq. 4-1, where L^k stands for the different ligands (hydroxyl ion, organics, *etc.*) present in solution.

The thermodynamic solubility is one of the most important parameters to consider in migration studies as it represents the capacity of a given solid phase to dissolve under given geochemical boundary conditions and defines the maximum possible concentration in the aqueous phase of the elements composing it.

$$\text{Solubility} = [M]_{TOTAL} = [M^i] + [ML^{i+k}] + [ML_2^{i+2k}] + \dots \quad (\text{eq. 4-1})$$

The distribution of all aqueous chemical species of Mⁱ or Orgⁱ in a system is defined by IUPAC as the element chemical speciation and is therefore dependent on the nature of the solution.

In general, the precipitation of a contaminant to form a solid (non-colloidal) phase is often favourable from an environmental point of view, because it limits the contaminant concentration in the aqueous phase and limits its transport. Precipitation (or co-precipitation) can be a relevant retention/uptake process under the alkaline conditions generated by cementitious materials. However, the complexation phenomena existing between radionuclides and certain organic molecules (ligands) influence the RN speciation by eventually outcompeting hydrolysis under alkaline to hyperalkaline pH conditions. RN-organics complex formation is potentially related to significant changes in RN solubility.

4.2.2 Speciation/solubility in the presence of organic ligands

Regarding speciation/solubility of RN in the presence of organic ligands, the OECD Nuclear Energy Agency review work remains a major reference (Hummel *et al.*, 2005b; carried out within the framework of the Thermochemical Database Project NEA-TDB Phase II). The work focused on the complexes of U, Np, Pu, Am, Tc, Se, Ni and Zr, as well as interactions with the major competing elements Na, K, Mg and Ca with selected organic ligands (oxalate, citrate, EDTA and α-ISA). This is a very extensive work but still not complete. Rather few information for the conditions of interest is available for trivalent actinides, Np, Pu(IV), U(IV) and for Th(IV) since a quite large variability in the experimental data has been detected and, above all, because data are rarely obtained under the hyperalkaline conditions typical for cementitious environments (Felipe-Sotelo *et al.*, 2015). NEA-TDB is preparing an update of the previous organics volume within the current Phase V.

Two additional reviews carried out by Gaona *et al.* (2008) and Rai and Kitamura (2017) enrich the selection on available thermodynamic data concerning complexation of RN by ISA and/or gluconic acid (GLU), present as gluconate species in alkaline to hyperalkaline pH conditions. In the work of Gaona *et al.* (2008), the available thermodynamic data for An(IV)–ISA/GLU complexes have been reviewed and re-calculated to ensure the internal consistency of the stability constants assessed. Further modelling exercises, estimations based on Linear Free-Energy Relationships (LFER) among tetravalent actinides, as well as direct analogies between ISA and GLU complexes have also been performed. This approach has led to the definition of a speciation scheme for the complexes of Th(IV), U(IV), Np(IV) and Pu(IV) with ISA and GLU forming in alkaline to hyperalkaline pH conditions, both in the absence and presence of calcium. Rai and Kitamura (2017) reviewed and recommended equilibrium constant values for ISA complexation reactions involving Ca, Fe(III), Th, Np(IV), and U(VI). The authors considered that the available data for Pu(IV), U(IV), and Am(III) were extremely limited and based on ill-defined/controlled experimental techniques and should be used for scoping studies only. Obviously, even for the most studied organic ligands like ISA, many knowledge gaps on contaminant-organic interaction reactions still exist. Another similar example from the literature are the reported stability constants for actinide-EDTA complexes that vary by orders of magnitude (Cartwright *et al.*, 2007).

A more recent experimental study in the ISA system was performed by Tasi *et al.* (2018a) providing the most comprehensive thermodynamic dataset available to date for the system Pu^{3+} – Pu^{4+} – OH^- – Cl^- – ISA^- – $\text{H}_2\text{O}(\text{l})$, that is valid under a wide range of conditions relevant for nuclear waste disposal (see FIGURE 4-1 below).

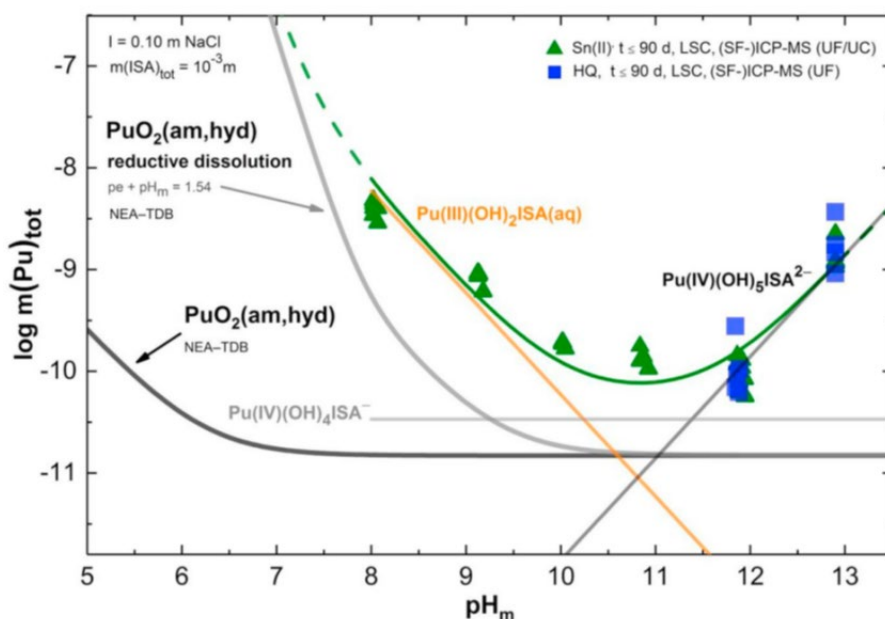


FIGURE 4-1: Experimentally measured $m(\text{Pu})_{\text{tot}}$ in equilibrium with $\text{PuO}_2(\text{ncr,hyd})$ at $I = 0.10 \text{ m NaCl}$ in $\text{Sn}(\text{II})$ -buffered systems with $\text{pH}_m = 8.0$ – 12.9 in the presence of $m(\text{ISA})_{\text{tot}} = 10^{-3} \text{ m}$ and in hydroquinone-buffered systems, at $\text{pH}_m > 11$ with $m(\text{ISA})_{\text{tot}} = 10^{-3} \text{ m}$.

Solubility curves (solid and dashed) in green (with $m(\text{ISA})_{\text{tot}} = 10^{-3} \text{ m}$) for $\text{Pu}(\text{IV})\text{O}_2(\text{ncr,hyd})$ in the presence of ISA are calculated (at $I = 0.10 \text{ m NaCl}$) using the chemical and thermodynamic models derived by Tasi *et al.* (2018a). Black and grey solid lines correspond to the thermodynamically calculated solubility of $\text{PuO}_2(\text{am,hyd})$ in the absence of ISA, calculated using equilibrium constants reported in the NEA-TDB (Guillaumont *et al.*, 2003) (Fig. 4-1 taken from Tasi *et al.*, 2018a).

It should be noted that the Supporting Information linked to this paper by Tasi *et al.* provides a recent “Review of previous experimental studies on the complexation behaviour of ISA with tri- and tetravalent actinides” by the same authors.

Considering other organic ligands targeted in CORI, the studies from Reiller *et al.* (2017) and Fromentin and Reiller (2018) needs to be mentioned. The authors investigated the complexation of Eu(III) by adipic acid, a major hydrosoluble degradation product of γ -irradiated polyesterurethane. The formation of a complex between Eu^{3+} and Adip^{2-} was confirmed by time resolved laser-induced fluorescence spectroscopy (TRLFS) investigations and the complexation constant was extrapolated from experimental data. This led to a discussion of previous data published by Wang *et al.* (2000). Using the same kind of spectroscopic properties, Wang *et al.* (1999) had also studied the complexation of lanthanide(III) with aliphatic dicarboxylic acids, and particularly with phthalate, isophthalate and terephthalate. Fromentin and Reiller (2018) concluded that the formation of EuAdip^+ could only occur at weakly acidic to mildly basic pH values ($4 < \text{pH} < 9$). Under the studied conditions ($0.3 \text{ mol kg}_w^{-1}$ adipate / $0.5 \text{ mol kg}_w^{-1}$ NaClO_4) adipate does not seem to be able to complex Eu(III) and outcompete hydrolysis in alkaline media with $\text{pH} > 10$. A predominance diagram of the Eu(III)-adipate system is given below in FIGURE 4-2.

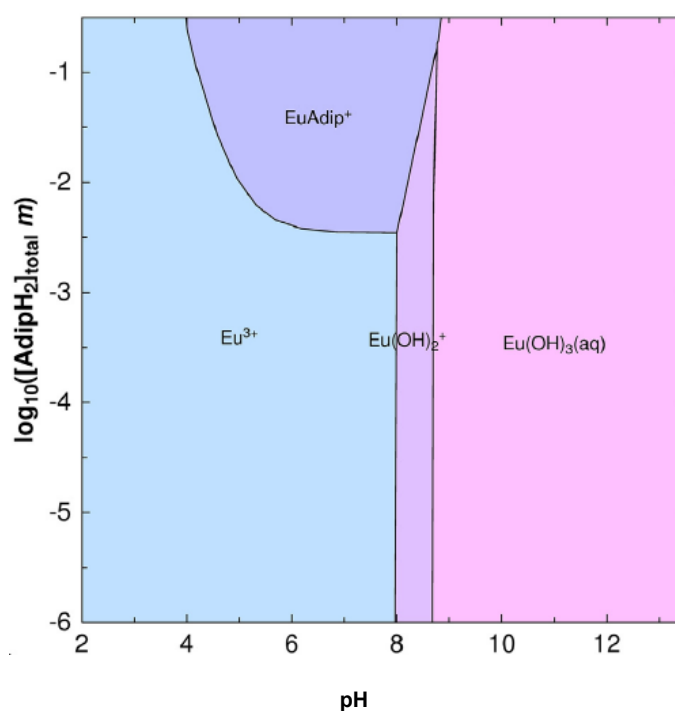


FIGURE 4-2: Predominance diagrams of Eu(III) $10^{-6} \text{ mol} \cdot \text{kg}_w^{-1}$ vs. pH with increasing total adipic acid concentration, $I=0.1 \text{ mol} \cdot \text{kg}_w^{-1}$ (NaClO_4) at $P(\text{CO}_2)=10^{-12} \text{ atm}$. Diagram obtained using Phreeplot software (Kinniburgh and Cooper, 2011) (Fig. 4-2 taken from Fromentin and Reiller, 2018).

Very recently in 2020, Fromentin and Reiller (2020) studied interactions between hydro-soluble degradation products from a radio-oxidized polyesterurethane and Eu(III). In their work (using gamma irradiation at 1000 kGy and 31 days in a pH 13.3 artificial cement water at 60°C), the main hydro-soluble degradation products are adipic acid and butane-1,4-diol. The use of TRLFS showed the existence of several types of Eu(III) complexes depending on pH ranges. The fluorescence of europium was

investigated as a function of total organic carbon content and pH and has indicated at least two relevant Eu(III) complexes. However, it should be noticed that the interpretation of complexation at pH > 10, and especially at pH 13.3, is not straightforward.

Rojo et al. (2021) studied the effect of GLU on the solubility/speciation of Nd(III)/Cm(III) in alkaline NaCl and CaCl₂ solutions. In NaCl solutions, the solubility of Nd(OH)₃(s) remains mostly unaffected with [GLU]_{tot} = 10⁻³ M, whereas a clear increase in solubility is observed in dilute CaCl₂ solutions with the same [GLU]_{tot} and pH_c ≥ 11. Under similar conditions, TRLFS measurements indicate the formation of ternary Ca-Cm(III)-GLU complexes. Density functional theory calculations provide additional support to the formation of stable ternary Ca-Nd(III)-GLU aqueous complexes. In concentrated CaCl₂ solutions, GLU does not affect the solubility of Nd(III) due to the competition with Ca-GLU complexes.

The workability of cements is usually improved by the addition of organic additives like superplasticizers, a group of several different chemical substances. Several studies have been dedicated to the complexation of RN or heavy metals by such molecules under cementitious environments (Glaus *et al.*, 2003; Young, 2012; Wieland *et al.*, 2014; García *et al.*, 2018a; Baston *et al.*, 2019).

A recent study on operational solubility of Eu(III) in contact with degraded by radiolysis PNS and PCE superplasticiser in alkaline solution has been presented by Legand et al. (2023) based on the PhD work of Legand (2023). As shown in FIGURE 4-3, three different media were investigated as a function of dose (0-250 kGy): undiluted PCE alkaline solutions (FIGURE 4-3a), diluted PCE alkaline solutions (FIGURE 4-3b) and extracted pore solutions of the grout (FIGURE 4-3c). Similar trends are observed for PNS superplasticizer. The addition of SP in alkaline solution leads to increase the Eu(III) solubility with the dose. However, no significant impact of coupled effect of radiolysis for doses lower than 250 kGy, and alkaline hydrolysis (pH 12.9) of SPs on Eu(III) solubility in pore solution (SP-grout with 1 and 2 wt% of PCE and PNS, respectively) were observed. The small amount of degraded molecules leached in pore solution has a weak effect on Eu(III) solubility.

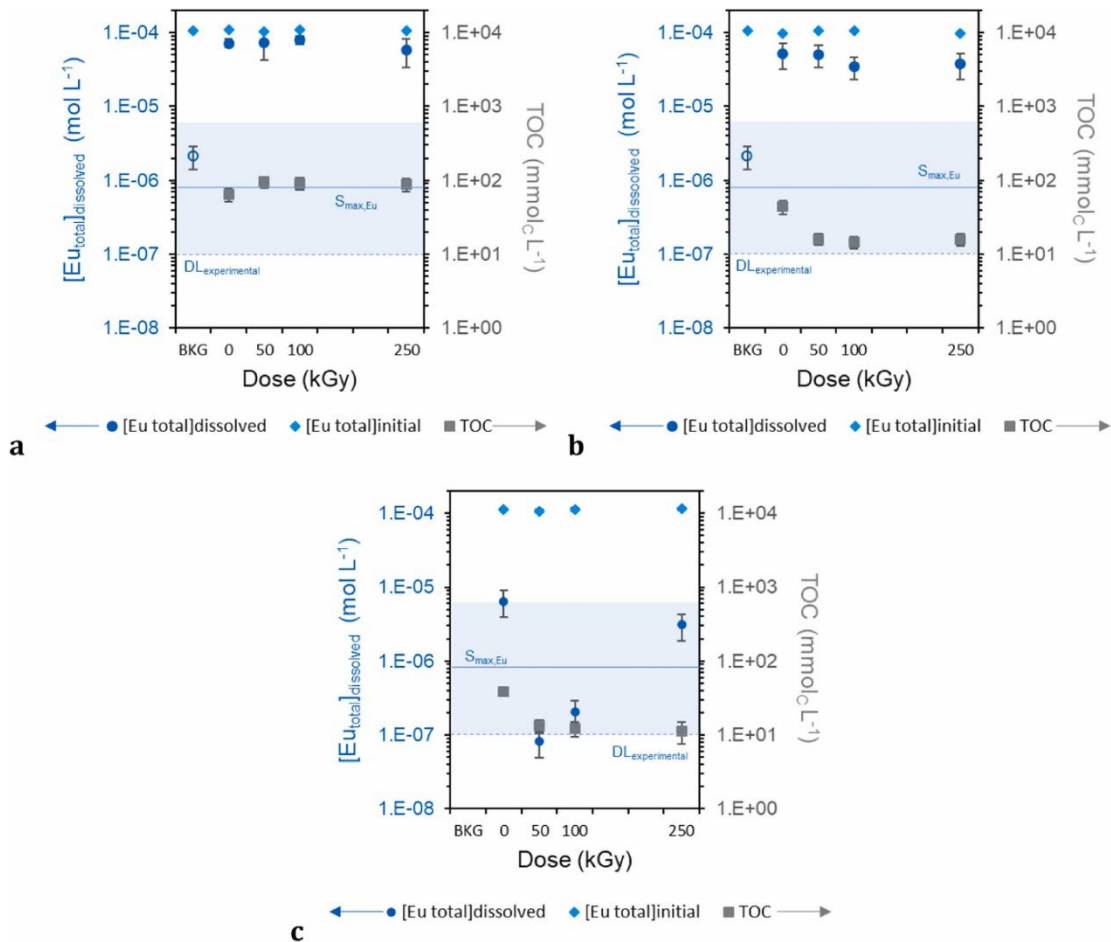


FIGURE 4-3: Concentration of total initial Eu (mol L⁻¹, blue diamonds), total dissolved Eu (mol L⁻¹, blue circles) and TOC content (mmol^c L⁻¹, grey squares) in alkaline solution (without SP, BKG), in undiluted PCE alkaline solutions (a), in diluted PCE alkaline solutions (b) and in extracted pore solutions (c) as a function of dose (from 0 to 250 kGy): Eu solubility limits in the medium S_{max, Eu} (mol L⁻¹, blue plain line) with combined uncertainty (blue shaded area), experimental detection limit DL_{experimental} (mol L⁻¹, blue dotted line). (Fig. 4-3 taken from Legend *et al.*, 2023).

4.2.3 Speciation/solubility calculations

Predictive geochemical modelling is commonly used to assess the chemical speciation of an element in a specific environment. Predictions are developed based on thermodynamic equilibrium modelling and speciation software, *e.g.* PHREEQC geochemical code (Parkhurst and Appelo, 2013). Apart from the NEA-TDB Project mentioned earlier, which provides a most valuable set of critically reviewed and consistent thermodynamic data recommended for use but is as such not complete in terms of the systems and species covered, other specific thermodynamic databases were developed in the field of radioactive waste management with clearly better usability.

The PSI/Nagra Chemical Thermodynamic Database 12/07 (PSI/Nagra TDB 12/07; Thoenen *et al.*, 2014) was prepared to support the ongoing safety assessments in the framework of the “Sachplan Geologische Tiefenlager” for the planned repositories for low- and intermediate-level and for high-level radioactive waste in Switzerland.

The ThermoChimie database (Giffaut *et al.*, 2014) is managed by the French, Belgian and British waste management agencies; Andra, Ondraf-Niras and RWM, respectively. Since its initial creation by Andra in 1996, ThermoChimie has been based on (i) previous thermodynamic database compilations; (ii) open

scientific literature; (iii) data obtained by means of specific experimental programs on actinides and fission products carried out under the auspices of Andra or other reputable experimental programs endorsed by Nuclear Waste Management organizations and research institutions; (iv) estimations (Giffaut *et al.*, 2014). Thus, as shown in TABLE 3-3, many RN thermodynamic data addressing the systems studied in CORI are available in this database.

Organic ligands can have a significant impact on RN complexation reactions in the aqueous phase and hence on radionuclide speciation and/or solubility. Based on thermodynamic databases, these effects can be constrained by (geo)chemical calculations in several cases, although a significant numbers of ligand systems remain under-defined. In the preparation phase of EURAD CORI it was decided that CORI shall not carry out studies specifically targeting the development of new thermodynamic data for databases. Several data gaps remain open for these indispensable fundamental input data. Data which are required in order to establish a detailed scientific mechanistic understanding of radionuclide-organic-cement ternary systems.

4.3 Radionuclide uptake in cementitious materials

4.3.1 Uptake of RN onto cementitious materials

Exhaustive studies have been carried out during the past decades to derive quantitative data and mechanistic understanding of radionuclide uptake onto cementitious materials. These works were mainly performed in the context of radioactive waste disposal and take into account (i) different kinds of cementitious materials, (ii) the influence of their different potential degradation stages on chemical processes, and (iii) the uptake onto several constitutive pure phases (see SOTA Chapter 5).

The uptake is quantified by a solid liquid distribution coefficient noted K_d (or distribution ratio R_d) (generally in $L \cdot kg^{-1}$) and defined by:

$$K_d = \frac{C_{ads}}{C_e} = \frac{n_0 - n_e}{m} \frac{V}{n_e} \quad (\text{eq. 4-2})$$

where C_{ads} ($mol \cdot kg^{-1}$) is the concentration of adsorbed species per mass of sorbent, C_e ($mol \cdot L^{-1}$) the concentration of the species in solution at equilibrium, n_0 (moles) and n_e (moles) the initial and equilibrium molar quantity in solution, V is the volume of solution and m is the dry mass of solid sorbent.

The distribution coefficient is an experimentally determined parameter quantifying the distribution of a chemical species between a given fluid and solid material sample under certain conditions, including the attainment of constant aqueous concentrations of the species of interest. This parameter represents the sum of all the phenomena that are able to remove an element from the aqueous phase, *i.e.* by adsorption on the surface of the solid matrix, incorporation inside some of the solid matrix mineral phases or precipitation in solution with other species. The most relevant retention process often is adsorption. To isolate the contribution of adsorption processes on radionuclide retention, precipitation must be avoided in experiments with respect to the respective solubility limits.

In the particular context, the scientific community benefits from two important reviews published in 2016 and 2018.

The first one is the book “Radionuclide and Metal Sorption on Cement and Concrete” from Ochs *et al.* (2016) published by Springer. This book contains a full state-of-the-art assessment and a critical evaluation of the type and magnitude of sorption and incorporation processes in hydrated cement systems, responsible for the retention properties of cementitious materials towards radionuclides and metals from a variety of radioactive and industrial waste. In Ochs *et al.* (2016), the sorption values for Cl, I, Cs, Sr, Ra, Ag, Ca, Ni, C, Th, U, Pu, Np, Pa, Am, Se, Mo, Tc, Pd, Pb, Nb, Sn, H, Be, Zr are summarized and the original studies referenced. This review was commissioned by Ondraf-Niras in the context of near-surface disposal and contributes to improved process understanding and scientific argumentation. It is used for selecting “best estimate” sorption values for the radionuclides/metals and deriving lower and upper limits for these values.

The second publication (Tits and Wieland, 2018) is based on the research programme that had been carried out for many years by the Laboratory for Waste Management (LES) at the Paul Scherrer Institute in Switzerland with the aim to understand the interaction processes of actinides and lanthanides with cementitious materials both on a microscopic and macroscopic scale. This PSI public report contains an overview of batch sorption studies with actinides and lanthanides in different redox states and on various cementitious materials carried out at the LES. The actinides and lanthanides investigated include Eu(III) and Am(III), Th(IV), Np(IV), Np(V) and Np(VI) and U(VI). The experimental results and interpretations provided in this report aim to:

- quantify the actinide/lanthanide uptake by hardened cement paste (HCP) and C-S-H phases,
- describe the effects of cement paste / C-S-H composition, cement pore water composition and pH on actinide/lanthanide sorption by cementitious materials, and
- discuss the mechanisms driving the uptake of actinides by cement paste and C-S-H phases.

The aim of the present SOTA is not to copy and repeat previously published work. The entire book by Ochs *et al.* (2016) was dedicated to such a detailed bibliographic review. We strongly encourage readers to refer to both previously mentioned documents, which provide a relatively exhaustive bibliographic base on a specific cementitious material/radionuclide system. In combination with the work performed in CORI Task 3 on binary systems (cement/organic), the work planned in CORI Task 4 on ternary systems (cement/organic/radionuclide) extends knowledge beyond the present State-of-the-Art.

4.3.2 Uptake of RN in the presence of organic ligands

Many of the studies about the effects of organics on RN retention/uptake can be considered as only quasi-qualitative, as their aim is to compare retention values of the contaminant in the presence or absence of the organic component. This basic approach, merely based on direct experimental evidences and no comprehensive system understanding, may not be enough for safety assessment of nuclear waste disposals (Payne *et al.*, 2013) in certain cases. The numerical value of the distribution coefficient depends on several factor (pH, ionic strength (I), adsorbate concentration, *etc.*) K_d values cannot be extrapolated to conditions different from those adopted in the experiment and therefore a strong motivation exists to establish a full mechanistic approach based on detailed scientific understanding.

In their recent review about the possible “*reduction of radionuclide uptake in hydrated cement systems by organic complexing agents*”, carried out for the Swedish Nuclear Fuel and Waste Management Company (SKB), Ochs *et al.* (2014) examined the fate of different RN or other species (C, Ca, halogens, Cs, alkaline earth elements, Ag, Cd, Pd, Ni/Co, An(III)/Ln(III), Ac, An(IV), An(V), An(VI), Zr, Sn, Tc, Nb, Se, Mo, Pb, Po) in the presence of ISA, EDTA, NTA, GLU, citrate, oxalate and degradation products of a UP2 filter aid. The study was as far as possible based on experimental evidence directly applicable to

the ternary systems considered. The finding was that much of the information was only available for ISA, and the conclusions for many other ligands were based on ISA by analogy. This can be understood as a lack in well-established experimental data.

Cellulose degradation under hyperalkaline conditions, conditions typical of cementitious environments, leading to the isosaccharinic acid, ISA (Pavasars *et al.*, 2003), is a quite well-established process. ISA is probably the most studied organic ligand in the frame of radioactive waste disposals because it has shown high capacity to complex radionuclides (Humphreys *et al.* 2010; Kuippers *et al.*, 2018 and references therein), especially actinides.

Diesen *et al.* (2017) studied the impact of cellulose degradation products, present as a mixture in an artificial cement pore water (pH 12.5). Different amounts of Eu(III), as freshly precipitated solid europium hydroxide, were added to this mixture. After filtration, Portland cement was added to the solutions. From their measurements, the authors concluded that under the experimental conditions applied, the extent of adsorption of the formed organic europium complexes to cement was low ($<9 \mu\text{mol Eu}\cdot\text{g}^{-1}$ of cement) in comparison to data for adsorption of europium onto cement without the presence of organic degradation products reported in literature. Their study stressed the need for further information regarding the mobility of these complexes under disposal conditions.

The possible effects of competitive ions (Na, Ca or Fe) on ISA-RN complexation have been mentioned in the literature, but the information necessary for a better description of their overall role is not enough (Kuippers *et al.*, 2018).

Organic products with chelating functions (EDTA or nitrilotriacetic acid, NTA) may be present in appreciable concentration in many nuclear installations. They are mainly generated during effluent extraction processes. Many different studies showed its capability of strongly chelating tri- and tetravalent actinides (May *et al.*, 2012; Reinoso Maset *et al.*, 2012) enhancing their mobility in different substrates. EDTA was clearly involved in RN migration at the Oak Ridge National Laboratory, USA, (Killey *et al.*, 1984). However, Reinoso-Maset *et al.* (2013) also showed that this effect is not the same for all the organic-RN systems. For example, the mobility of Cs within silica/sand was not affected by the presence of EDTA. EDTA has also a limited effect onto U migration, probably due to the presence of other cations in solution (Mg, Ca) which may form stronger complexes with EDTA than U. The presence of other ligands (as, for example carbonates, phosphates) are particularly important in U retention, and thus the competition between organic ligand (and inorganic) should be considered as well.

A mechanistic approach to the understanding and description of retention processes in complex materials like cement needs the application of a bottom-up approach, focusing on the behaviour of the main sorbing minerals (e.g. C-S-H phases). Molecular dynamic simulation is an appealing modern technique to increase the knowledge on mechanisms of RN-organic and cement interactions. In particular, the key role of Ca as a linking “bridge” between the surface of cement (or C-S-H) and polyhydroxocarboxylic acids (ISA or gluconic acid) has been already reported (Androniuk and Kalinchev, (2020); Jo *et al.* (2022); Poiteau *et al.* (2008).

Concerning retention data, the studies on the potential role of cement superplasticizers on RN suggest that their impact on RN mobilisation should be negligible (Wieland *et al.*, 2014; NDA, 2017; Garcia *et al.*, 2018b; Baston *et al.*, 2019). However, not much is known about the long-term evolution of cement-bound superplasticizers in hardened concrete. Some authors mention that uncertainties remain as to whether RN behaviour would be the same when studying crushed or intact material. There is a lack of fundamental understanding on that subject.

In some cases, the presence of organics has been observed to increase contaminant adsorption (Kornilovich *et al.*, 2006; Barger and Koretsky, 2011), hypothetically due to the formation of solid-organic-contaminant (S-O-C) ternary complexes, adsorbed on the solid surfaces.

A mechanistic analysis of RN-cement-organic interactions needs focused experiments to understand the extent of the effects of organics on RN retention, but also a thermodynamic description of the aqueous and solid species formed.

4.4 Radionuclide diffusion in cementitious materials

Diffusion is one of the most important transport processes in porous media. Diffusion is controlled by concentration gradients. Therefore, ions and molecules generally move from regions with high concentration to regions with lower concentration. The determination of diffusion coefficients in cement is important not only for describing RN migration, but also for predicting the movement of all the ions that can contribute to cement degradation affecting its main properties.

It is out of the scope of the present document to deal in detail with the mathematic treatment of diffusion, which is widely addressed in the literature (*e.g.* Crank, 1975). We would simply remind that the diffusion theory is based on the first and second Fick's laws. The first Fick's law states that the mass flux per unit cross-sectional area, F [$\text{kg}\cdot\text{m}^{-2}\cdot\text{s}^{-1}$], is directly proportional to the concentration, C [$\text{kg}\cdot\text{m}^{-3}$], gradient and, for a one-dimension simplification, is expressed as:

$$F = -D \frac{\partial C}{\partial x} \quad (\text{eq. 4-3})$$

The diffusion coefficient, D [$\text{m}^2\cdot\text{s}^{-1}$] is the proportionality constant between concentration gradient and flux and determines the rate at which ions and/or molecules spread. The concentration of ions/molecules in the porewater, C , depends on time t [s] and distance x [m], and the conservation of the mass leads to the Fick's second law, expressed in its one-dimensional approximation as:

$$\frac{\partial C}{\partial t} = D \frac{\partial^2 C}{\partial x^2} \quad (\text{eq. 4-4})$$

It is important to remark that diffusion in porous media is more complex than in free water, as it is affected by the characteristics of the solid material, especially its porous structure. The variable geometry of solid structures is defined by geometric terms such as tortuosity (τ) or constrictivity (δ), which cannot be straightforwardly measured. Not all the pores are connected and the volume available for diffusion and contributing to solute transport is related to connected pores. Thus, in porous media, the cross-sectional area available for diffusion is limited by its porosity (ϵ).

The diffusion coefficient of a species in free water, D_w , will be related to the diffusion coefficient in a porous material, D_p , in the following way:

$$D_p = \frac{\delta}{\tau^2} D_w \quad (\text{eq. 4-5})$$

The effective diffusion coefficient, D_e , takes account of the smaller cross-sectional area available for diffusion in porous media and is defined by:

$$D_e = \varepsilon \cdot D_p \quad (\text{eq. 4-6})$$

Another mechanism that affects diffusion in the cementitious porous media is the retention on the solid surfaces, because it retards ions migration. To account for retention processes, it is necessary to define another parameter, the apparent diffusion coefficient, D_a , which is defined as:

$$D_a = \frac{D_e}{(\varepsilon + \rho \cdot K_d)} = \frac{D_e}{\alpha} \quad (\text{eq. 4-7})$$

ρ is the dry density of the solid and α is a parameter known as capacity factor, which includes retention through the distribution coefficient, K_d . If a solute is non-sorbing ($K_d = 0 \text{ m}^3 \cdot \text{kg}^{-1}$) then the capacity factor is equivalent to the porosity.

To determine these transport parameters different experimental set-ups must be designed, based on the characteristic of the RN or ion that shall be studied. Depending on the constraint of the experiment, different analytical solutions to the Ficks' laws exists (Crank, 1975) but experimental results can also be analysed by numerical methodologies. The most used classical experimental techniques to measure the diffusion coefficients of chemical species are: Through-Diffusion (TD); In-Diffusion (ID) and Out-Diffusion (OD) (Flury and Gimmi; 2002).

Even if diffusion processes in HCP, concrete, or mortars have been studied over the last years, data available in the open literature are relatively scarce. Most of data deal with diffusion of conservative tracers as tritiated water (HTO) or Cl^- , I^- or low sorbing species (Atkinson and Nickerson, 1984; Sarrot *et al.*, 1991; Bucur *et al.*, 2010; Felipe-Sotelo *et al.* 2014; van Es *et al.*, 2015; Akagi *et al.*, 2018; Shafikhani and Chidiac, 2019). García-Gutiérrez *et al.* (2018) analysed Cs diffusion in mortars from different cements.

Some compilation of diffusion coefficients from safety analyses studies exist (Albinsson *et al.*, 1993; Mattigod *et al.*, 2001; Wieland, 2014) which are often related to the specific materials and/or chemical conditions of interest for each repository design. In general, markedly different diffusion behavior are observed for different cement formulations (Grambow *et al.*, 2020).

Due to the specific property of each cementitious material, it is difficult to draw strong general conclusions. Nevertheless, for the same formulations, it can be stated that D_e decreases when the water to cement ratio decreases (being the material less porous) (Jakob *et al.*, 1999; Yamaguchi *et al.*, 2009).

The scarceness of diffusion data in cement-based materials can be partly explained by the experimental difficulties related to the work with them. The chemical conditions generated by the cement, implies high adsorption and/or low solubility for many elements, thus diffusion tests with moderately and high sorbing species need long time (in the order of months to years). This means that in through diffusion experiments, even after several months, the RN may not have appeared in the outlet deposit. Similarly, in in-diffusion experiment, the diffusion profile may be too short (just several micrometers) to be adequately analyzed. In these cases, only the upper limit of diffusion coefficients can be estimated, but not the real one. The application of new methodologies for diffusion experiments as microprobe techniques are certainly welcomed to partially overcome these drawbacks. For example, Suyiama *et al.* (2008) analyzed uranium diffusion in OPC and another Portland cement containing 30% ash (FAC) analyzing the diffusion profiles by laser ablation microprobe inductively coupled plasma mass spectrometry and determining both D_e and D_a (for OPC: $D_a = \sim 4 \times 10^{-16} \text{ m}^2 \cdot \text{s}^{-1}$; $D_e = \sim 3 \times 10^{-11} \text{ m}^2 \cdot \text{s}^{-1}$, and for FAC: $D_a = \sim 2 \times 10^{-17} \text{ m}^2 \cdot \text{s}^{-1}$; $D_e = \sim 6 \times 10^{-13} \text{ m}^2 \cdot \text{s}^{-1}$).

Furthermore, it is quite complicated to maintain the physicochemical conditions and the cementitious materials stable during the whole experiment duration. Dissolution/precipitation processes may take place, resulting in changes within the solid (e.g. porosity, mineralogy). RN incorporation within existing or freshly formed phases may occur, and the existence of no-reversible retention processes can also entangle the interpretation of diffusion data. This means that, often, simple diffusion/retention models cannot be applied for the interpretation of diffusion data. The lack of data is reflected also in the studies about RN diffusion in the presence of organic ligands that are much less available compared to retention *batch* experiments.

For what concerns the effects of the organic on RN diffusion, some information can be found on cellulose degradation products. Holgersson *et al.* (1998) analyzed the effects of gluco-isosaccharinate on the diffusion process of Cs, Ni, Pm and Th in a Portland cement by means of through diffusion experiments. The authors observed only the breakthrough of HTO and Cs, but not of Ni, Pm or Th. The effect of the organic on Cs diffusion was considered negligible.

Felipe-Sotelo *et al.* (2016) analyzed the migration of selenium in cementitious backfill (Nirex reference vault backfill, NRVB, and PFA/OPC) in the presence of cellulose degradation products. No sign of breakthrough was evidenced after one year, for either of both solids, in agreement with the very low solubility of selenium under alkaline conditions and presence of Ca. Felipe-Sotelo *et al.* (2017) also analyzed U and Th diffusion through intact cylinders of NRVB by in-diffusion experiments and did not observe breakthrough for either U or Th, both in the absence and presence of cellulose degradation products.

Detailed quantitative data about RN-organic complexes diffusive transport in cementitious materials remain a largely open issue.

4.5 CORI results: RN migration in cement-organic systems

The work performed in Task 4 of CORI features experimental studies on binary systems (radionuclides + cement) and ternary systems (radionuclides + organics + cement). Studies in the binary system are required to assess the specific effect of organic compounds in the higher complexity ternary systems. The new studies in CORI have extended knowledge beyond the already published data in the literature. In this chapter, main results from CORI are described to update information in the previous D3.1 SOTA document in view of the new research in CORI.

Considering the high complexity of the ternary systems studied in CORI Task 4 and the several variations regarding the investigated radionuclide, organic ligand and cement(phase) types, it is challenging to provide results in a short summary. In the subsequent rather detailed sub-chapters focusing on specific groups of radionuclides, the new data and improved process understanding generated in CORI Task 4 are described along the investigated types of organics.

Main **general observations** regarding radionuclide retention in the ternary system RN-organic-cement derived from the work in CORI are as follows:

- In many investigated cases the **effect of organic species** on the solubility or sorption of RNs was zero or minor. This is especially true if considering “realistic” organics concentrations in solution as expected for many repository settings.
- New **quantitative data** on radionuclide retention on cement-based materials under presence of organics were derived. The strong variations used in CORI regarding cement, degradation

stages, organics and radionuclides open perspectives **to systematize findings into material/radionuclide groups** having expected „weak“, „moderate“, „strong“ impact on sorption retention. (See also the subsequent sub-chapters).

- **A strong effect of dissolved [Ca]** on the chemical speciation, reaction mechanisms and quantification was observed. This fundamental understanding represents a new input for a more realistic description of the chemical system. It should be emphasized, that a **comprehensive understanding of speciation** (and thermodynamics) is **essential** for in-depths data interpretation.
- Differences between the **real leachates** from Task 2 and the **proxy ligands** were observed regarding impact on radionuclide retention. The real leachates tend to cause a stronger decrease in radionuclide sorption, which is also related to the organic concentrations.

The **radionuclides** studied in Task 4 were: ^{134}Cs , ^{36}Cl , Pb(stable), ^{63}Ni , ^{152}Eu , Nd(stable), ^{241}Am , ^{248}Cm , $^{232,234}\text{Th}$, $^{238,239}\text{Pu}$ and $^{233,238}\text{U}$, spanning a wide range of chemical characteristics. **Cement materials** investigated in Task 4 were CEM I, CEM III, CEM IV and CEM V hardened cement paste (HCP) at various degradation stages. Pure solid phases such as portlandite, C-A-S-H, AFt and AFm-phases were investigated to improve process understanding. Some studies were performed using the “reference cement” material (RCM) defined in CORI, which is a CEM I HCP, (producer CEMEX Prachovice, Czech Republic) provided by the Czech team in CORI. A large variety of **organic molecules** was investigated in CORI Task 4, including ISA, EDTA, NTA, Citrate, formate, oxalate, acetate, phthalate, gluconate but also more complex mixture such as superplasticizer, real degradation product of cellulose, PCE or IER.

The most relevant RN/organic migration results gathered within WP3 CORI are compiled in the public CORI Deliverable D3.6,7,8 – (Altmaier *et al.* (2024)). The reader is referred to this document for further detail on technical results and discussions. Likewise, reference is made to peer-reviewed publications obtained in WP3 CORI (Almendros-Ginestà *et al.* (2023); Burešová *et al.* (2023); Dettmann *et al.* (2022); Drtinová *et al.* (2023); Friedrich *et al.* (2023); Kittnerová *et al.* (2023); Kretschmar *et al.* (2020); Maragkou *et al.* (2021), Missana *et al.* (2022a&b), Stietz *et al.* (2023 a&b), Szabo *et al.* (2022a&b, 2023a&b) and Tasi *et al.* (2021).

4.5.1 Results obtained in CORI for U(VI)

In binary systems (radionuclides + cement), the retention of U(VI), expressed as distribution ratio R_d , is significant ($R_d > 10^5$ L/kg) at low U concentration in solution for all matrices investigated. The nature of cement (RCM vs. HCP CEM V/A) has less effect than the alteration state of the matrix. The maximum retention of U(VI) is observed for stage II of cement degradation, where the Ca concentration in solution is buffered by portlandite *i.e.* at around 22 mM for pH 12.5. Desorption experiments performed for stage II and stage III reveal a reversible uptake mechanism. These results confirmed what was also observed in literature (see Ochs *et al.*, 2016). Uranium shows an extremely strong binding affinity to all investigated forms of CASH ($R_d = 10^{5.5}$ L/kg), *i.e.* with Ca/Si and Al/Si ratios: 1.2-0.05 (pH= 11.3 ± 0.2) and 1.2-0.02 (pH= 10.2 ± 0.1). For CSH (Ca/Si = 0.8), the affinity of U(VI) is similar ($R_d = 10^{5.1}$ L/kg). From long term diffusion experiments (*i.e.* 505 days), a limited penetration depth of around 40 µm was determined for HCP at stage II in absence of organics. These results are consistent with a migration behaviour of U(VI) dominated by strong sorption and/or very slow diffusion processes.

The effect of organics on U(VI) retention depends on the nature of the organic ligand and on its concentration in the ternary system (CEM-ORG-RN). This is discussed in more detail below.

α -ISA: No large effect is observed regarding the $R_d(U(VI)/CASH)$ value in presence of α -ISA, while a minor increase of the solubility of U(VI) in presence of 10^{-3} M of ISA is measured in similar solution. For the ternary system U(VI)-ISA-HCP, one main result is the existence of a threshold value for ISA concentration in solution ($[ISA]_{eq} = 2 \times 10^{-4}$ mol L⁻¹) above which uranium uptake strongly decreases. The same behaviour was reported by Poiteau *et al.* (2018) for a CEM I HCP at stage I and III for which the ISA threshold concentration is in the same order of magnitude or slightly higher, *i.e.* about 10^{-3} mol L⁻¹ compared to 2×10^{-4} mol·L⁻¹. Similar observations have been recently reported for the uptake of Nb(V) (CEM I HCP stage I) by Çevirim-Papaioannou *et al.* (2023) and Pu(IV) (CEM I HCP stage II) by Tasi *et al.* (2021). Almendros *et al.* (2024) also observed a slight increase of U(VI) adsorption in portlandite, which can be explained by the formation of ternary U(VI)-ISA-portlandite complexes. From diffusion experiment in HCP at stage III, first data are consistent with a deeper penetration of uranium inside the degraded zone of the HCP which could be (at least partly) linked to the change of mineralogy in the degraded zone and the presence of ISA. The effect of presence of cellulose RDP onto U(VI) sorption was also investigated on fresh and stage II RCM samples. A clear decrease in R_d was observed for the degraded RCM (two orders of magnitude at the higher total ISA content (α -ISA and β -ISA) of 3×10^3 M in the cellulose RDP). The effect of the RDP on uranium adsorption in fresh RCM was negligible.

GLU and PBTC: The influence of GLU and PBTC on U(VI) retention by C-S-H with a C/S ratio of 0.8 was investigated. For a concentration of 10^{-2} M of GLU, the $\log(R_d)$ of U(VI) decreases from 5.1 in absence of GLU to 4.8 ± 0.1 . Regarding the U(VI) uptake, no clear trend can be seen in the tests with different addition sequences of U(VI) and GLU, thus indicating that GLU has only a very small influence on the U(VI) retention by C-S-H under these conditions. Concerning PBTC, the U(VI) retention by C(A)SH decrease when PBTC species are present at relatively high concentrations.

EDTA: For solutions reflecting the degradation stage II of cement, the solubility of U(VI) in presence of EDTA after long contact time is similar to the one without organics ($\sim 10^{-7}$ M). Under similar conditions, the U(VI) sorption is still significant ($R_d \sim 10^5$ L/kg) for HCP CEM V/A independently of the introduced EDTA concentration and contact time in the ternary system. At stage III/IV and for initial EDTA concentrations up to 10^{-3} M, the R_d value tends to decrease, suggesting a saturation of sorption sites. In spectroscopic investigations, the U(VI) fluorescence spectra evolution suggest that the EDTA interacts with U(VI) complexes at the highest concentration. Characterisation of the CSH-U(VI)-EDTA system showed an effect of the presence of carbonate. Under N₂ atmosphere the presence of EDTA in solution caused (slightly) lower R_d values due to stabilization of U(VI) in solution in the form of EDTA complexes. However, higher K_d values were observed when EDTA solutions were contacted with the C-S-H-U(VI) phase, because of the formation of ternary C-S-H-U(VI)-EDTA surfaces complexes, which stabilize U(VI) onto the C-S-H phase. On the other hand, under ambient atmosphere, U(VI) carbonate complexes govern the U(VI) chemistry in solution, resulting generally in lower R_d values. Similarly, under 1% CO₂ U(VI)-carbonate complexes govern the U(VI) chemistry in solution and result in the formation of ternary carbonate solid phases. EDTA ligand forms stable complexes with U(VI) in aqueous C-S-H suspensions.

Phthalate: The presence of phthalate had no significant effect on the retention of U(VI) on HCP CEM V/A at stage II or III/IV, similarly to what was observed for U(VI) retention in portlandite.

Superplasticiser: The number of studies performed with superplasticisers and U(VI) were limited. Two different commercial products were used for the experiments. The first one (SIKA) is based on modified melamine (SIKAMENT™ 200 R, Sika, Spain) and the second one (MG) is the Master Glenium SKY 886 (BASF), an innovative superplasticizer based on the latest generation of polycarboxylate ether (PCE) polymers. Batch sorption tests were carried out with “realistic” concentrations of superplasticizers (5% wt). Under these conditions, the effect of superplasticizers in the CSH was negligible. The presence of SIKA also slightly affected U(VI) sorption in fresh cements (CEM I, CEM IV and CEM V), whereas MG produced a decrease of 20% and 10% in the $\log(R_d)$ in CEM IV and CEM V, respectively.

4.5.2 Results obtained in CORI for Th(IV)/Pu(IV)

Th(IV) and Pu(IV) strongly sorb on fresh HCP under reducing and hyperalkaline conditions in the absence of organic ligands.

α-ISA: ISA clearly affects the uptake of Th(IV) and Pu(IV) as can be shown in adsorption experiments (with 2 orders of magnitude less uptake). The decrease of Pu(IV) adsorption in the presence of ISA was also observed in portlandite. Diffusion experiments also show deeper Pu(IV) in-diffusion in the presence of ISA within 118 days.

EDTA: The HCP-An(IV)-EDTA system with fresh HCP leads to a quantitative uptake of Th(IV) and Pu(IV) on HCP. Almost no difference is observed regarding the order of RN ligand addition, indicating negligible influence of EDTA on the retention of Th(IV) or Pu(IV) on HCP after 72 hours of contact time.

GLU: Concerning the HCP-Pu(IV)-GLU system, much lower R_d values for Pu(IV) are obtained in the ternary system compared to the binary HCP-Pu(IV) system. When Pu(IV) was added first, the uptake was higher than with initial GLU present, but lower compared to the binary system. This may be an indication that Pu(IV) desorbs after GLU addition. The order of addition affects Pu(IV) uptake on HCP, suggesting GLU occupies sorption sites, acting as a competitive element for the actinide retention. The order of additions of An(IV) and GLU have significantly influence of the uptake of An(IV) on HCP (pH > 13) during short contact times (72 h).

Further concerning the effect of GLU, the Pu(IV)-CSH-GLU and Pu(IV)-(AFm-ettringite)-GLU systems were investigated. At $[GLU] > 10^{-4}$ M, the Pu(IV) uptake is decreased in both C-S-H phases with high (1.4) and low (0.8) Ca:Si ratio and presence of redox buffer (*i.e.* HQ and Sn(II)). In the case of Pu(IV)-(AFm-ettringite)-GLU system, Pu uptake by AFm phases and ettringite has been observed, with log R_d of (5.6 ± 1.0) and (5.7 ± 1.1) (with R_d values reported in L/kg), respectively. Similar effects were observed for the uptake of Pu(IV) by AFm phases and ettringite: the presence of GLU at concentrations higher than 10^{-4} M decreases the R_d of Pu(IV). The impact of GLU on the retention of Pu(IV) by AFm phases and ettringite was stronger than that observed for C-S-H phases.

UP2W degradation products: The solubility of Pu(IV) in cement porewater solutions was moderately affected by the presence of HIBA, HBA or GTA. The uptake of $^{242}\text{Pu(III/IV)}$ by HCP in the degradation stage II was investigated in the absence and presence of the proxy ligands (HIBA, HBA or GTA) and the UP2W degradation leachate generated in Task 2. The presence of proxy ligands slightly decreased the distribution ratios for $^{242}\text{Pu(III/IV)}$ for $[L]_{\text{tot}} > 10^{-2}$ M. However, this effect is less evident due to the dispersion of the data and the increase of the detection limits for plutonium with increasing ligand concentrations. As for $^{63}\text{Ni(II)}$ and $^{152}\text{Eu(III)}$, the presence of the degradation leachate induces a moderate decrease in the uptake of $^{242}\text{Pu(IV)}$ by HCP, as compared to the sorption in the presence of the proxy ligands.

Superplasticiser: Pu(IV) sorption tests on fresh cements were done with Pu(IV) and presence of MG or SIKA (5 wt.%). The presence of SIKA significantly decreased Pu(IV) sorption in CEM V (47%), but the effect was also notable in CEM I (20%) and CEM IV (9%). The effect of MG was stronger decreasing the Log(R_d) of 41%, 44 % and 61 % for CEM I, CEM IV and CEM V, respectively. Batch sorption tests with Pu(IV) on portlandite and fresh and degraded (stage II) RCM in the presence of variable concentration of superplasticizers, confirmed the potential of decreasing the retention of the actinide, which can be also attributed to the non-negligible adsorption of the additives on the solid surface.

4.5.3 Results obtained in CORI for Eu(III)/ Cm(III)/ Pu(III)

α-ISA: A significant decrease in R_d values was previously observed for Eu(III) and Pu(III) in the presence of α -ISA synthesized in the laboratory. The effects of cellulose RDP degraded by radiolysis and hydrolysis on the adsorption of Eu(III) and Pu(III) on fresh and stage II RCM were investigated. In the case of Eu(III) and Pu(III) no large difference between the two stages was observed. The RDP have a non-negligible effect on the adsorption of all the studied RN. For the Eu(III)-RCM-RDP system at stage II, the effects produced by cellulose RDP on Eu(III) diffusion were depending on the TOC content of the RDP obtained either by only hydrolysis or hydrolysis and radiolysis. The effect of ISA on Eu(III) retention in portlandite is relevant (about 2 orders of magnitude). The diffusivity of Eu(III) is then higher with a factor of 250 in presence of high TOC content.

GLU: In the ternary $^{152}\text{Eu(III)-C-S-H-GLU}$ system, high uptake of Eu(III) was observed on C-S-H phases in the absence of organic ligands and under hyper-alkaline conditions. GLU has a negligible effect on $^{152}\text{Eu(III)}$ retention on C-S-H 0.8 at $[\text{GLU}] < 10^{-2}$ M, whereas a moderate decrease in retention is observed for higher GLU concentrations $[\text{GLU}] = 10^{-1.5}$ M and for longer equilibration times. For C-S-H 1.4, a strong decrease of Eu(III) retention was observed for $[\text{GLU}] > 10^{-3}$ M. In the $^{248}\text{Cm(III)-C-S-H-GLU}$ system, TRLFS analysis showed that Cm(III) is mostly incorporated in the C-S-H phase structure both in the presence and in absence of GLU. Conversely, for C-S-H 1.4, the formation Ca-Cm(III)-GLU-(OH) aqueous complexes is observed at $[\text{GLU}] \geq 10^{-2.5}$ M, thus preventing the incorporation of Cm(III) into the C-S-H structure. The results obtained in this framework support that the retention decrease of Eu(III) on C-S-H 1.4 in the presence of GLU is due to the formation of Ca-Eu(III)-GLU-(OH) species, thus highlighting the relevant role of Ca in the formation of Ca-Ac(III)/Ln(III)-L-(OH) complexes, as previously reported by Rojo et al. (2021).

Phthalate: The uptake/retention and migration behaviour of $^{241}\text{Am(III)}$ and $^{152}\text{Eu(III)}$ in the presence of phthalate on C-A-S-H phases and HCP (CEM V) were investigated. At phthalate concentrations above 10^{-3} mol kg^{-1} a distinct decrease of R_d values was observed. This reduction of the $^{241}\text{Am(III)}$ and $^{152}\text{Eu(III)}$ uptake in the presence of phthalate is suggested to be a consequence of the destabilisation/dissolution of C-S-H/C-A-S-H due to increasing Ca-complexation by phthalate in solution. In contrast, in sorption experiments with pure synthesised C-A-S-H (Ca/Si ratio 1.6), only a minor effect of the phthalate addition on the retention behaviour of Am(III) and Eu(III) was observed. In the absence of organics and at phthalate concentrations up to 10 mM, the R_d values of Am(III) and Eu(III) were in the order of 10^5 to 10^7 L kg^{-1} . Only at very high phthalate concentrations (10^{-1} mol kg^{-1}), a slight decrease in the radionuclide uptake was found.

UP2W degradation products: The uptake of $^{152}\text{Eu(III)}$ by HCP in the degradation stage II was investigated in the absence and presence of proxy ligands (HIBA, HBA, GTA) and the UP2W degradation leachate generated in CORI Task 2. The presence of proxy ligands has a negligible effect on the uptake of $^{152}\text{Eu(III)}$ up to $[\text{L}]_{\text{tot}} = 0.1$ M. The presence of the degradation leachate induces a moderate decrease in the uptake of $^{152}\text{Eu(III)}$ by HCP, as compared to the sorption in the presence of the proxy ligands. These observations possibly reflect that the multiple functionalities (-COOH, -OH, amide groups) expected in the macromolecules (10–15 kDa) present in the degradation leachate, can offer further binding / chelating capabilities compared to the small organic proxy ligands with at most bidentate binding.

Superplasticiser: The presence of superplasticizers does not affect the retention of Pu(III) and Eu(III) in CSH, however a non-negligible decrease of sorption is observed in fresh HCP for these RNs in the presence of 5%wt of superplasticizers. In particular, the presence of Sika clearly affects Eu(III) sorption in CEM I (-13% in $\text{Log}(R_d)$) and CEM V (-33 %), but much less in CEM IV. Again MG has a larger effect in all the cements with a reduction observed in the $\text{log}(R_d)$ values for Eu(III) by 51%; 58% and 67% for CEM I, CEM IV and CEM V, respectively. It is of interest to further investigate the role of superplasticisers in diffusion tests with Eu(III) and Pu(III) with the superplasticizer added during casting.

Organics with observed negligible impact: The effect of **citrate** on the Cm(III), Pu(III) and Eu(III) adsorption on CSH phases, AFm phases and ettringite was investigated. Citrate has a negligible impact on Pu(III) and Eu(III) retention by C-S-H phases. It was observed to reduce Pu(III) retention by AFm phases and ettringite only at $[CIT]_{tot} > 10^{-2}$ M. No effect of **EDTA** on Eu(III) adsorption kinetic in HCP CEM III was observed. Concerning **formate**, the effect on $^{242}\text{Pu(III)}$ and $^{152}\text{Eu(III)}$ uptake by C-S-H phases (Ca:Si = 0.8, 1.4) was negligible. The effect of formate on $^{242}\text{Pu(III)}$ adsorption on AFm phases and ettringite was likewise negligible. In the case of diisooctyl **phthalate** (DIOP), no significant effects were observed for sorption experiments with Pu(III/IV) and Am(III). Negligible effects regarding the presence of **adipates** or **oxalate** on Pu(III) or Am(III) adsorption on HCP CEM I at stage II were observed. Based on thermodynamic calculations, the affinity of **tri-methyl-amine** (TMA), which is a degradation product of basic anion exchange resins to form complexes with Am(III) or Eu(III) in HCP CEM V/A conditions is supposed to be low. A small effect of TMA on the mobility of these RNs is presumed and unlikely effects of TMA on Ca-bearing cement hydration phases are expected.

4.5.4 Results obtained in CORI for Pb(II)/Ni(II)

EDTA: The sorption reduction factor values (SRF) for Pb(II) in HCP CEM I and CEM III showed a limited effect of the presence of phthalate or EDTA, while depending of the Ca:Si ratio, the affinity of Pb(II) for CSH is more affected the presence of EDTA. For CSH 1.2, a maximum of SRF is observed for EDTA concentration at 5×10^{-3} M.

Formic acid: The solubility of Ni(II) is about $2 \cdot 10^{-7}$ M for fresh cement porewater conditions. When formic acid is added to the system, the resulting Ni(II) concentrations in solution are not significantly influenced. The $^{63}\text{Ni(II)}$ uptake was evaluated on non-degraded and degraded cement pastes based on CEM I and CEM V. The presence of formic acid, at a concentration of 10^{-3} M was found to have an impact on $^{63}\text{Ni(II)}$ uptake on non-degraded CEM I HCP and to a lower extent on degraded cement, *i.e.* moderately lower R_d values were obtained for nickel sorption in the ternary systems. On CEM V HCP, the presence of formic acid, at a concentration of 10^{-3} M was found to have an inverse impact on $^{63}\text{Ni(II)}$ uptake: higher R_d values were obtained for nickel sorption in the ternary system.

α -ISA: Ni(II) sorption on HCP was higher for advanced degradation stages than on fresh HCP. Additionally, the real degradation products (RDP) of cellulose had a much stronger impact than pure α -ISA on Ni(II) retention. This result suggests that not only α -ISA has a sorption reduction power but other products from the degradation of cellulose should eventually be considered, too. The presence of cellulose RDP on Ni(II) adsorption on fresh and stage II RCM show higher effects in the case of RCM degraded at stage II compared to fresh cement. Whereas significant decreases in R_d values were previously observed for Eu(III) and Pu(III/IV) in the presence of α -ISA synthesized in the laboratory, this effect was not been observed for Ni(II). This can be an indication that some of the still not identified cellulose degradation products obtained by hydrolysis and radiolysis might have stronger effects than pure α -ISA on Ni retention. The adsorption behaviour of Ni was also analysed in the CSH phases at different Ca/Si ratios, indicating that adsorption increases as the Ca/Si decreases. The effect of the organic on radionuclide retention in the Ni-CSH- α -ISA system is quite limited. Diffusion experiments of Ni(II) in the presence/absence of α -ISA in HCP stage II did not exhibit a variation in the diffusion coefficients within the experimental errors.

EDTA and phthalate: The HCP-Ni(II)-EDTA and HCP-Ni(II)-phthalate systems were investigated with HCP CEM V/A (or RCM) degraded at stage II and IV with a focus on investigating the solubility, sorption kinetics and performing diffusion experiments. The trends obtained with U(VI) are also observed for $^{63}\text{Ni(II)}$. At stage III/IV and for higher EDTA concentration, the evolution of R_d values with the organic concentration suggests a competition effect and/or a saturation of the sorption site

for EDTA concentration higher than 10^{-4} M. No significant effects were observed due the presence of phthalate on the retention of Ni(II) in HCP at stage II or stage III/IV. The penetration of $^{63}\text{Ni(II)}$ (or $^{63}\text{Ni(II)-ORG}$ complex) into the solid is quite limited and restricted to the very surface of the HCP sample. The presence of EDTA or phthalate does slightly enhance the $^{63}\text{Ni(II)}$ diffusion.

UP2W degradation products: GTA, HIBA and HBA induce a slight increase in the solubility of Ni(II) at $[\text{L}]_{\text{tot}} = 0.1$ M, thus hinting at the formation of stable Ni(II)-GTA, -HIBA and -HBA complexes under hyperalkaline conditions. The comparison of these results with solubility data in the presence of ISA confirms the stronger complexation properties of the latter ligand. Even though HIBA and HBA are carboxylic acids containing one alcohol group, this comparison shows that additional alcohol groups are required to efficiently chelate the metal ion and outcompete hydrolysis. The uptake of $^{63}\text{Ni(II)}$, by HCP in the degradation stage II was investigated under the absence and presence of proxy ligands (HIBA, HBA, GTA) and the UP2W degradation leachate generated in Task 2. A slight decrease in the distribution ratios for $^{63}\text{Ni(II)}$ was observed only at $[\text{L}]_{\text{tot}} > 10^{-2}$ M.

Superplasticiser: Sorption tests were carried out on fresh cements samples with Ni(II) in the presence of MG or SIKA (5 wt%). MG slightly affects Ni(II) adsorption, with observed variations within the experimental uncertainty. The maximum decrease in $\log(R_d)$ was observed for CEM V in the presence of SIKA. However, a very limited effect on nickel diffusion was observed in tests carried out with cements casted in the presence of SPs. The Ni(II) leaching behaviour was similar in the cement with and without superplasticizers.

4.6 References Chapter 4

- Abrahamsen L., Arnold T., Brinkmann H., Leys N., Merroun M., Mijndonckx K., Moll H., Polvika P., Ševců A., Small J., Vikman M., Wouters K., 2015. A Review of Anthropogenic Organic Wastes and Their Degradation Behaviour. MIND Project, Deliverable 1.1.
- Akagi Y., Katoa H, Tachi Y., Sakamoto H., 2018. Diffusion and sorption behavior of HTO, Cs, I and U in mortar. *Progress in Nuclear Science and Technology* 5, pp. 233–236.
- Albinsson Y., Andersson K., Borjesson S, Allard B. 1993. Diffusion of radionuclides in concrete/bentonite systems. SKB Technical Report 93-29. Swedish Nuclear Fuel and Waste Management Co.
- Almendros-Ginestà, O., Missana, T., García-Gutiérrez, M., Alonso, U., 2023. Analysis of radionuclide retention by the cement hydrate phase portlandite: A novel modelling approach. *Progress in Nuclear Energy* 159, 104636. <https://doi.org/10.1016/j.pnucene.2023.104636> .
- Almendros-Ginestà, O., Clavero M.A., García-Gutiérrez, M., Missana T., 2024. Role of isosaccharinate and phthalate on Ni, U, Pu and Eu retention on portlandite (Submitted). Also available as CIEMAT/PAFP/EURAD/1-24 Report.
- Altmaier M., Ricard D., Vandenborre J., Garcia D., Henocq P., Macé N., Missana T. (2024): Final report of results generated in CORI. Final Deliverables D3.6, D3.7 and D.8 of the HORIZON 2020 project EURAD. EC Grant agreement no: 847593.
- Andra, 2005. Dossier 2005 Argile. Référentiel de comportement des radionucléides et des toxiques chimiques d'un stockage dans le Callovo-Oxfordien jusqu'à l'homme, Site de Meuse/Haute-Marne, Book 1/2: Chapters 1-4. ANDRA.
- Andra, 2005. Dossier 2005 Argile. Tome "Architecture et gestion du stockage géologique". ANDRA
- Androniuk I., Landesman C., Henocq P., Kalinichev A.G., 2017. Adsorption of gluconate and uranyl on C-S-H phases: Combination of wet chemistry experiments and molecular dynamics simulations for the binary systems. *Physics and Chemistry of the Earth, Parts A/B/C* 99, pp. 194–203.
- Androniuk I., Kalinichev A.G., 2020. Molecular dynamics simulation of the interaction of uranium (VI) with the C-S-H phase of cement in the presence of gluconate. *Applied geochemistry* 113, pp. 104496.
- Atkinson A., Nickerson A.K., 1984. The diffusion of ions through water-saturated cement. *J. Mater. Sci.* 19, pp. 3068–3078.
- Barger M., Koretsky C.M., 2011. The influence of citric acid, EDTA and fulvic acid on U(VI) sorption onto kaolinite. *Applied Geochemistry* 26, pp. 158–161.
- Baston, G., Dawson, J., Farahani, B., Saunders, R., Schofield, J., Smith, V., 2019. Further studies to underpin the use of PCE Superplasticisers in the Packaging of Low-heat-generating Wastes. Updates on the effects of radiolysis products on sorption and solubility. NDA Report no. RWM/Contr/19/035; p. 124). NDA;
- Bayliss S., Ewart F.T., Howse R.M., Smith-Briggs J.L., Thomason H.P., Willmott H.A., 1988. The solubility and sorption of lead-210 and carbon-14 in a nearfield environment. *Mat.Res.Soc.Symp. Proc.* 112, 33–42.
- Bucur C., Olteanu M., Cristache C., Pavelescu M., 2010. Radionuclide Transport through cement matrices. *Rev. Chim.* 61(5), pp. 458–461.
- Burešová, M., Kittnerová, J., Drtinová, B., 2023. Comparative study of Eu and U sorption on cementitious materials in the presence of organic substances. *J Radioanal Nucl Chem* 332, 1499–1504. <https://doi.org/10.1007/s10967-022-08705-3>.

- Cartwright A.J., May C., Worsfold P.J., Keith-Roach M.J., 2007. Characterisation of Th-RDTA and Th-NTA species by electrospray ionisation-mass spectrometry. *Anal. Chim Acta* 590, pp. 125–131.
- Çevirim-Papaioannou, N., Jo, Y., Franke, K., Fuss, M., De Blochouse, B., Altmaier, M., Gaona, X., 2022. Uptake of niobium by cement systems relevant for nuclear waste disposal: Impact of ISA and chloride. *Cement and Concrete Research* 153, 106690. <https://doi.org/10.1016/j.cemconres.2021.106690>.
- Crank J., 1975. *The mathematic of diffusion*, Oxford Science Publications.
- Dettmann, S., Huittinen, N.M., Jahn, N., Kretzschmar, J., Kumke, M.U., Kutyma, T., Lohmann, J., Reich, T., Schmeide, K., Shams Aldin Azzam, S., Spittler, L., Stietz, J., 2023. Influence of gluconate on the retention of Eu(III), Am(III), Th(IV), Pu(IV), and U(VI) by C-S-H (C/S = 0.8). *Front. Nucl. Eng.* 2, 1124856. <https://doi.org/10.3389/fnuen.2023.1124856>.
- Diesen V., Forsberg K., Jonsson M., 2017. Effects of cellulose degradation products on the mobility of Eu(III) in repositories for low and intermediate level radioactive waste. *Journal of Hazardous Materials* 340, 384–389.
- Drtinová, B., Kittnerová, J., Bergelová, K., Burešová, M., Baborová, L., 2023. Sorption of lead on cementitious materials in presence of organics. *Front. Nucl. Eng.* 1, 1095233. <https://doi.org/10.3389/fnuen.2022.1095233>.
- Felipe-Sotelo M., Hinchliff J., Drury B., Evans N.D.M., Williams S., Read D., 2014. Radial diffusion of radiocaesium and radioiodide through cementitious backfill. *Physics and Chemistry of the Earth*, 70/71, pp. 60–70.
- Felipe-Sotelo M., Edgar M., Beattie T., Warwick P., Evans N.D.M., Read D., 2015. Effect of anthropogenic organic complexants on the solubility of Ni, Th, U(IV) and U(VI). *Journal of Hazardous Materials* 300, pp. 553–560.
- Felipe-Sotelo M., Hinchliff J., Evans N.D.M., Read D., 2016. Solubility constraints affecting the migration of selenium through the cementitious backfill of a geological disposal facility. *Journal of Hazardous Materials* 305, pp. 21–29.
- Felipe-Sotelo M., Hinchliff J., Field L.P., Milodowski A.E., Preedy, O., Read, D., 2017. Retardation of uranium and thorium by a cementitious backfill developed for radioactive waste disposal. *Chemosphere* 179, pp. 127–138.
- Flury M, Gimmi T.F., 2002. 6.2 Solute Diffusion. in *Methods of Soil Analysis: Part 4 Physical Methods*. Soil Science Society of America, print ISBN:9780891188414, Online ISBN:9780891188933, pp. 1323–1351).
- Friedrich, S., Sieber, C., Drobot, B., Tsushima, S., Barkleit, A., Schmeide, K., Stumpf, T., Kretzschmar, J., 2023. Eu(III) and Cm(III) Complexation by the Aminocarboxylates NTA, EDTA, and EGTA Studied with NMR, TRLFS, and ITC—An Improved Approach to More Robust Thermodynamics. *Molecules* 28, 4881. <https://doi.org/10.3390/molecules28124881>.
- Fromentin E, Reiller P.E., 2018. Influence of adipic acid on the speciation of Eu(III): Review of thermodynamic data in NaCl and NaClO₄ media, and a new determination of Eu-adipate complexation constant in 0.5 mol·kgw⁻¹ NaClO₄ medium by time-resolved luminescence spectroscopy. *Inorganica Chimica Acta* 482, pp. 588–596.
- Fromentin E, Reiller P.E., 2020. Interactions between hydro-soluble degradation products from a radio-oxidized polyesterurethane and Eu(III) in contexts of repositories for low and intermediate level radioactive waste. *Radiochim. Acta* 108(5), pp. 383–395.
- Gaona X., Montoya V., Colàs E., Grivé M., Duro L., 2008. Review of the complexation of tetravalent actinides by ISA and gluconate under alkaline to hyperalkaline conditions. *J. Contam. Hydrol.* 102, pp. 217–227.

- Garcia D., Grivé M., Duro L., Brassines S., de Pablo J., 2018b. Effects of superplasticizers on Ni behaviour in cementitious materials. *J. of Radioanalytical and Nuclear Chemistry* 317(1), pp. 397–407.
- Garcia D., Grivé M., Duro L., Brassinnes S., de Pablo J., 2018a. The potential role of the degradation products of cement superplasticizers on the mobility of radionuclides. *Applied geochemistry* 98, pp. 1–9.
- García-Gutiérrez M., Missana T., Mingarro M. Morejón M., Cormenzana J.L. 2018. Cesium diffusion in mortars from different cements used in radioactive waste repositories. *Applied Geochemistry* 98, pp.10-16.
- Giffaut E., Grivé M., Blanc P., Vieillard Ph., Colàs E., Gailhanou H., Gaboreau S., Marty N., Madé B., Duro L., 2014. Andra thermodynamic database for performance assessment: ThermoChimie. *Applied geochemistry* 49, pp. 225–236.
- Glaus, M. A., Laube, A., & Van Loon, L. R., 2003. A generic procedure for the assessment of the effect of concrete admixtures on the sorption of radionuclides on cement: Concept and selected results. *MRS Online Proceedings Library Archive*, 807.
- Grambow B., López-García M., Olmeda J., Grivé M., Marty N.C.M., Grangeon S., Claret F., Lange S., Deissmann G., Klinkenberg M., Bosbach D., Bucur C., Florea I., Dobrin R., Isaacs M., Read D., Kittnerová J., Drtinová B., Vopalka D., Cevirim-Papaioannou N., Ait-Mouheb N., Gaona X., Altmaier M., Nedyalkova L., Lothenbach B.h., Tits J., Landesman C., Rasamimanana C., Ribet S., 2020. Retention and diffusion of radioactive and toxic species on cementitious systems: Main outcome of the CEBAMA project. *Applied Geochemistry* 112, 104480.
- Grenthe, I., Gaona, X., Plyasunov, A. V., Rao, L., Runde, W. H., Grambow, B., Konings, R. J. M., Smith, A.L., Moore, E. E. (2020). Second Update on the Chemical Thermodynamics of Uranium, Neptunium, Plutonium, Americium and Technetium, OECD Nuclear Energy Agency Data Bank, Eds., OECD Publications, Paris, France.
- Guillaumont R., Fanghänel T., Neck V., Fuger J., Palmer D.A., Grenthe I., Rand M.H., 2003. Update on the Chemical Thermodynamics of Uranium, Neptunium, Plutonium, Americium and Technetium. Elsevier, North Holland, Amsterdam, p. 959.
- Holgersson S., Albinsson Y., Allard B., Boren H., Pavasars I, Engkvist I., 1998. Effects of Gluco-iso-saccharinate on Cs, Ni, Pm and Th Sorption onto, and Diffusion into Cement. *Radiochim. Acta* 82, pp. 393–398.
- Hummel W., Anderegg G., Puigdomènech I., Rao L. and Tochiyama O., 2005a. The OECD/NEA TDB review of selected organic ligands. *Radiochim. Acta* 93, pp. 719–725.
- Hummel W., Anderegg G., Puigdomènech I., Rao L., Tochiyama O., 2005b. Chemical Thermodynamics of Compounds and Complexes of U, Np, Pu, Am, Tc, Se, Ni, and Zr with Selected Organic Ligands, Chemical Thermodynamic 9. Elsevier ISBN: 978-0-444-51402-8, North Holland, Amsterdam, p. 1088.
- Humphreys P.N., Laws A., Dawson J., 2010. A Review of Cellulose Degradation and the Fate of Degradation Products Under Repository Conditions. Technical Report SERCO/TAS/002274/001/Issue2.
- Jakob A., Sarott F.-A., Spieler P., 1999. Diffusion and sorption on hardened cement paste - experiments and modelling results. PSI Bericht Nr. 99-05, Paul Scherrer Institut, Nuclear Energy and Safety Research Department, Laboratory for Waste Management (NES / LES).
- Jo, Y., Androniuk, I., Çevirim-Papaioannou, N., De Blochouse, B., Altmaier, M., Gaona, X., 2022. Uptake of chloride and iso-saccharinic acid by cement: Sorption and molecular dynamics studies on HCP (CEM I) and C-S-H phases. *Cement and Concrete Research* 157, 106831. <https://doi.org/10.1016/j.cemconres.2022.106831>.

- Keith-Roach M.J., 2008. The speciation, stability, solubility and biodegradation of organic co-contaminant radionuclide complexes: a review. *Science of the Total Environment*, 396, pp. 1–11.
- Killey R.D.W., McHug J.O., Champ D.R., Cooper E.L., Young J.L., 1984. Subsurface Co-60 migration from a low-level waste disposal site. *Environmental Science and Technology* 165, pp. 277–304.
- Kinniburgh D., Cooper D.M., 2011. Creating graphical output with PHREEQC. <<http://www.phreeplot.org>>.
- Kittnerová, J., Drtinová, B., Štamberg, K., Deissmann, G., Lange, S., Evans, N., 2023. Study of Radium Behavior in Contact With Calcium-Silicate-Hydrates. *Journal of Nuclear Engineering and Radiation Science* 9, 011901. <https://doi.org/10.1115/1.4055160>.
- Kornilovich BY., Pshinko G.N., Bogolepov A.A., 2006. Effects of EDTA and NDTA on sorption of U(VI) on the clay fraction of soil. *Radiochemistry* 48(6), pp. 584–587.
- Kretzschmar, J., Tsushima, S., Drobot, B., Steudtner, R., Schmeide, K., Stumpf, T., 2020. Trimeric uranyl(VI)–citrate forms Na^+ , Ca^{2+} , and La^{3+} sandwich complexes in aqueous solution. *Chem. Commun.* 56, 13133–13136. <https://doi.org/10.1039/D0CC05460G>.
- Kretzschmar, J., Tsushima, S., Lucks, C., Jäckel, E., Meyer, R., Steudtner, R., Müller, K., Rossberg, A., Schmeide, K., Brendler, V., 2021. Dimeric and Trimeric Uranyl(VI)–Citrate Complexes in Aqueous Solution. *Inorg. Chem.* 60, 7998–8010. <https://doi.org/10.1021/acs.inorgchem.1c00522>.
- Kuippers G., Boothman C., Bagshaw H., Ward M., Beard R., Bryan N., Lloyd J.R., 2018. The biogeochemical fate of Ni, during microbial ISA degradation; implications for nuclear waste disposal. *Scientific Reports*, 8: 8753, www.nature.com/scientificreports.
- Legend S. (2023) Effets de la radiolyse sur le transfert et la spéciation de radionucléides en milieu cimentaire adjuvanté, PhD manuscript.
- Legend, S., Macé, N., Muzeau, B., Le Tutour, P., Therias, S., Reiller, P.E., 2023. Radiolysis effect on Eu(III)-superplasticiser interactions in artificial cement and squeezed cement pore waters. *Journal of Hazardous Materials* 443, 130269. <https://doi.org/10.1016/j.jhazmat.2022.130269>.
- Maragkou, E., Pashalidis, I., 2021. Investigations on the Interaction of EDTA with Calcium Silicate Hydrate and Its Impact on the U(VI) Sorption. *Coatings* 11, 1037. <https://doi.org/10.3390/coatings11091037>.
- Mattigod S.V., Whyatt G.A., Serne R.J., Martin P.F., Schwab, K.E., Wood M.I., 2001. Diffusion and Leaching of Selected Radionuclides (Iodine-129, Technetium-99, and Uranium) through Category 3 Waste Encasement Concrete and Soil Fill Material. Pacific Northwest National Laboratory (No. PNNL-13639), Richland, Wa 99352, USA.
- May C.C., Young L., Worsfold P.J., Heath S., Bryan N.D., Keith-Roach M.J., 2012. The effects of EDTA on the groundwater transport of Th through sand. *Water Research* 46, pp. 4870–4882.
- Means J.L., Crear D.A., 1978. Migration of radioactive wastes: radionuclide mobilization by complexing agents. *Science* 200, pp. 1480–1481.
- Missana, T., García-Gutiérrez, M., Alonso, U., Almendros-Ginestá, O., 2022a. Nickel retention by calcium silicate hydrate phases: Evaluation of the role of the Ca/Si ratio on adsorption and precipitation processes. *Applied Geochemistry* 137, 105197. <https://doi.org/10.1016/j.apgeochem.2022.105197>.
- Missana, T., García-Gutiérrez, M., Alonso, U., Fernández, A.M., 2022b. Effects of the presence of isosaccharinate on nickel adsorption by calcium silicate hydrate (CSH) gels: Experimental analysis and surface complexation modelling. *Journal of Environmental Chemical Engineering* 10, 108500. <https://doi.org/10.1016/j.jece.2022.108500>.
- NDA, 2017. The impact of the use of polycarboxylate ether superplasticisers for the packaging of low heat generating wastes on GDF post-closure safety. NDA Report no. NDA/RWM/135. NDA.

- Ochs M., Mallants D. and Wang L., 2016. Radionuclide and metal sorption on cement and concrete. Topics in Safety, Risk, Reliability and Quality, Volume 29. ©Springer International Publishing Switzerland, ISSN 1566-0443.
- Ochs M., Talerico C., 2006. Development of Models and Datasets for Radionuclide Retention by Cementitious Materials, Andra 2005 report 2006, C.RP.0BMG.06.0001A.
- Ochs M., Talerico C., Lothenbach B., Giffaut E., 2003. Systematic trends and empirical modelling of lead uptake by cements and cement minerals, Mat.Res.Soc.Symp. Proc. 757, 693–698.
- Parkhurst, D., Appelo, C., 2013. Description of input and examples for PHREEQC version 3. A Computer Program for Speciation, Batch-Reaction, One-Dimensional Transport, and Inverse Geochemical Calculations. U.S Geological Survey Techniques and Methods 6, A43.
- Pavasars I., Hagberg J., Borén H., Allard B., 2003. Alkaline degradation of cellulose: mechanisms and kinetics. Journal of Polymers and the Environment 11 (2), pp. 39–47.
- Payne T.E, Brendler V., Ochs M., Baeyens B., Browne P.L., Davis J.A., Ekberg C., Kulik D.A., Lutzenkirchen J., Missana T., Tachi Y., Van Loon L.R., Altmann S., 2013. Guidelines for thermodynamic sorption modelling in the context of radioactive waste disposal. Environmental Modelling and Software 42, pp. 1–14.
- Pointeau I., 2000. Etude mécanistique et modélisation de la rétention de radionucléides par les silicates de calcium hydrates (CSH) des ciments. Ph.D. dissertation, University of Reims, France.
- Pointeau, I., Coreau, N., Reiller, P.E., 2008. Uptake of anionic radionuclides onto degraded cement pastes and competing effect of organic ligands. Radiochimica Acta 96, 367–374.
- Rai D, Kitamura A., 2017. Thermodynamic equilibrium constants for important isosaccharinate reactions: a review. J. Chem. Therm. 114, pp. 135–143.
- Reiller, P.E., Fromentin, E., Ferry, M., Dannoux-Papin, A., Badji, H., Tabarant, M., Vercoüter, T., 2017. Complexing power of hydro-soluble degradation products from irradiated polyvinylchloride: influence on $\text{Eu}(\text{OH})_{3(s)}$ solubility and $\text{Eu}(\text{III})$ speciation in neutral to alkaline environment. Radiochimica Acta 105. <https://doi.org/10.1515/ract-2016-2691>.
- Reinoso-Maset E., Worsfold P.J., Keith-Roach M.J., 2012. The effects of EDTA, NTA, picolinic acid on Th mobility in ternary system with natural sand. Environmental Pollution 162, pp. 399–405.
- Reinoso-Maset E., Worsfold P.J., Keith-Roach M.J., 2013. Effect of organic complexing agents on the interactions of Cs, Sr and U with silica and natural sands. Chemosphere 91, pp. 948–954.
- Rojo, H., Gaona, X., Rabung, T., Polly, R., García-Gutiérrez, M., Missana, T., Altmaier, M., 2021. Complexation of Nd(III)/Cm(III) with gluconate in alkaline NaCl and CaCl_2 solutions: Solubility, TRLFS and DFT studies. Applied Geochemistry 126, 104864. <https://doi.org/10.1016/j.apgeochem.2020.104864>.
- Santschi P.H., Xu C., Zhang S., Schwehr K.A., Lin P., Yeager C.M., Kaplan D.I., 2017. Recent advances in the detection of specific natural organic compounds as carriers for radionuclides in soil and water environments, with examples of radioiodine and plutonium. J. Environ. Radioact 171, pp. 226–233.
- Sarott F.-A., Bradbury M.H., Pandolfo P., Spieler P., 1991. Diffusion and adsorption studies on hardened cement paste and the effect of carbonation on diffusion rates. Cement and Concrete Research 22, pp. 439–444.
- Stietz, J., Amayri, S., Häußler, V., Scholze, R., Reich, T., 2023a. The Uptake of Actinides by Hardened Cement Paste in High-Salinity Pore Water. Minerals 13, 1380. <https://doi.org/10.3390/min13111380>.
- Stietz J., Amayri S., Häußler V., Prieur D. and Reich, T. 2023b. Uptake of Pu(IV) by hardened cement paste in the presence gluconate at high and low ionic strengths. Front. Nucl. Eng. 2:1268767. <https://doi.org/10.3389/fnuen.2023.1268767>.

- Shafikhani M, Chidiac S.E., 2019. Quantification of concrete chloride diffusion coefficients – A critical review. *Cement and Concrete Composites* 99, pp. 225-250.
- Sugiyama D., Chida T., Cowper M., 2008. Laser ablation microprobe inductively coupled plasma mass spectrometry study on diffusion of uranium into cement materials. *Radiochim. Acta* 96, pp. 747–752.
- Szabo, P.G., Tasi, A.G., Gaona, X., Maier, A.C., Hedström, S., Altmaier, M., Geckeis, H., 2023a. Impact of the degradation leachate of the polyacrylonitrile-based material UP2W on the retention of Ni(II), Eu(III) and Pu(IV) by cement. *Dalton Trans.* 52, 13324–13331. <https://doi.org/10.1039/D3DT02122J>.
- Szabo, P.G., Tasi, A.G., Gaona, X., Maier, A.C., Hedström, S., Altmaier, M., Geckeis, H., 2023b. Uptake of Ni(II), Eu(III) and Pu(III/IV) by Hardened Cement Paste in the Presence of Proxy Ligands for the Degradation of Polyacrylonitrile. *Front. Nucl. Eng.* 2, 1117413. <https://doi.org/10.3389/fnuen.2023.1117413>.
- Szabo, P.G., Tasi, A.G., Gaona, X., Maier, A.C., Hedström, S., Altmaier, M., Geckeis, H., 2022a. Uptake of selected organic ligands by hardened cement paste: Studies on proxy ligands for the degradation of polyacrylonitrile and general considerations on the role of different functionalities in the uptake process. *Front. Nucl. Eng.* 1, 997398. <https://doi.org/10.3389/fnuen.2022.997398>.
- Szabo, P.G., Tasi, A.G., Gaona, X., Polly, R., Maier, A.C., Hedström, S., Altmaier, M., Geckeis, H., 2022b. Solubility of Ca(II), Ni(II), Nd(III) and Pu(IV) in the presence of proxy ligands for the degradation of polyacrylonitrile in cementitious systems. *Dalton Trans.* 51, 9432–9444. <https://doi.org/10.1039/D2DT01409B>.
- Tasi A., Gaona X., Fellhauer D., Böttle M, Rothe J., Dardenne K., Polly R., Grivé M., Colàs E., Bruno J., Källström K., Altmaier M., Geckeis H., 2018a. Thermodynamic description of the plutonium – α -D-isosaccharinic acid system I: Solubility, complexation and redox behaviour. *Applied geochemistry* 98, pp. 247–264 (+ Supporting Information).
- Tasi, A., Gaona, X., Fellhauer, D., Böttle, M., Rothe, J., Dardenne, K., Polly, R., Grivé, M., Colàs, E., Bruno, J., Källström, K., Altmaier, M., Geckeis, H., 2018b. Thermodynamic description of the plutonium – α -D-isosaccharinic acid system II: Formation of quaternary Ca(II)–Pu(IV)–OH–ISA complexes. *Applied Geochemistry* 98, 351–366. <https://doi.org/10.1016/j.apgeochem.2018.06.014>
- Tasi, A., Gaona, X., Rabung, Th., Fellhauer, D., Rothe, J., Dardenne, K., Lützenkirchen, J., Grivé, M., Colàs, E., Bruno, J., Källström, K., Altmaier, M., Geckeis, H., 2021. Plutonium retention in the isosaccharinate – cement system. *Applied Geochemistry* 126, 104862. <https://doi.org/10.1016/j.apgeochem.2020.104862>.
- ThermoChimie v10a, <https://www.thermochimie-tdb.com/>.
- Thoenen T., Hummel W., Berner U., Curti E., 2014. The PSI/Nagra chemical thermodynamic database 12/07. PSI Bericht Nr. 14-04, ISSN 1019-0643, Paul Scherrer Institut, Nuclear Energy and Safety Research Department, Laboratory for Waste Management (NES / LES).
- Tits J., Wieland E., 2018. Actinide Sorption by Cementitious Materials. PSI Bericht Nr. 18-02, ISSN 1019-0643, Paul Scherrer Institut, Nuclear Energy and Safety Research Department, Laboratory for Waste Management (NES / LES).
- van Es E., Hinchliff J., Felipe-Sotelo M., Milodowski A.E., Field L.P., Evans N.D.M., Read, D., 2015. Retention of chlorine-36 by a cementitious backfill. *Mineral. Mag.* 79, pp. 1297–1305.
- Wang Z.-M., van de Burgt L.J., Choppin G.R., 1999. Spectroscopic study of lanthanide(III) complexes with carboxylic acids. *Inorganica Chimica Acta* 293, pp. 167–177.
- Wang Z.-M., van de Burgt L.J., Choppin G.R., 2000. Spectroscopic study of lanthanide(III) complexes with aliphatic dicarboxylic acids. *Inorganica Chimica Acta* 310, pp. 248–256.
- Wieland E., Lothenbach B., Glaus M.A., Thoenen T. Schwyn B., 2014. Influence of superplasticizers on the long-term properties of cement pastes and possible impact on radionuclide uptake in a cement-based repository for radioactive waste. *Applied geochemistry* 49, pp. 126–142.

- Wieland E., 2014. Sorption Data Base for the Cementitious Near Field of L/ILW and ILW Repositories for Provisional Safety Analyses for SGT-E2. Nagra Technical Report 14-08, Nagra, Wettingen, Switzerland.
- Yamaguchi T., Negishi K., Hoshino S., Tanaka T., 2009. Modeling of diffusive mass transport in micropores in cement based materials. *Cement and Concrete Research* 39, pp. 1149–1155.
- Young A.J., 2012. The stability of cement superplasticiser and its effect on radionuclide behaviour. Ph.D thesis, Loughborough University, U.K..

5. Fundamental cement chemistry

Authors: Virginie Blin [CEA]; David Garcia [KIT (Amphos21)]; Pierre Henocq [Andra], Tiziana Missana [CIEMAT]

This chapter summarizes fundamental aspects and knowledge on the chemistry of cement-based materials.

Cement-based materials have been massively used in civil engineering for more than one hundred years. They also represent a main component in radioactive waste disposal facilities, in terms of being considered for use as engineered barriers and packages. The chemistry of ordinary cement is well-known. In particular, H.W.F. Taylor (1992) in his outstanding work described the main cement components and their hydration processes. The minerals formed by the hydration of cement, called cement hydrates, have been deeply characterized during the last decades. The Calcium Silicate Hydrates (C-S-H) are the main cement hydrate; they are closely related to the fundamental properties of cement-based materials. This is explaining the large number of scientific papers on this cement hydrate.

This document presents a synthesis of the cement chemistry according to the current cement types, outlining the anhydrous cement composition and the different hydrated phases. Finally, the chemical evolution of the cementitious matrix in the context of a deep geological repository is described.

5.1 Anhydrous cement

The chemical properties of the cement-based materials and their mineralogy depend on the chemical composition of cement (Taylor, 1992). Different types of cement are available; their use depends on the environmental exposure (sulfate for instance), the design of the concrete structure (massive elements for instance), or the economical point of view (use of Supplementary Cementitious Materials). Consequently, this section presents the main components of the ordinary cement and the various types of cement made with Supplementary Cement Materials (SCMs).

The solid phases in anhydrous cement are expressed in the form of oxides such as CaO, SiO₂, Al₂O₃ and Fe₂O₃, which are the main components. The nomenclature of these oxides is defined as follows:

- C = CaO
- A = Al₂O₃
- S = SiO₂
- s = SO₃
- F = Fe₂O₃
- M = MgO
- c = CO₂

Cement powder is a mix of clinker and gypsum (around 5%). The main components of clinker are: (i) C3S (alite), (ii) C2S (belite), (iii) C3A, and (iv) C4AF (Taylor, 1992). This composition corresponds to the ordinary Portland cement called CEM I. Other types of cement are mixes composed of cement CEM I and SCMs. The main SCMs are (i) blast-furnace slag, (ii) fly ash, and (iii) silica fume (Lothenbach *et al.*, 2011; Snellings *et al.*, 2012). Binary, ternary and even quaternary cements can be made with these supplementary materials. We can distinguish the cement types (i) CEM III composed with CEM I and slag, and (ii) CEM V, a ternary cement composed by CEM I, fly ash and slag. The ternary diagram in FIGURE 5-1 illustrates different types of cement and their components regarding their Ca, Si and Al contents.

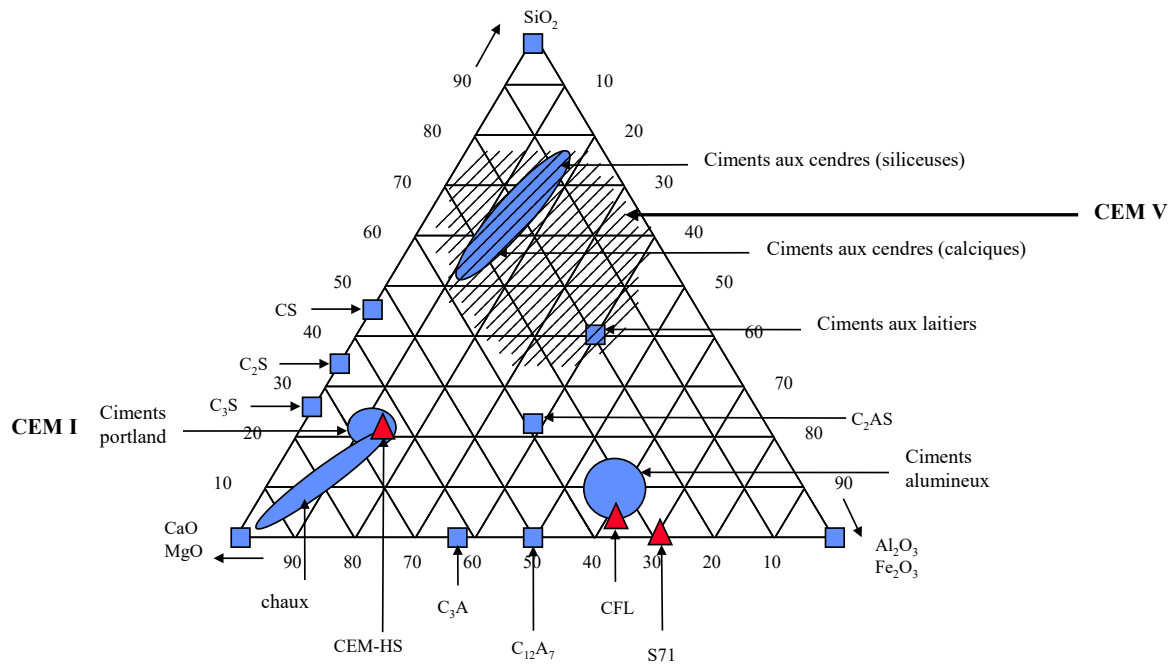


FIGURE 5-1: Ternary diagram CaO-SiO₂-Al₂O₃ showing the compositions of the main types of cement (from Damtoft *et al.*, 1999).

5.2 Cement hydrates

Once cement is hydrated with water, solid phases including water molecules are formed. These mineral phases are called cement hydrates. Hydration of C3S and C2S leads to the formation of Calcium Silicate Hydrates (C-S-H) and portlandite (CH), while ettringite (AFt), AFm phases, and calcium alumina hydrates are formed from C3A and C4AF (Taylor, 1992; Strutzman, 1999; Glasser, 2011). Because of their high specific surface area, C-S-H mostly contribute to the radionuclide retention capacity. However, the other minerals can also contribute, especially AFm phases, for some radionuclides.

Regarding their significant impact of the radionuclide behaviour and on the overall properties of cement-based materials, C-S-H are specifically described in terms of thermodynamic (Gartner & Jenings, 1987; Chen *et al.*, 2004; Lothenbach & Nonat, 2015; Walker *et al.*, 2016) and, also, electrokinetic properties (Nachbaur *et al.*, 1998; Viallis-Terrisse *et al.*, 2001; Henocq, 2005). One of the main characteristics of

C-S-H is the variable stoichiometry characterized by the molar ratio Ca/Si (C/S) between 0.6 and 1.7. This stoichiometry can be illustrated by the relationship between the C/S and the calcium concentration in solution as illustrated in FIGURE 5-2.

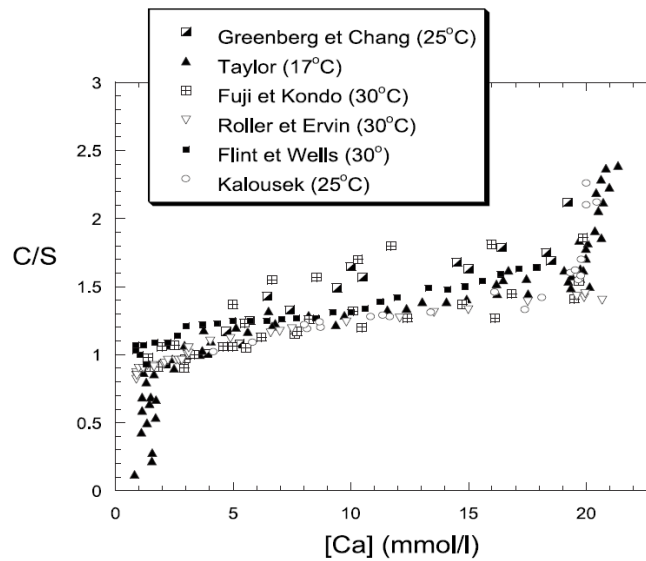


FIGURE 5-2: Solubility of C-S-H: C/S as a function of calcium concentration in a solution in equilibrium with the C-S-H from Berner (1992) and Henocq (2005).

In a pristine cement-based material, the C/S ratio of C-S-H is expected to be higher than 1.45 (near 1.75 (Taylor, 1993); 1.7 (Jennings, 2000)). That means, according to FIGURE 5-2, that the degradation of cementitious materials is associated with a decalcification of C-S-H. Nevertheless, it is important to note that in sound cement-based materials, the initial alkali content in the pore solution induces a high pH (pH>13) and modifies the chemical equilibrium of C-S-H by decreasing the calcium concentration in solution as shown in FIGURE 5-3 (Hong & Glasser, 1999; Henocq, 2005).

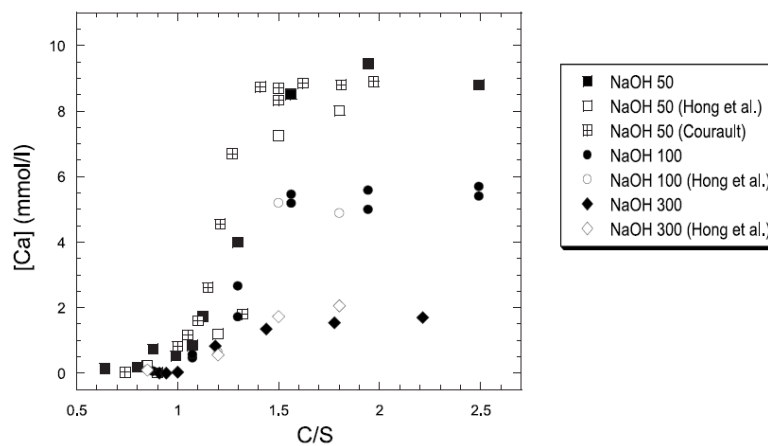


FIGURE 5-3: Solubility of C-S-H: calcium concentration as a function of C/S for different NaOH concentrations (from Henocq, 2005).

The characterization of the main cement hydrates in terms of thermodynamic properties such as solubility have motivated many works of interest (Damidot *et al.*, 2011; Lothenbach & Winnefeld, 2006; Roosz *et al.*, 2018), not only on C-S-H as aforementioned, but also on AFm phases (Matschei *et al.*, 2007), ettringite (Myneni *et al.*, 1998; Perkins & Palmer, 1999), and portlandite (Duchesne & Reardon, 1995).

C-S-H have a nanostructure defined by the *dreierketten* chain structure (Hamid, 1981). The nanostructure evolves as a function of C/S ratio. As shown by ^{29}Si NMR technique in *FIGURE 5-4*, this evolution is characterized by long silicon tetrahedra chains for low C/S ratio (Q_2 tetrahedra) which are gradually broken as the C/S ratio increases (Q_1 tetrahedra) (Cong & Kirkpatrick, 1996; Zanni *et al.*, 1996; Klur *et al.*, 1998; Roosz *et al.*, 2018). In parallel, there is also an evolution of the amount of layers per C-S-H grain: for C-S-H (C/S=1.0), stacks of 3 or 6 layers were observed while for C-S-H (C/S=1.2), particle stacks of 4 to 8 layers were observed (Gaboreau *et al.*, 2020). These structure evolutions with C/S ratio involve a decrease of the specific surface area as C/S increases. Consequently, that has consequences on the sorption properties.

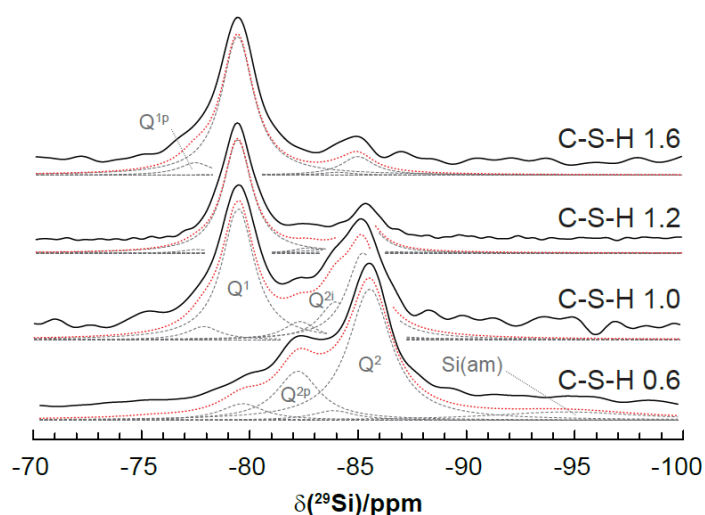


FIGURE 5-4: ^{29}Si NMR spectra of C-S-H samples with various C/S ratios (from Roosz, 2016).

For ordinary cement, C-S-H is the main hydration product together with CH. However, for cement-based materials that include SCMs, the alumina content is much higher than ordinary cement, and as a consequence, alumina substitution into the C-S-H structure occurs to form C-A-S-H (Faucon *et al.*, 1998; L'Hôpital *et al.*, 2015). The physico-chemical properties of C-A-S-H are assumed to be similar to those of C-S-H in terms of alkali sorption (Bach *et al.*, 2013; Chappex & Scrivener, 2012) contrary to the observations by Hong & Glasser (2002). Regardless of these chemical aspects, the hydration of cementitious mixes with SCMs involved a pozzolanic reaction between portlandite produced from C3S and C2S, and silica and alumina released from the hydration of SCMs (*FIGURE 5-5*). The effect of the pozzolanic reaction is a densification of the matrix with more C-A-S-H, decreasing the transport and improving mechanical properties.

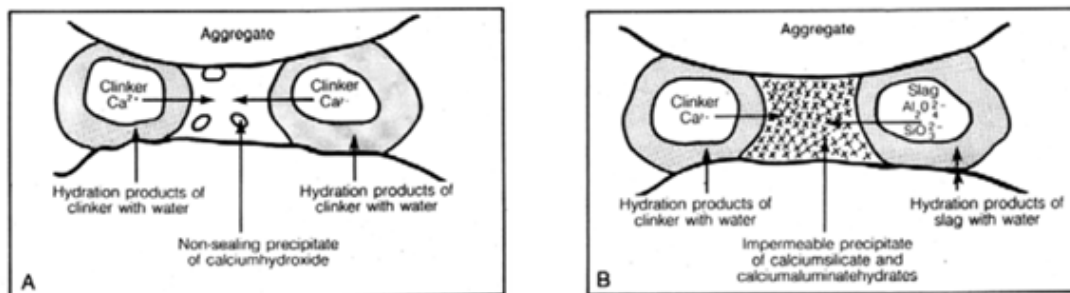


FIGURE 5-5: Effect of the pozzolanic reaction: A) hydration of ordinary Portland cement, and B) hydration of a cement/slag mix (from Surech & Nagaraju (2015)).

As aforementioned, the other main cement hydrates are ettringite, AFm phases, hydrotalcite and possibly hydrogarnet or gypsum. These solid phases, even if their content and specific surface area can be negligible compared to the ones of C-S-H, have a role in terms of radionuclide retention (oxy-anions for ettringite and AFm) and chemical evolution in certain environments (sulfate attack for example).

5.3 Pore solution

The cement-based materials are porous materials with a porosity around 10% for concrete and 40% for hydrated cement pastes (HCPs) (Fagerlund, 2006; Tracz, 2016). For pristine materials in fully saturated conditions, this porous volume is filled with a solution in equilibrium with the cement hydrates. For ordinary cements, the pore solution composition is controlled by the portlandite solubility and the alkali content implying a high pH and, consequently, alkaline conditions. Andersson *et al.* (1989) characterized the pore solution of hydrated cement pastes for various cement types including the major ionic species as well as E_h and pH. This work showed that the composition of the pore solution is dependent on the chemical composition of cement but generally controlled by NaOH and KOH contents which imply a high pH (~13.3). Moreover, Andersson *et al.* (1989) mostly measured a positive redox potential E_h (~100 mV), i.e. oxidizing conditions, except when blast-furnace slag was used in the material and reducing conditions were observed ($E_h = -377$ mV).

The chemical composition of cement may include toxic chemicals or other species as trace elements which then can be present in the pore solution at trace concentrations. The main trace elements are mostly Ba, Ni, Sr, Pb, Co or Li (Hillier *et al.*, 1999; Achternbosch *et al.*, 2005; Young, 2012). The trace elements can be released in the environment under leaching and, probably, could compete with radionuclides in terms of sorption. Additionally, they can also participate in ion-exchange with active elements as described in González-Siso (2018).

As an example, TABLE 5-1 gives the concentration of the main species in the pore solution of a CEM V hydrated cement paste (Olmeda *et al.*, 2017).

TABLE 5-1: Pore solution composition from CEM-V/A HCP samples at 102 days of curing (Olmeda *et al.*, 2017).

Pore solution properties	
pH	13.3
Species	Concentration (mmol/kg)
Ca	1.4
S	1.6
Na	72
K	210

5.4 Superplasticizers

Cement admixtures are an essential component of concrete. Usually, they are used for enhancing the workability of the fresh mix and/or for reducing the water content. Superplasticisers are synthetic chemicals consisting of high molecular weight - water soluble polymers. Solubility is ensured by the presence of adequate hydroxyl, sulfonate or carboxylate groups attached to the main organic repeat unit which is usually anionic in nature (Ramachadran, 1996). Different types of superplasticizers are available (Young, 2012), (i) sulfonated melamine, (ii) sulfonated naphthalene formaldehyde, (iii) lignosulfonates, and (iv) polycarboxylates. The latter has been widely used since one decade.

The influence of superplasticizers is assumed to be negligible in most of the applications in civil engineering. However, not much is known about the long-term evolution of cement-bound SP in hardened concrete. Keith-Roach and Höglund (2018) referred in their review some studies where the use SP improve mechanical properties as porosity or reduce the Cl⁻ concentration of cement porewaters, which is beneficial for long-term structural properties of concrete. The same authors also indicated that no significant effect of SP was found on the kind or amount of hydration products or pore solution composition. In addition, in radioactive waste management, the role of superplasticizers with regard to radionuclide complexation with organic molecules motivated a number of studies (Glaus *et al.*, 2003; Young, 2012; Wieland *et al.*, 2014; Garcia *et al.*, 2018). Regarding the sorption properties of the admixtures on cement-based materials, sorption values remain low compared to that of radionuclide sorption (Glaus *et al.*, 2006; Wieland *et al.*, 2014).

5.5 Chemical evolution

As described previously, the cement-based materials are in equilibrium at high pH conditions. Consequently, in a natural environment, *i.e.* around pH 7, cement-based materials are chemically

unstable. The consequences, in presence of natural waters, are the leaching of selected species into the pore solution such as Na and K, and a gradual dissolution of cement hydrates leading to a degradation of the cement-based materials. This degradation evolves with time, regarding the mineralogical composition. The pH is the main parameter illustrating this degradation process and its evolution is an indicator on the degradation level. A universal description has been adopted for characterizing the chemical evolution of the cement-based materials under disposal conditions (Ochs *et al.*, 2016). This description is based on four degradation stages (I up to IV). Each step is related to the time scale under the assumptions specific for Dessel site and physicochemical processes of some key minerals as follows (Ochs *et al.*, 2016):

- **Stage I (13.5 > pH > 12.5, 3 years):** The pristine cement-based materials have a hyperalkaline pore water (pH ~ 13.5). In contact with natural waters, alkalis (Na and K) are gradually removed from the pore volume until very low Na and K concentrations. The lower pH limit (pH = 12.5) corresponds to the thermodynamic equilibrium with portlandite in free alkali solution.
- **Stage II (pH = 12.5, 3,500 years):** the pH of the pore fluid is controlled by the solubility of portlandite. Typically, the pore solution is composed by Ca cations (0.02 mol/kg) and OH⁻ (0.035 mol/kg). The duration of this step depends on the portlandite content which acts as a buffer.
- **Stage III (12.5 > pH > 10, 36,400 years):** after the complete dissolution of portlandite (state II), the C-S-H phase is gradually decalcified from a C/S ratio of 1.5 down to C/S = 0.7. The pore solution is mainly controlled by Ca-concentration which evolves from 0.02 mol/kg down to 0.001 mol/kg; cations are balanced by OH⁻ ions for high C/S ratios and Si(OH)_nx species (n=2,3 and x=-2,-1 respectively) for the lowest C/S ratios.
- **Stage IV (10 > pH):** Once C-S-H are completely dissolved, calcite (in the presence of carbonate) and silica control the pore fluid chemistry.

FIGURE 5-6 presents a schematic description of the degradation of cement-based materials with the corresponding pH decrease as a function of time and the definition of the degradation stages as described above.

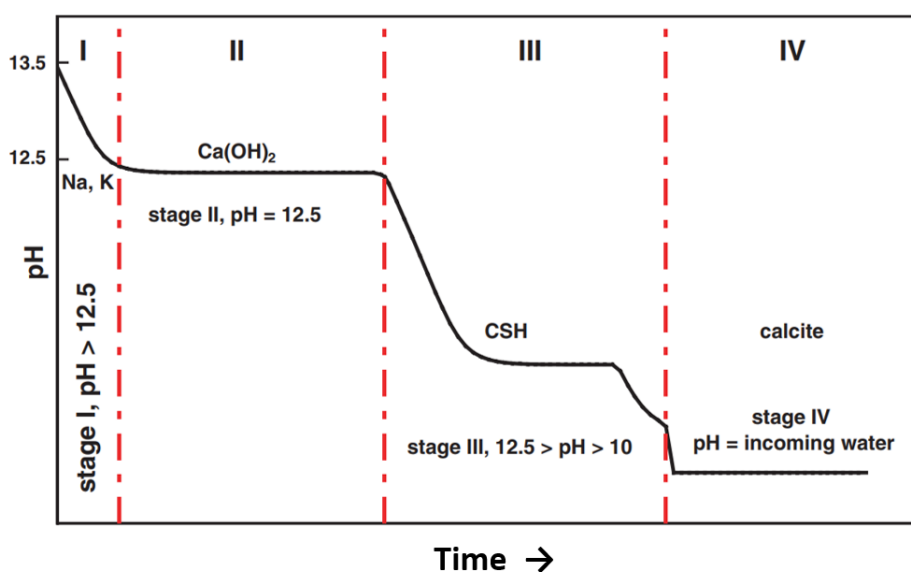


FIGURE 5-6: Schematic diagram illustrating the evolution of pH associated to the gradual degradation of cement-based materials defining four degradation stages (I to IV) (adj. from Ochs *et al.*, 2016).

5.6 Effect of the sorption on chemical properties

The sorption of species in solution, or more generally their interactions with the cementitious matrix, depends on the chemical and physical properties of the cement hydrates, mostly C-S-H. This part is not dedicated to a wide overview of radionuclide sorption in cement-based materials (for which one can refer to Evans (2008) and Ochs *et al.* (2016) regarding radionuclide sorption). It rather discusses the role of sorption processes on the chemical equilibrium of the cement hydrates, especially C-S-H. An example of this is the effect of the sorption of alkalis (Na and K) on cement hydrates regarding the composition of the pore solution (Brouwers, 2003). Also, alkali sorption is high for low C/S C-S-H. The amount of cations (Na^+) fixed by C-S-H is then balanced in the solution by calcium ions released by C-S-H increasing the Ca concentration as shown in FIGURE 5-7 (Henocq, 2017). As expected, the release of calcium increases as the liquid/solid (L/S) ratio decreases, and consequently, for high concentrations of NaCl (up to 1 M), the Ca concentration can be 30 times higher compared to the free-alkali C-S-H (for L/S=20).

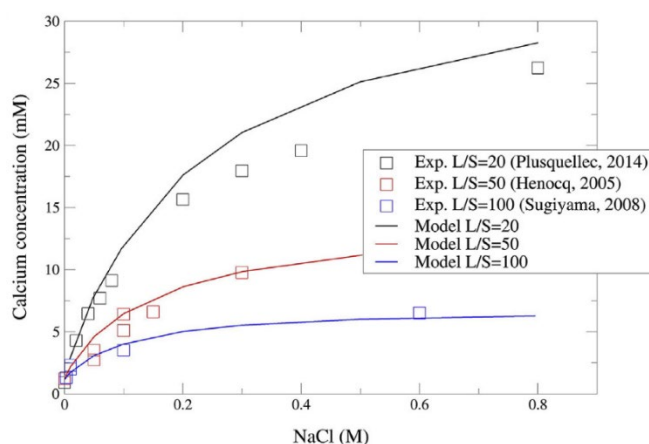


FIGURE 5-7: Effect of the Na^+ sorption on the chemistry of C-S-H: evolution of the calcium concentration of C-S-H ($C/S=0.8$) at equilibrium as a function of NaCl concentration with different liquid-to-solid ratios (L/S). Experiments and modelling (Henocq, 2017).

The cations such as Na^+ species are favourably sorbed on C-S-H with a low C/S ratio. This sorption dramatically falls as the C/S ratio increases (Henocq, 2017). The mechanisms induced in the observations in FIGURE 5-7 are minor in the case of the chemical system defined by a pristine hydrated cement paste. However, they would occur in the case of degraded cement-based materials.

5.7 CORI Results: effects of organics sorption on chemical properties

Measurements were performed in CORI to investigate the effect of the sorption of selected organic molecules on the chemical properties of the cementitious systems, i.e. HCP or individual phases. In particular, the zeta potential of various systems such as C-S-H, ettringite, portlandite or HCPs was measured under systematic variation of added organics concentrations. The zeta potential is related to the surface charge of particles in solution and can be an important factor in sorption processes. This type of information can therefore potentially provide additional understanding regarding the sorption processes and their impact on the chemistry of the studied system. For example, if the sorption of organic molecules modifies the surface charge of C-S-H under given conditions, this would potentially have an effect on the sorption of other species such as radionuclides. In addition of organic molecules, superplasticizers have also been studied.

5.7.1 Organic molecules

The effect of ISA on the surface charge was studied in ettringite and portlandite systems. FIGURE 5-8 presents the measured of zeta potential as a function of ISA concentration. It can be observed that the zeta potential evolves rapidly even in presence of low organics concentrations.

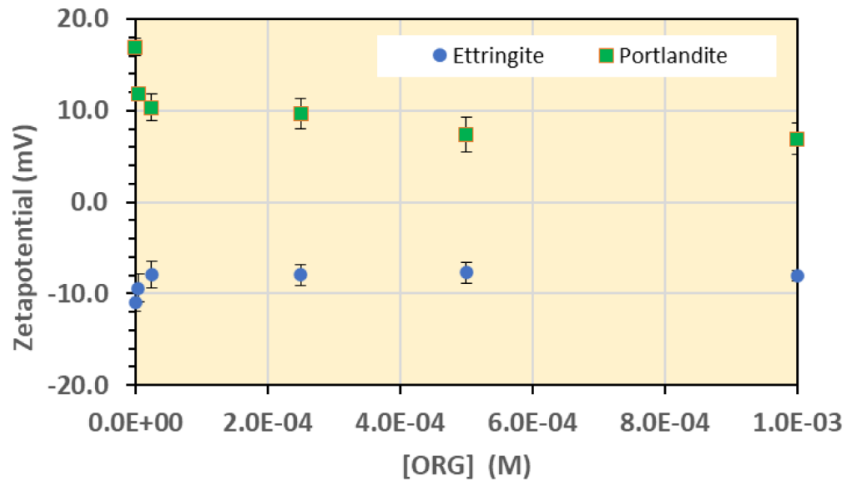
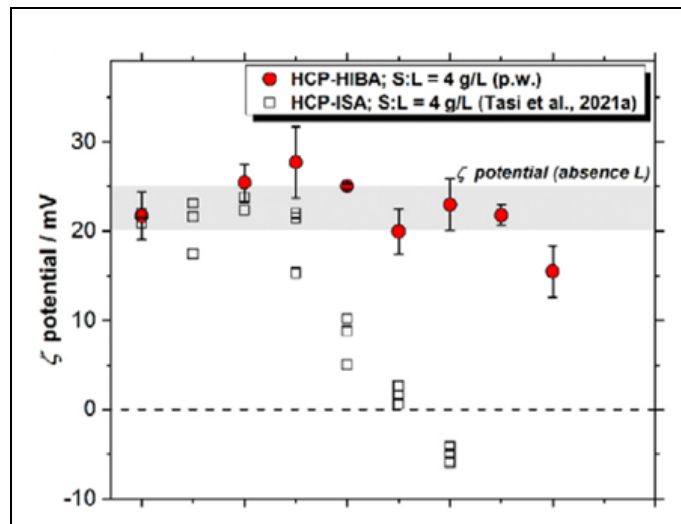


FIGURE 5-8: Influence of ISA concentration on zeta potential of ettringite and portlandite.

Further studies were performed on the evolution of the zeta potential of HCP particles in presence of HIBA, HBA and glutaric acid in comparison with ISA reported by Tasi et al. (2021). The conditions of this study correspond to the degradation stage II (pH=12.5). The measurements showed that HBA and HIBA molecules have no effect on the zeta potential and then further on the surface charge of HCP particles (FIGURE 5-9(top), shown for HIBA). Contrary to HBA and HIBA, glutaric acid has a significant effect on zeta potential at higher concentrations comparable to ISA.



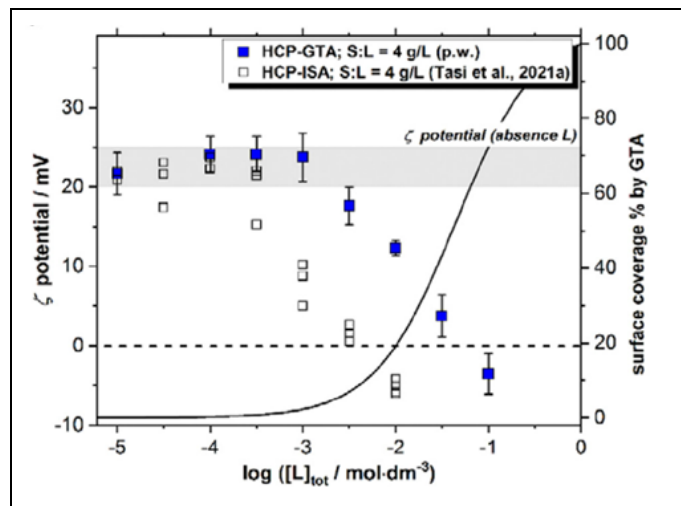


FIGURE 5-9: Zeta potentials of suspended HCP particles in the presence of proxy ligands at $10^{-5} M \leq [L]_{tot} \leq 0.1M$: (Top, previous page) HIBA, (Bottom) GTA. Zeta potentials reported in the literature for the HCP-ISA system are included for comparison (Tasi et al., 2021). Grey zones correspond to the zeta potentials representative of HCP (CEM I) in the degradation stage II and absence of organic ligands.

5.7.2 Superplasticizers

One of the main new insights highlighted in the updated SOTA concerns the superplasticizers which were particularly studied in for a larger variety of cementitious systems. Two commercial superplasticizers were considered here: the first one (SIKA) based on modified melamine (SIKAMENT™ 200 R, Sika, Spain), and the second product (MG) being the Master Glenium SKY 886 (BASF). This is an innovative superplasticizer based on latest generation of polycarboxylate ether (PCE) polymers. FIGURES 5-10 and 5-11 show the effect of the superplasticizers MG and SIKA on the surface properties (through the zeta potential measurements) of individual cement phases, C-S-H and portlandite. These results indicate that the surface charge is significantly modified, from positive to negative values. The surface of these cement hydrates becomes negatively charged with a higher effect of the superplasticizer SIKA.

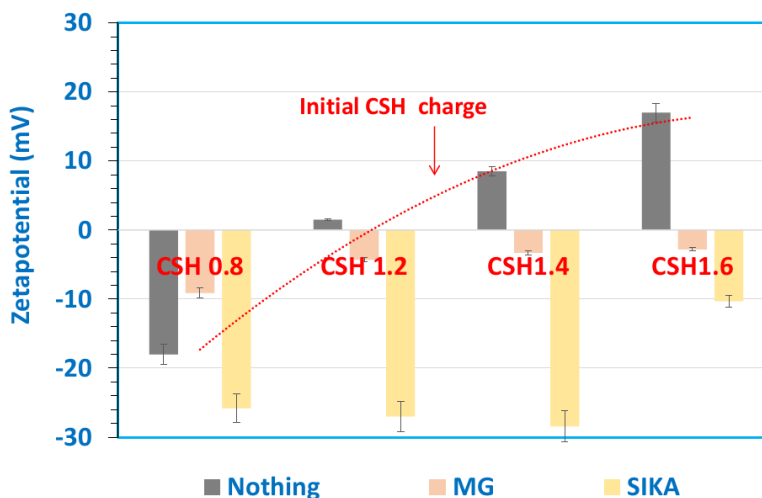


FIGURE 5-10: Zeta potential of C-S-H with various C/S in the presence of superplasticizers (MG and SIKA) in comparison with pure C-S-H (“Nothing”).

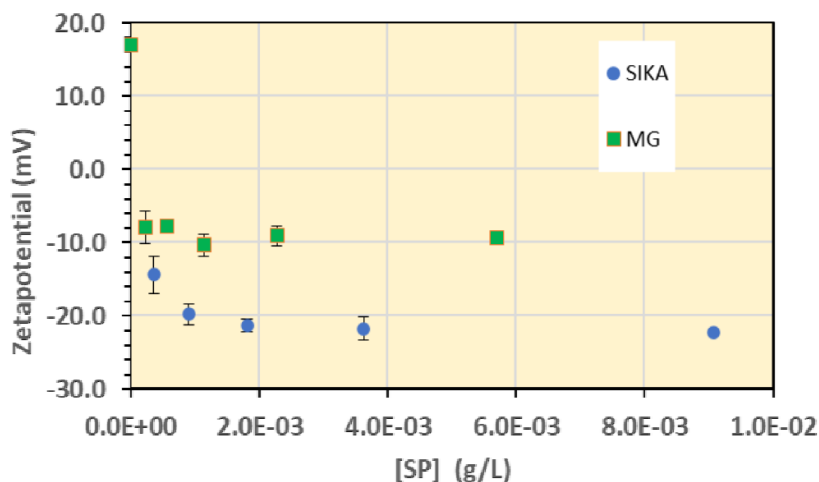


FIGURE 5-11: Zeta potential of portlandite in the presence of superplasticizers (MG and SIKA).

FIGURE 5-12 shows the zeta potential of HCP particles for two types of cement in the fresh state (stage I), CEM I and CEM V (FIGURE 5-12(a)), and also for the CEM I HCP at two degradation stages, fresh and stage II (FIGURE 5-12(b)). These measurements did not show any influence of superplasticizers, and the cement type at the fresh state. On the other hand, the superplasticizers inhibit differences between the fresh and degraded stages. In particular, the positive charge of the degraded HCP becomes negative.

These experiments on the surface charge of various cementitious systems in solution have evidenced a significant effect of the superplasticizers, especially PCE, which modify the surface properties, and consequently, can have an impact on the sorption behaviour of other species.

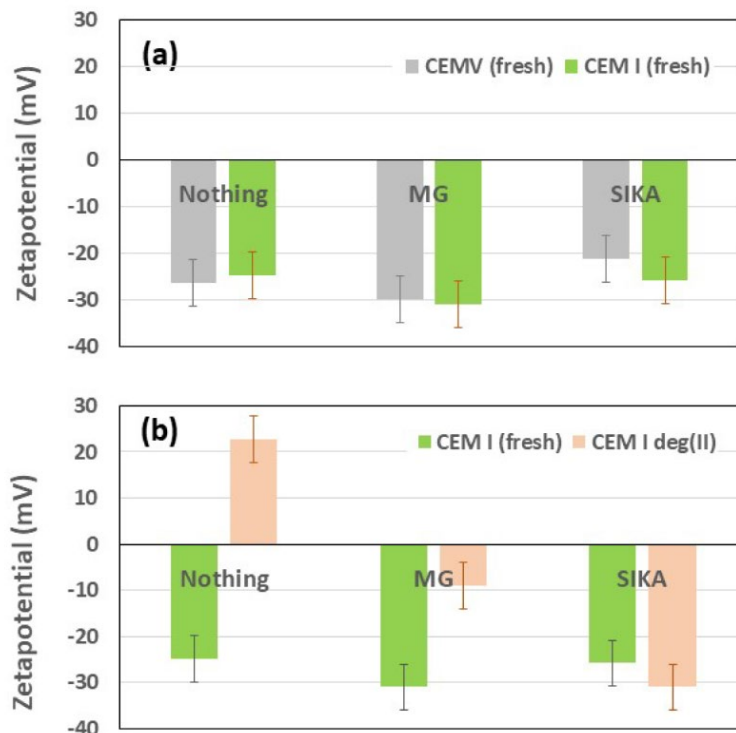


FIGURE 5-12: Zeta potential of HCP particles in the presence of superplasticizers (MG and SIKA).

5.8 Conclusion

The cement-based materials form a complex chemical system, which is not in equilibrium in most of the cases, especially in the context of a deep geological radioactive waste repository. The cementitious matrix is composed of several minerals, which play a role for the chemical evolution and the related radionuclide sorption processes. There is a good knowledge regarding the cement chemistry and a wide literature dedicated to the various cement types, which allows to characterize their chemical evolution with time and their contribution in terms of sorption.

5.9 References Chapter 5

- Achternbosch, M., Bräutigam, K. R., Hartlieb, N., Kupsch, C., Richers, U., & Stemmermann, P. (2005). Impact of the use of waste on trace element concentrations in cement and concrete. *Waste management & research*, 23(4), 328-337.
- Andersson K., Allard B., Bengtsson M., Magnusson B. (1989) Chemical composition of cement pore solutions. *Cement and Concrete Research* 19, 327-332
- Bach, T. T. H., Chabas, E., Pochard, I., Coumes, C. C. D., Haas, J., Frizon, F., & Nonat, A. (2013). Retention of alkali ions by hydrated low-pH cements: Mechanism and Na⁺/K⁺ selectivity. *Cement and Concrete Research*, 51, 14-21.
- Berner, U. R. (1992). Evolution of pore water chemistry during degradation of cement in a radioactive waste repository environment. *Waste management*, 12(2-3), 201-219.
- Brouwers, H. J. H. (2003). Alkali concentrations of pore solution in hydrating OPC. *Cement and Concrete Research*, 33(2), 191-196.
- Chappex, T., & Scrivener, K. (2012). Alkali fixation of C–S–H in blended cement pastes and its relation to alkali silica reaction. *Cement and Concrete Research*, 42(8), 1049-1054.
- Chen, J. J., Thomas, J. J., Taylor, H. F., & Jennings, H. M. (2004). Solubility and structure of calcium silicate hydrate. *Cement and concrete research*, 34(9), 1499-1519.
- Cong, X., & Kirkpatrick, R. J. (1996). ²⁹Si MAS NMR study of the structure of calcium silicate hydrate. *Advanced Cement Based Materials*, 3(3-4), 144-156.
- Damidot, D., Lothenbach, B., Herfort, D., & Glasser, F. P. (2011). Thermodynamics and cement science. *Cement and Concrete Research*, 41(7), 679-695.
- Damtoft, J. S., Herfort, D., & Yde, E. (1999, May). Concrete binders, mineral additions and chemical admixtures: state of the art and challenges for the 21st century. In *Creating With Concrete: Opening and Leader Papers of the Proceedings of the International Congress held at the University of Dundee, Scotland, UK on 6-10 September 1999* (pp. 153-168). Thomas Telford Publishing.
- Duchesne, J., & Reardon, E. J. (1995). Measurement and prediction of portlandite solubility in alkali solutions. *Cement and Concrete Research*, 25(5), 1043-1053.
- Fagerlund, G. (2006). Porosity and specific surface of Portland cement paste: an analysis of experimental work performed by Åke Grudemo during the years 1973-1979. Division of Building Materials, Lund Institute of Technology, Lund University.
- Faucon, P., Petit, J. C., Charpentier, T., Jacquinet, J. F., & Adenot, F. (1999). Silicon substitution for aluminum in calcium silicate hydrates. *Journal of the American Ceramic Society*, 82(5), 1307-1312.
- Frias, M., & de Rojas, M. I. S. (2002). Total and soluble chromium, nickel and cobalt content in the main materials used in the manufacturing of Spanish commercial cements. *Cement and Concrete Research*, 32(3), 435-440.
- Gaboreau, S., Grangeon, S., Claret, F., Ihiwakrim, D., Ersen, O., Montouillout, V., & Carteret, C. (2020). Hydration properties and interlayer organization in synthetic CSH. *Langmuir*.
- García, D., Grivé, M., Duro, L., Brassinnes, S., & de Pablo, J. (2018). The potential role of the degradation products of cement superplasticizers on the mobility of radionuclides. *Applied Geochemistry*, 98, 1-9.
- Gartner, E. M., & Jennings, H. M. (1987). Thermodynamics of calcium silicate hydrates and their solutions. *Journal of the American Ceramic Society*, 70(10), 743-749.

- Glasser, F. (2011). Application of inorganic cements to the conditioning and immobilisation of radioactive wastes. In Handbook of advanced radioactive waste conditioning technologies (pp. 67-135). Woodhead Publishing.
- Glaus, M. A., Laube, A., & Van Loon, L. R. (2003). A generic procedure for the assessment of the effect of concrete admixtures on the sorption of radionuclides on cement: Concept and selected results. MRS Online Proceedings Library Archive, 807.
- Glaus, M. A., Laube, A., & Van Loon, L. R. (2006). Solid–liquid distribution of selected concrete admixtures in hardened cement pastes. Waste Management, 26(7), 741-751.
- González-Siso M. R. (2018). Determination of key master variables and radionuclide behaviour in the Swedish Final Repository environment. PhD Thesis. Universitat Politècnica de Catalunya.
- Hamid, S. A. (1981). The crystal structure of the 11Å natural tobermorite $\text{Ca}_{2.25}[\text{Si}_3\text{O}_{7.5}(\text{OH})_{1.5}] \cdot \text{H}_2\text{O}$. Zeitschrift für Kristallographie-Crystalline Materials, 154(3-4), 189-198.
- Henocq, P. (2005). Modeling ionic interactions on the surface of calcium silicate hydrates. French. PhD Thesis. Laval University.
- Hillier, S. R., Sangha, C. M., Plunkett, B. A., & Walden, P. J. (1999). Long-term leaching of toxic trace metals from Portland cement concrete. Cement and Concrete Research, 29(4), 515-521.
- Hong, S. Y., & Glasser, F. P. (1999). Alkali binding in cement pastes: Part I. The CSH phase. Cement and Concrete Research, 29(12), 1893-1903.
- Hong, S. Y., & Glasser, F. P. (2002). Alkali sorption by CSH and CASH gels: Part II. Role of alumina. Cement and Concrete Research, 32(7), 1101-1111.
- Jennings, H. M. (2000). A model for the microstructure of calcium silicate hydrate in cement paste. Cement and concrete research, 30(1), 101-116.
- Keith-Roach, M. and Höglund L. O. (2018). Review of the long-term risks associated with the use of superplasticizers. POSIVA.
- Klur, I., Pollet, B., Virlet, J., & Nonat, A. (1998). CSH structure evolution with calcium content by multinuclear NMR. In Nuclear magnetic resonance spectroscopy of cement-based materials (pp. 119-141). Springer, Berlin, Heidelberg.
- L'Hôpital, E., Lothenbach, B., Le Saout, G., Kulik, D., & Scrivener, K. (2015). Incorporation of aluminium in calcium-silicate-hydrates. Cement and Concrete Research, 75, 91-103.
- Lothenbach, B. & Winnefeld F. (2006), Thermodynamic modelling of the hydration of Portland cement. Cement and Concrete Research 36, 209-226.
- Lothenbach, B., Scrivener, K., & Hooton, R. D. (2011). Supplementary cementitious materials. Cement and concrete research, 41(12), 1244-1256.
- Lothenbach, B., & Nonat, A. (2015). Calcium silicate hydrates: solid and liquid phase composition. Cement and Concrete Research, 78, 57-70.
- Matschei, T., Lothenbach, B., & Glasser, F. P. (2007). The AFm phase in Portland cement. Cement and Concrete Research, 37(2), 118-130.
- Myneni, S. C., Traina, S. J., & Logan, T. J. (1998). Ettringite solubility and geochemistry of the $\text{Ca}(\text{OH})_2$ – $\text{Al}_2(\text{SO}_4)_3$ – H_2O system at 1 atm pressure and 298 K. Chemical Geology, 148(1-2), 1-19.
- Nachbaur L., Nkinamubanzi P. C., Nonat A., Mutin J.-C. (1998) Electrokinetic properties which control the coagulation of silicate cement suspensions during early age hydration. Journal of Colloid and Interface Science 202, 261
- Ochs, M., Mallants, D., & Wang, L. (2016). Radionuclide and metal sorption on cement and concrete. Springer.

- Olmeda, J., Henocq, P., Giffaut, E., & Grivé, M. (2017). Modelling of chemical degradation of blended cement-based materials by leaching cycles with Callovo-Oxfordian porewater. *Physics and Chemistry of the Earth, Parts A/B/C*.
- Perkins, R. B., & Palmer, C. D. (1999). Solubility of ettringite ($\text{Ca}_6[\text{Al}(\text{OH})_6]_2(\text{SO}_4)_3 \cdot 26\text{H}_2\text{O}$) at 5–75°C. *Geochimica et Cosmochimica Acta*, 63(13-14), 1969-1980.
- Ramachandran, V. S. (1996). *Concrete admixtures handbook: properties, science and technology*. William Andrew.
- Roosz, C. (2016). *Propriétés thermodynamiques des phases cimentaires hydratées: C-S-H, C-A-S-H et M-S-H*. Thesis. Université de Poitiers.
- Roosz, C., Vieillard, P., Blanc, P., Gaboreau, S., Gailhanou, H., Braithwaite, D., ... & Madé, B. (2018). Thermodynamic properties of CSH, CASH and MSH phases: Results from direct measurements and predictive modelling. *Applied Geochemistry*, 92, 140-156.
- Snellings, R., Mertens, G., & Elsen, J. (2012). Supplementary cementitious materials. *Reviews in Mineralogy and Geochemistry*, 74(1), 211-278.
- Stutzman, P. E. (1999). *Chemistry and structure of hydration products* (No. American Ceramic Society Bulletin).
- Suresh, D., & Nagaraju, K. (2015). Ground granulated blast slag (GGBS) in concrete—a review. *IOSR journal of mechanical and civil engineering*, 12(4), 76-82.
- Taylor H.F.W. (1992) *Cement Chemistry*, 2nd edition, Academic Press.
- Taylor, H. F. W. (1993). Nanostructure of C-S-H: Current status. *Advanced cement based materials*, 1(1), 38-46.
- Tracz, T. (2016). Open porosity of cement pastes and their gas permeability. *Bulletin of the Polish Academy of Sciences. Technical Sciences*, 64(4).
- Viallis-Terrisse H., Nonat A., Petit J.-C. (2001) Zeta-potential study of Calcium Silicate Hydrates interacting with alkaline cations. *Journal of Colloid and Interface Science* 244, 58-65
- Walker, C. S., Sutou, S., Oda, C., Mihara, M., & Honda, A. (2016). Calcium silicate hydrate (CSH) gel solubility data and a discrete solid phase model at 25 C based on two binary non-ideal solid solutions. *Cement and Concrete Research*, 79, 1-30.
- Wieland, E., Lothenbach, B., Glaus, M. A., Thoenen, T., & Schwyn, B. (2014). Influence of superplasticizers on the long-term properties of cement pastes and possible impact on radionuclide uptake in a cement-based repository for radioactive waste. *Applied geochemistry*, 49, 126-142.
- Young A.J. (2012) *The stability of cement superplasticiser and its effect on radionuclide behaviour*. Ph.D thesis, Loughborough University, U.K.
- Zanni, H., Rassem-Bertolo, R., Masse, S., Fernandez, L., Nieto, P., & Bresson, B. (1996). A spectroscopic NMR investigation of the calcium silicate hydrates present in cement and concrete. *Magnetic resonance imaging*, 14(7-8), 827-831.